Analysis of Passive Cooling And Heating of Ventilation Air in a Buried Intake Culvert

Daniel Løchen Slobodinski

EPT-M-2013-108

MASTER THESIS

for

Stud.techn. Daniel Loechen Slobodinski

Spring 2013

Analyses of passive cooling and heating of ventilation air in a buried intake culvert

Analyse av passiv kjøling og oppvarming av ventilasjonsluft i en nedgravd inntakskulvert

Background and objective

Buried pipes or ducts, also mentioned as culverts, can be used for cooling or preheating of supply air for ventilation in buildings. In hot summer periods, the thermal mass in the culvert can be cooled by night ventilation, and in the following day the ventilation air can be cooled by the thermal mass of the culvert and the surrounding ground. In the winter time, heat from the surrounding ground can contribute with preheating of intake air for ventilation. In spring and fall it seems beneficial to have an alternative air intake to avoid the culvert to cool intake air when the outside air temperature is below the air temperature used for ventilation supply to rooms.

Heat transfer between airflow and culvert walls and heat conduction in the ground are the two important parameters for the cooling or heating power of the supply air culvert. The heat transfer coefficient between airflow and culvert walls can be enhanced by installing an axial fan, causing rotational flow and increased turbulence, at the culvert entrance.

The goal for this thesis is twofold; one is to model and demonstrate, by CFD simulations, the difference in heat transfer to the wall between uniform and rotational inlet flow into the culvert. The other goal is to improve modeling of earth conduction and to simulate realistic cooling and heating power, over a year, for a supply air culvert.

The following tasks are to be considered:

1. A literature review of heat transfer for air in ducts shall be performed.

2. CFD-simulations, with and without rotational flow at the inlet, shall be performed for a duct. The difference in heat transfer to the wall shall be demonstrated and evaluated along with data from literature.

3. Heat transfer between the culvert and the surrounding ground shall be modeled and the annual cooling and heating of intake air for ventilation shall be analyzed.

-- " --

Within 14 days of receiving the written text on the master thesis, the candidate shall submit a research plan for his project to the department.

When the thesis is evaluated, emphasis is put on processing of the results, and that they are presented in tabular and/or graphic form in a clear manner, and that they are analyzed carefully.

The thesis should be formulated as a research report with summary both in English and Norwegian, conclusion, literature references, table of contents etc. During the preparation of the text, the candidate should make an effort to produce a well-structured and easily readable report. In order to ease the evaluation of the thesis, it is important that the cross-references are correct. In the making of the report, strong emphasis should be placed on both a thorough discussion of the results and an orderly presentation.

The candidate is requested to initiate and keep close contact with his/her academic supervisor(s) throughout the working period. The candidate must follow the rules and regulations of NTNU as well as passive directions given by the Department of Energy and Process Engineering.

Risk assessment of the candidate's work shall be carried out according to the department's procedures. The risk assessment must be documented and included as part of the final report. Events related to the candidate's work adversely affecting the health, safety or security, must be documented and included as part of the final report. If the documentation on risk assessment represents a large number of pages, the full version is to be submitted electronically to the supervisor and an excerpt is included in the report.

Pursuant to "Regulations concerning the supplementary provisions to the technology study program/Master of Science" at NTNU §20, the Department reserves the permission to utilize all the results and data for teaching and research purposes as well as in future publications.
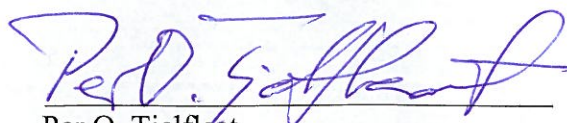
The final report is to be submitted digitally in DAIM. An executive summary of the thesis including title, student's name, supervisor's name, year, department name, and NTNU's logo and name, shall be submitted to the department as a separate pdf file. Based on an agreement with the supervisor, the final report and other material and documents may be given to the supervisor in digital format.

☐ Work to be done in lab (Water power lab, Fluids engineering lab, Thermal engineering lab)
☐ Field work

Department of Energy and Process Engineering, 18. February 2013

Olav Bolland
Department Head

Per O. Tjelflaat
Academic Supervisor

Research Advisor: Førsteamanuensis II Rasmus Høseggen

Preface

This report is a master thesis written at the Department of Energy and Process Engineering at The Norwegian University of Science and Technology during the spring of 2013.

I would like to thank my supervisor, Professor Per O. Tjelflaat for his invaluable guidance, support and help throughout the whole project assignment until this master thesis. Without him the project would not have been possible. I would also like give a big thank to my co-supervisor Rasmus Z. Høseggen for useful feedback on my model in ESP-r.

My fellow students Ragnhild Løge and Ida Auråen deserve a big thank for collaborating with me on ESP-r.

Last, but not least, I would like to express my sincerer gratitude to Martin A. Holst at EDR Medeso AS for always answering me quickly and thoroughly on all questions regarding the CFD model.

Abstract

Passive ventilation is becoming increasingly important due to more focus on limiting electricity for ventilation purposes. Underground culverts may be utilized to achieve preheating or precooling of the intake air. Therefore it represents a possible measure to reduce the electricity usage used for heating and cooling.

In order to assess the possible heating and cooling performance of a culvert situated at Grong primary school, the impact of rotational versus uniform inflow on the convective heat transfer has been examined in a CFD model. The results from this model have been compared to measurements performed at Grong and other similar experiments.

Based on this, a heat performance model was created in ESP-r incorporating a heat convection model and one-dimensional heat conduction model together with local weather data from Grong.

The model showed that the culvert might be used for heating during fall and winter when the ambient temperature is low compared to the ground temperature. For the spring, the culvert provides undesirable cooling. During the summer when the ambient temperature is high enough, the culvert can provide cooling in the hottest days.

Sammendrag

Passiv bygningsventilasjon blir stadig viktigere for å begrense bruken av strøm til ventilasjonsformål. Underjordiske kulverter kan brukes til å forvarme eller forkjøle inntakslufta. Derfor representerer de et mulig tiltak for å redusere strømbruken til oppvarming og kjøling.

For å vurdere den potensielle oppvarmings- eller kjølingsytelsen til kulverten ved Grong barneskole, ble påvirkninga på den termiske konveksjon undersøkt ved å se på forskjellen mellom uniform- kontra rotasjonsinnstrømning i en numerisk strømningsmodell. Resultatene fra denne ble sammenlignet med målinger foretatt i kulverten på Grong og andre liknende eksperimenter.

På grunnlag av dette, ble energiytelsesmodell laget i ESP-r. Denne inkluderte effekten av termisk konveksjon og endimensjonal varmeledning sammen med lokale værdata fra Grong.

Denne modellen viste at kulverten egner seg best til forvarming på høst og vinter når utetemperaturen er lav sammenlignet med bakketemperaturen. På våren gav den en uønsket kjøling. På sommeren, når utetemperaturen er høy nok, kan den kjøle inntakslufta når dette er ønskelig på de varmeste dagene.

Table of Contents

Lists

List Of Figures

List Of Tables

List Of Equation

1 Introduction

1.1 Background

Due to higher production of electricity in Europe, there has been an increase of emissions of greenhouse gases. In the HVAC sector, one uses considerable amounts of energy due to the heating and cooling demand of buildings. Especially the latter one has risen as a result of construction of low-energy buildings and passive houses these last few years.

Embedded ducts and pipes can be used for precooling and preheating of supply air in buildings. It is important to understand the heat transfer characteristics of convection between the air and the duct surfaces, and the thermal conduction throughout the duct structure until it reaches the surrounding ground.

1.2 Scope And Strategy

The goal of this assignment is to analyze the heat transfer conditions inside a concrete culvert situated at Grong primary school. Firstly a preliminary literature search will be performed in order to attain some knowledge on how to analyze and model such conditions, and then a computational fluid dynamics (CFD) model will be created. The main interests will be to analyze the difference in heat transfer characteristics between rotational flow and uniform flow at the duct inlet. Results from this model will be compared to results found in the literature search and evaluated.

Lastly the heating and cooling effect of the culvert will be evaluated, by using a model incorporating both the effects of convective heat transfer between the air and the culvert walls and conductive heat transfer to the ground. This model has already been made as a part of the preparation for the master thesis. It will be updated in terms of setting the heat transfer coefficient on the duct walls to a certain value, instead of using the default correlation from the program. Some simulations will be run to show the difference between the old and the new model.

1.3 Tools Used

Two programs will be used in this master thesis, namely Ansys Fluent and ESP-r.

Ansys Fluent is a renowned computational fluid dynamics program developed by Ansys Inc.

The building energy performance modeling program ESP-r will be used to analyze the amount of the heat transfer between the air and the ground in order to calculate the heating and cooling capacity of the culvert. ESP-r is an open source program developed at University of Stratchclyde in Glasgow.

1.4   Report Structure

The report starts with an introduction to simplified model of ground temperature distribution in the ground. Heat transfer by convection in ducts and what parameters affects this, supplied with different examples and graphs.

Before the results of CFD analysis, a description of how the model is built is presented. A similar approach will be done for ESP-r as well.

The most important findings will be discussed along with the representation of the results and also in the discussion section, followed by conclusion and a suggestion for further studies.

2 Ground Temperature Distribution

In an earth-to-air-heat-exchanger (ETAHE) the intake air is led through an underground duct, in which the air gets heated up or cooled down. Air temperature fluctuates very much compared to the ground temperature. To get a picture of how ground temperature varies with depth and time, one can simplify Fourier's Law by considering the ground as a semi-infinite media (Zhang 2009). By using ground surface temperature records, one can solve this equation and obtain:

Equation 1: Fourier's Law (Zhang 2009)

$$\rho_s cp_s \frac{\partial T_s}{\partial t} = \frac{\partial}{\partial z}\left(k_s \frac{dT_s}{dz}\right)$$

Equation 2: Undisturbed Ground Temperature (Zhang 2009)

$$T_s(z,t) = T_{s,m} - A_s \cdot \exp\left[-z\left(\frac{\pi}{365\alpha_s}\right)^{0,5}\right]\cos\left\{\frac{2\pi}{365}\left[t - t_0 - \frac{z}{2}\left(\frac{365}{\pi\alpha_s}\right)^{0,5}\right]\right\}$$

ρ_s = Soil density [kg/m³]

cp_s = Soil specific heat capacity [J/kgK]

T_s = Ground temperature [°C]

t = Time [day]

t_0 = Phase constant [day]

z = Ground depth [m]

k_s = Soil thermal conductivity [W/mK]

$T_{s,m}$ = Annual mean temperature [°C]

A_s = Amplitude of daily mean ground surface temperature in a year [°C]

α_s = Soil thermal diffusivity [m²/day]
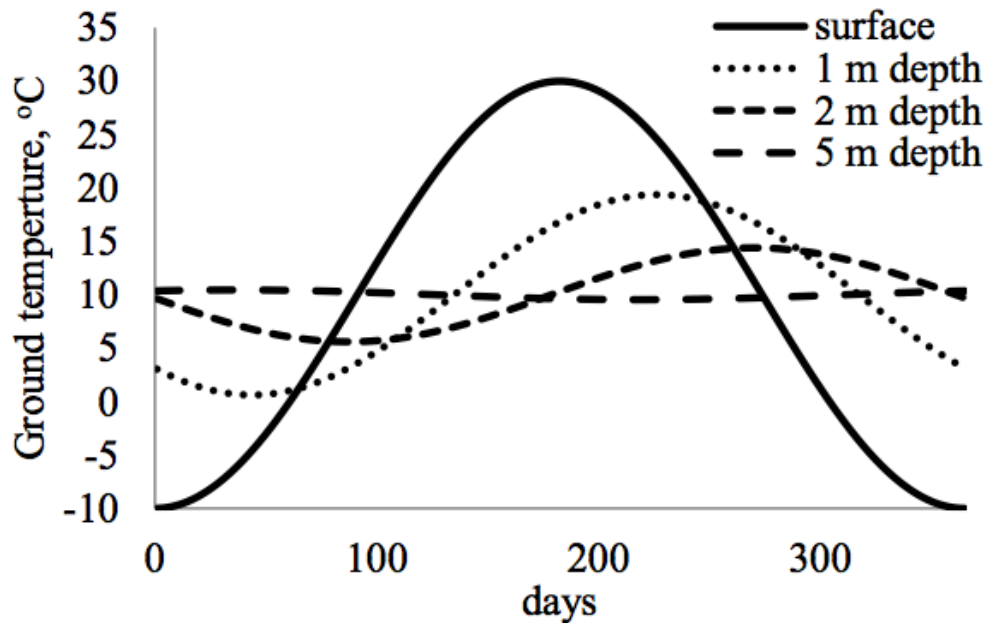
Figure 1: Annual Ground Temperature Variations At Different Depths (Zhang 2009)

The result of solving Equation 2 for a place with certain characteristics is shown above. Figure 1 shows how the fluctuations quickly dampen down with increasing depth. One notices the phase change, which moves the temperature amplitude to the right i.e. the peak temperature does not coincide with the middle of the summer (as with the surface temperature), but rather sometime in the fall deeper in the ground. (Labs 1979). I.e. an ETAHE will perform better at preheating air in the fall when the ground temperatures are higher rather than in the spring when the ground temperatures are at the lowest.

3   Heat Transfer For Air In Ducts

A duct is a system used in HVAC industry for supply and removal of ventilation air. They come in a variety of sizes and shapes. The most common ones are circular or square. In this assignment the main focus will be on the subterranean square ducts.

3.1   Variety Of Ducts

Depending on in what geographical place we find ourselves, people have different needs for ventilation. In desert regions, windcatchers have been used in combination with a culvert for cooling the intake air. A culvert is a duct typically placed underground. Some examples can be seen in old constructions in Iran (Roaf 2005). A windcatcher is a tall construction which purpose is to collect air by letting the wind pass through the openings in the upper part. At ambient conditions with very high temperatures, this air is not cold enough to cool the occupants. The air is being led through a duct, which causes the moving mass of air to exchange heat with the culvert walls convectively, thus cooling the air down a bit more.
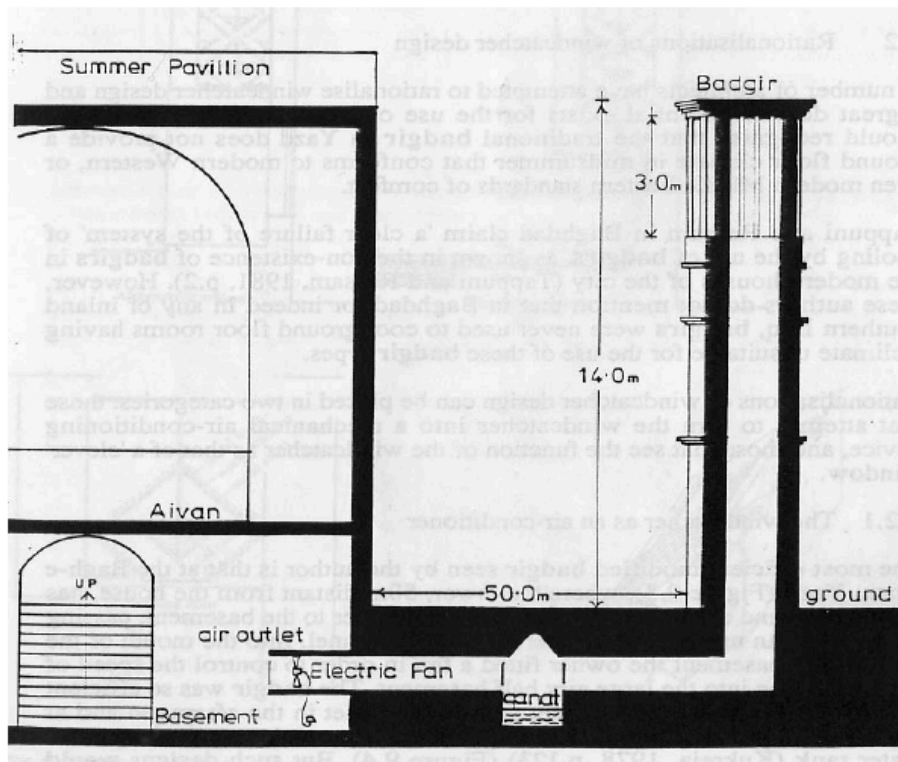
Figure 2: Section Through The Pavilion, Tower And Ganat At The Bagh-e Khan, Yazd (Roaf 2005)

The culvert walls are connected to the ground, which can lead the heat further out to the ground and store it there. Ground can be used as a thermal storage due to its relative stable temperatures as seen in Figure 1, and its massive thermal capacity.

Figure 3 shows a similar construction that cools the air in a different manner due to evaporation of water instead of convection and conduction into the surrounding ground. This is also an example found in Iran. In this culvert, the walls are drenched due to diffusion of water coming from a creek nearby. The walls in the culvert consist of bricks having a low conductivity, thus keeping the effect of the ground temperatures to a minimum. The depth of the culvert is not very deep in this case.
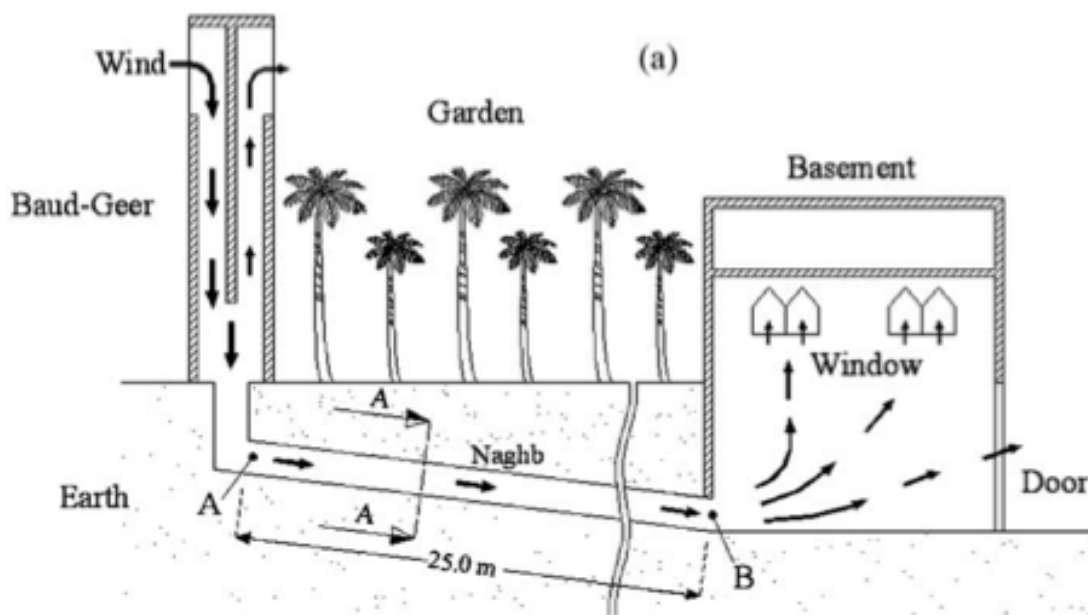
Figure 3: Schematic View Of The Air Way Through The Baud-Geer (Windcatcher) and Naghb (Culvert) (S.M. Jafarian 2009)

When the hot air enters the duct, it comes in contact with the moist walls causing water to evaporate. This heat is taken from the air, which will then have a lower temperature (S.M. Jafarian 2009).

Another setup utilized for cooling and heating of air is earth-tubes or e-tubes. An earth-tube system consists of a series of buried pipes in the ground. The system can be designed without any electrical components such as fans, when the pressure difference between the interior and exterior of building is sufficiently big. Or it can be connected to an air-handling unit or in a combination with a fan.
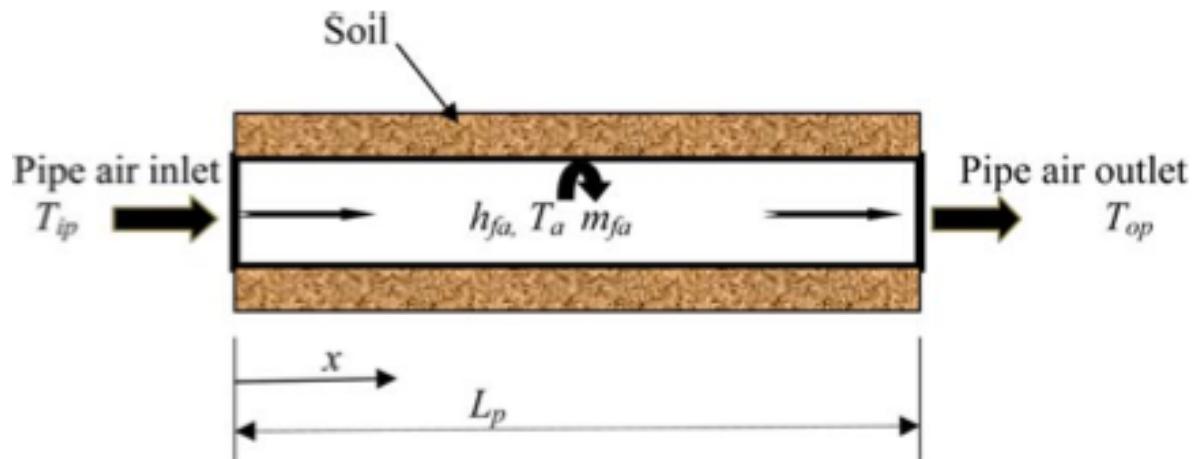
Figure 4: Air Through Earth-tube (Darkwa, Kokogiannakis et al. 2011)

Depending on the season, the earth-tubes can be used for cooling or heating the intake air. Earth-tubes are generally thinner and more light weighted than the concrete ducts thus giving them a smaller thermal mass. That makes them more sensitive to ground temperature variations than concrete culverts. In order to avoid problems with condensation inside the tubes, they are often installed with an inclination. The condensation will be safely discharged instead of being accumulated as puddles at the lowest points (Darkwa, Kokogiannakis et al. 2011).

3.2 Temperature Altering Processes For Air

As seen in the section above, there are mainly three processes able to affect the air temperature in ducts. These are:

- Heat convection between surface and air
- Evaporation of water
- Heat conduction from surface and into ground

The main focus in this assignment is to work out a way to be able to predict the amount heat convection with a given geometry and flow conditions, and also find a way to model the heat conduction in a credible way. The effects of evaporating water will not be considered.

3.2.1 Heat Transfer By Convection

In order to get a better grip of heat transfer in ducts, round ducts are first considered.

3.2.1.1 Entrance Region And Boundary Layers

Consider a fluid entering a pipe with uniform velocity and temperature profile, where the pipe has a constant temperature, the velocity profile and temperature profile will change along the length of the duct. Due to viscous forces, the velocity will be slowed down close to the duct walls, which will allow the air closest to wall to change in temperature. Thermal and velocity boundary layers will develop from the walls and grow further into the duct. From the entrance region to the point where these layers completely cover the cross section is referred to as the entrance region. After this point, the flow is considered fully developed (Lienhard 2005).

In Figure 5 the T_b is the fluid bulk mean temperature. This is the mass-averaged temperature at a certain length x into the pipe. Since T_w in this case is constantly higher than $T\infty$ (the uniform temperature of the fluid before entering the pipe), T_b will grow as the air traverses the duct. A crucial point here is that q_w, which refers to the local heat transfer rate at the wall, is higher at the entrance region and diminishes further into the pipe.

Equation 3: Local Heat Flux (Zhang 2009)

$$q_w" = h_x \left(T_{surf,x} - T_b \right)$$

Equation 4: Hydraulic Diameter (Zhang 2009)

$$D_h = \frac{4A}{P}$$

Equation 5: Local Nusselt Number (Zhang 2009)

$$Nu_x = \frac{h_x D_h}{k}$$

$q_w"$ = Local heat flux wall [W/m²]

$T_{surf,x}$ = Temperature surface [°C]

T_b = Bulk mean temperature of fluid [°C]

D_h = Hydraulic diameter [m]

A = Cross sectional area [m²]

P = Wetted perimeter of the cross section [m]

Nu_x = Local Nusselt number [non-dimensional]

h_x = Local convective heat transfer coefficient [W/m²K]

k = Thermal conductivity of fluid [W/mK]
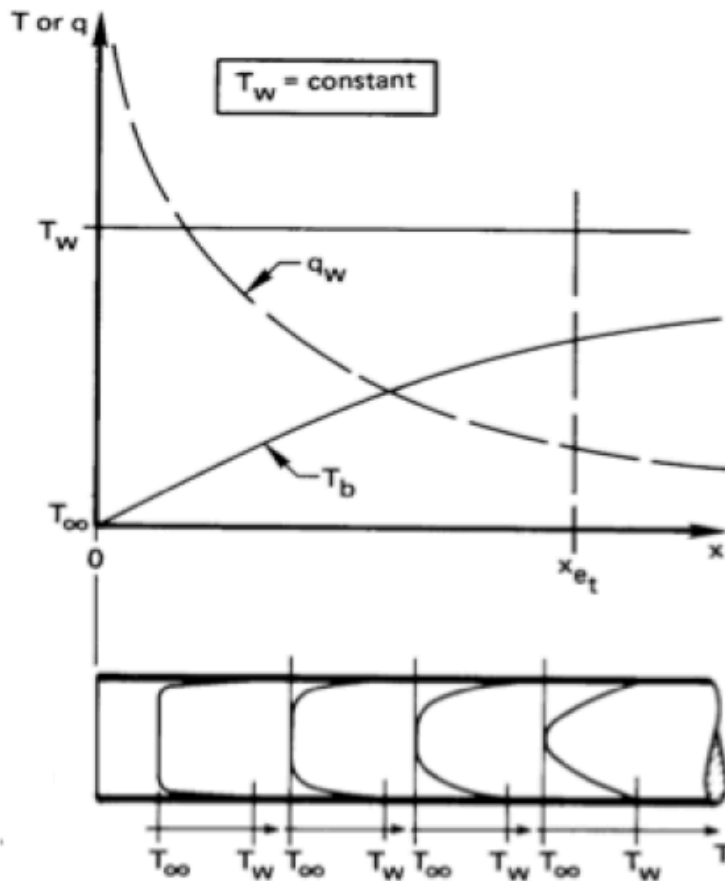
As can be seen in Equation 5, for a given geometry (constant hydraulic diameter) and a given fluid with constant thermal conductivity, Nu_x and h_x become proportional to each other. With this in mind, we can see how $Nu_{x,T}$ (subscript T indicates constant wall temperature) and h_x are expected to vary over the ducts length according to Figure 6. What strikes us is that the Nu_x is considerably higher in the entrance region, and then stabilizes on a flat level after a certain length x/D_h.

For ETAHE with small D_h and a big L, it is a reasonable assumption to assume turbulent conditions on the whole length. For instance a small pipe with a diameter of 10 cm and a total length of 20 meters, will have a length ratio $L/D_h = 20$. In this case, most of the flow will have a constant Nu_x.

However the duct at Grong is a large cross sectional ETAHE and is expected to have more complicated flow conditions, since the ratio L/D_h is not as large as in the above mentioned example. L/D_h is approximately 7 for the Grong case.
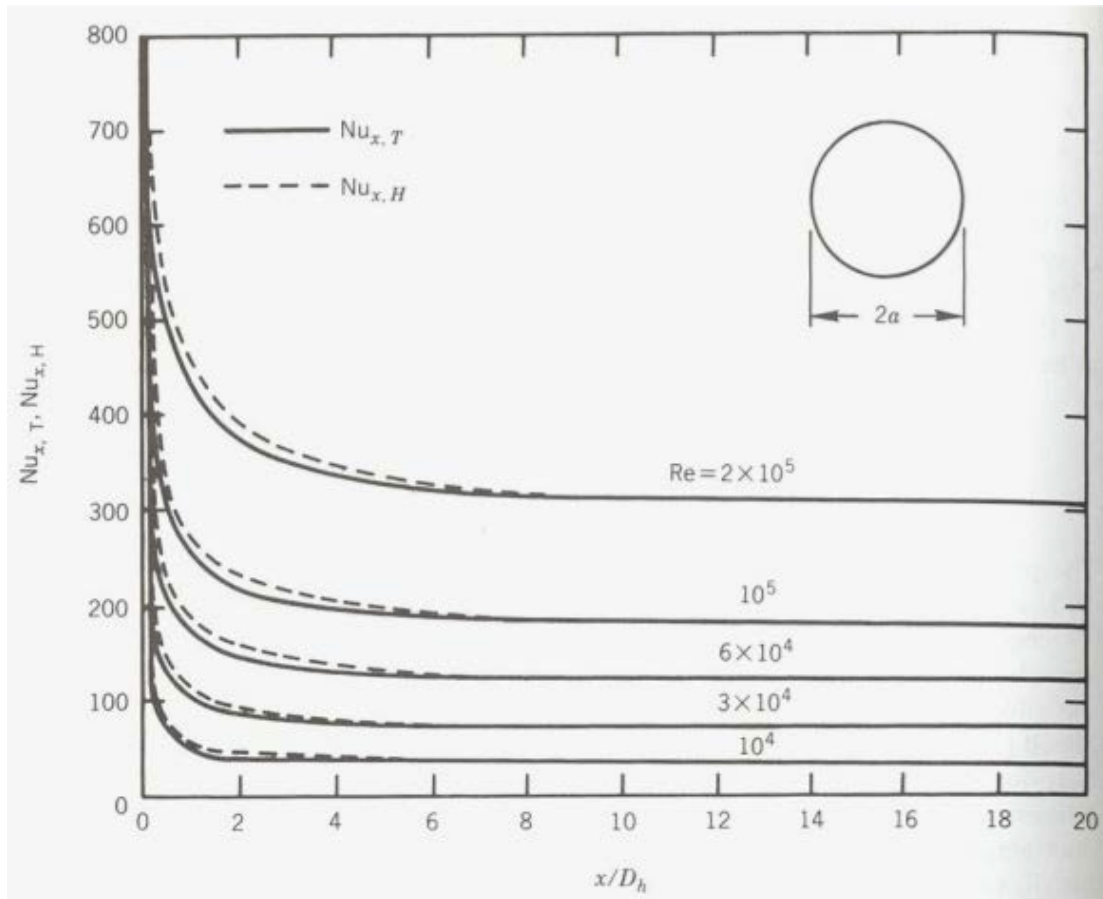
Figure 6: Local Nusselt Numbers For Simultaneously Developing Turbulent Flow In A Smooth Circular Duct For Pr =0,73 (Deisler 1953)

3.2.1.2 *Influencing Factors On The Heat Transfer Coefficient*

Four factors were identified as influential on heat transfer coefficient. These are not completely distinguishable, but rather intertwined. These are surface roughness, vortices, fan flow and buoyancy.

In ducts with rib-roughened surfaces, vortices will form close to the walls, as can be seen of Figure 7. Here φ is the rib head chamfer angle. In an example in which a heated wall with rib-roughened surface was subject to airflow at different Re, following conclusions was drawn. When Re_D increases, the boundary layer decreases. This will increase the heat transfer rate. But in addition to this, the vortices originating from the roughness elements as will add to the heat removal, thus enhancing the heat transfer coefficient (R. Karwa 1998).

Equation 6: Reynolds Number Based On General Length Parameter (Incropera and De Witt 1985)

$$\text{Re}_\chi = \frac{U\chi}{\nu}$$

Re_χ = Reynolds number for a parameter χ [non-dimensional]
U = Flow velocity [m/s]

v = Kinematic viscosity [m²/s]

χ = General length parameter (e.g. diameter, radius) [m]

SEQUENCE ① ② ③ ④ : VORTICES STARTING, GROWING AND THEN MOVING DOWNSTREAM

• Represents an anticlockwise rotating vortex

x Represents a clockwise rotating vortex
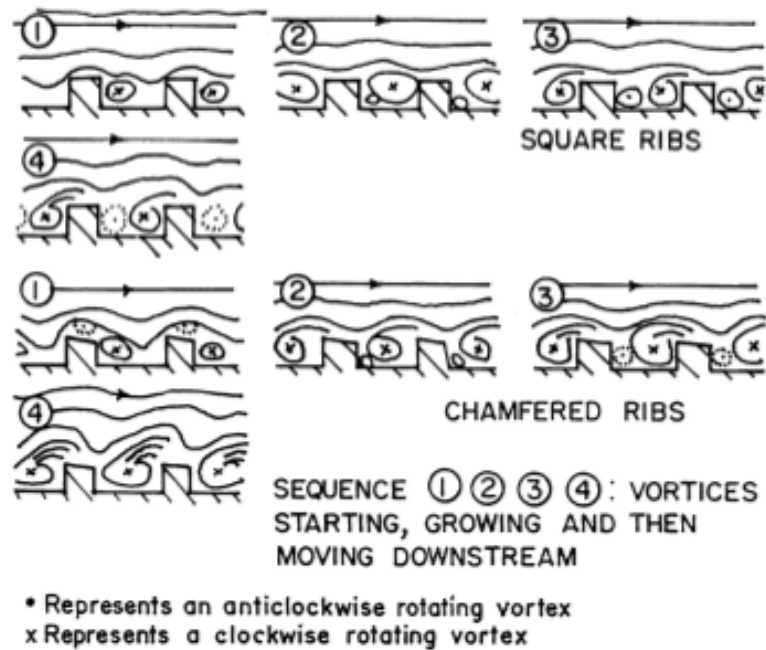
Figure 7: Flow Pattern For Square (φ=0°) And Chamfered Ribs (φ=10°) (F. Williams 1970)

However, an increase in the heat transfer coefficient by increasing the roughness will automatically lead to a bigger friction factor. This will increase the pressure loss in the duct, hence requiring more power to drive the flow. This is important to bear in mind when an enhancement in the heat transfer coefficient is desirable (Bejan 1982).

In another paper by T.Y. Chen and H.T. Shu the influence on the heat transfer due an axial fan was investigated. They let flow over a heated aluminum plate in a square duct with D_h = 0,07 m at varying Reynolds numbers. The flow at the inlet was either uniform or rotational due to an axial fan. In Figure 9, one can see how the flow field looks like after x/D = 2,86. Y is height, Z is the width of the duct and x is length in main flow direction. They investigated these two cases with and without a delta-wing vortex generator situated at x=0. The experimental setup is seen in Figure 8.
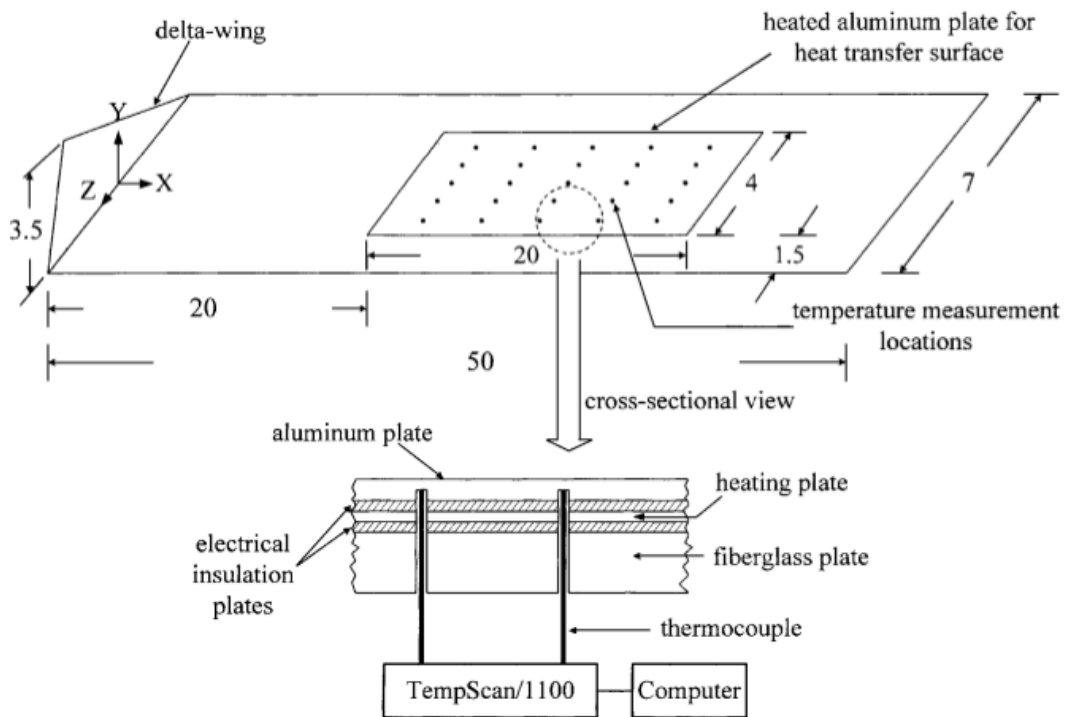
Figure 8: Experimental Setup. Delta Wing Vortex Generator Is Seen At Inlet. Unit: cm (T.Y. Chen 2003)
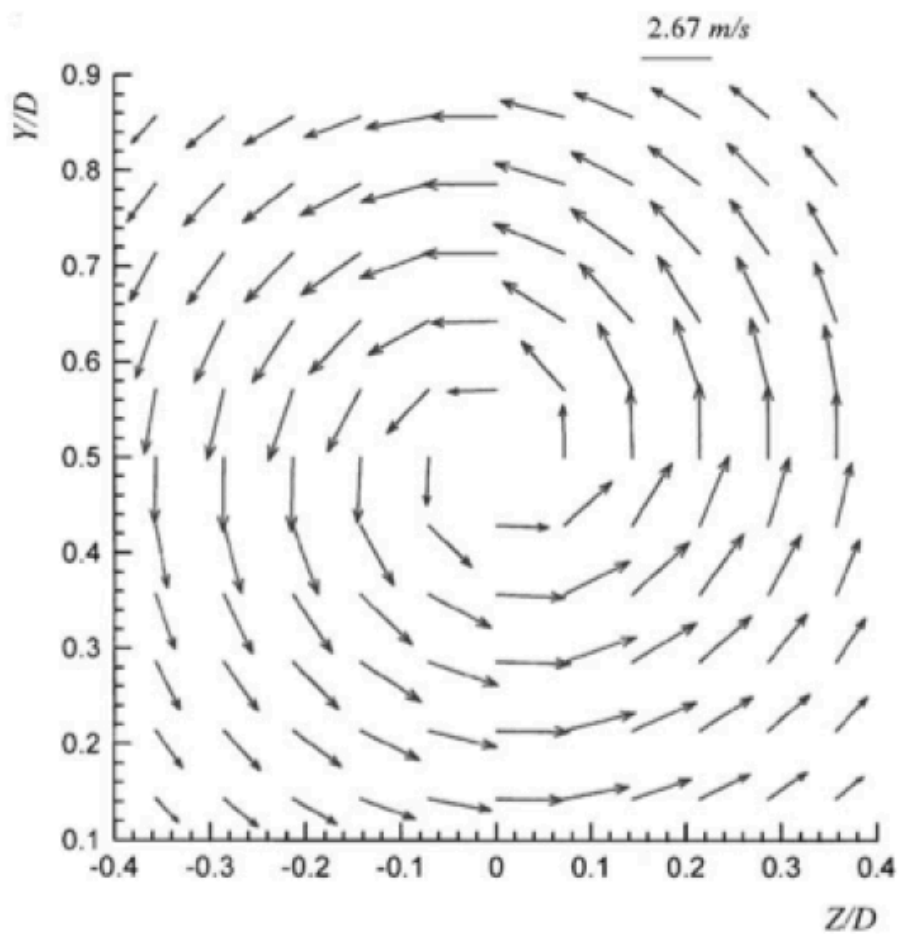
Figure 9: Fan Flow Of ReD= 11820 At X/D= 2,86 (T.Y. Chen 2003)

Their most important discovery was that the Nusselt number is increased in every case compared to uniform flow. The delta-wing increases the axial vorticity and the turbulent kinetic energy. However, in fan flow, the delta wing has a minor impact on the Nusselt number. (T.Y. Chen 2003) For Reynolds number of approximately 12 000, the Nusselt number increases from 40 (uniform) to 100 (fan flow). This again translates to an enhancement of the heat transfer coefficient from 16,9 W/m²K to 36,7 W/m²K, by using D= 0,07m, k_{air}= 0,0257 W/mK; in other words, an increase of 117,4% of the heat transfer coefficient from uniform to fan flow.
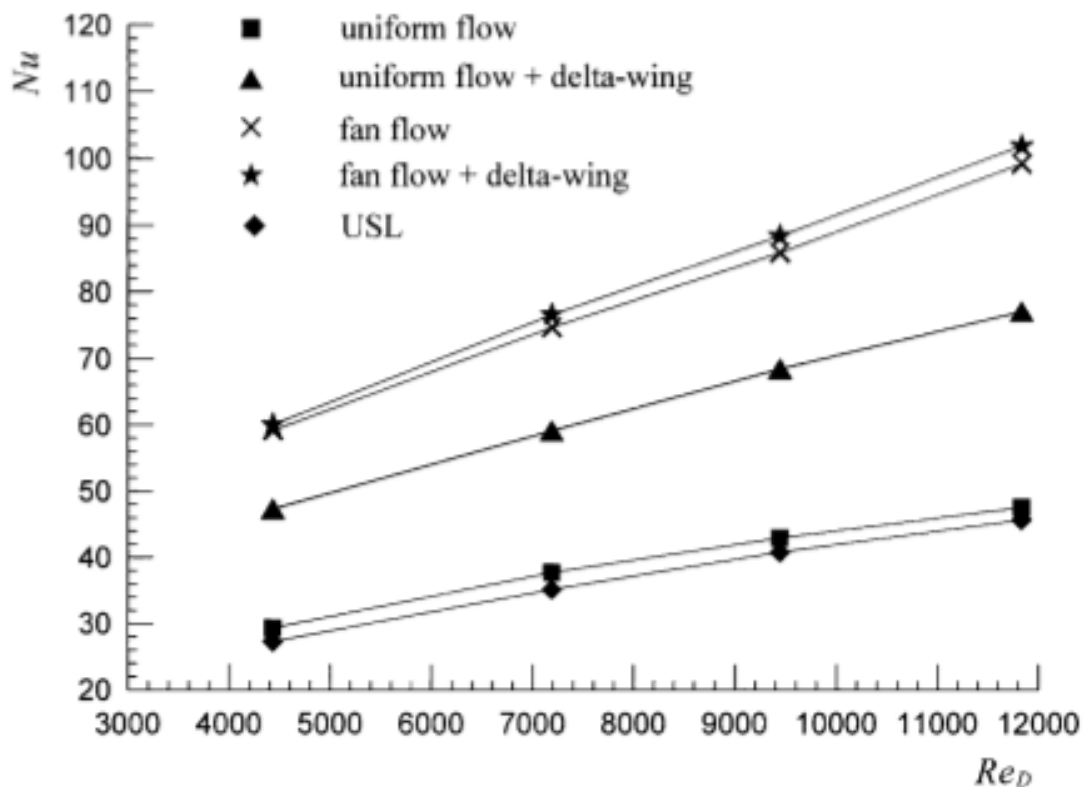
Figure 10: The Nusselt Numbers On The Heat Transfer Surface For The Investigated Flows VS. Reynold Number (T.Y. Chen 2003)

The strength of the rotational effect was measured in terms of axial vorticity. This is a measure of how much a flow rotates around the x-axis in this case. It was measured at different lengths inside the channel and normalized over the cross section and represented as seen in Figure 11. The vorticity falls along the duct. The vorticity is not measured for pure uniform flow. For the fan flow with and without the delta-wing the magnitude of the vorticity is almost identical.

13
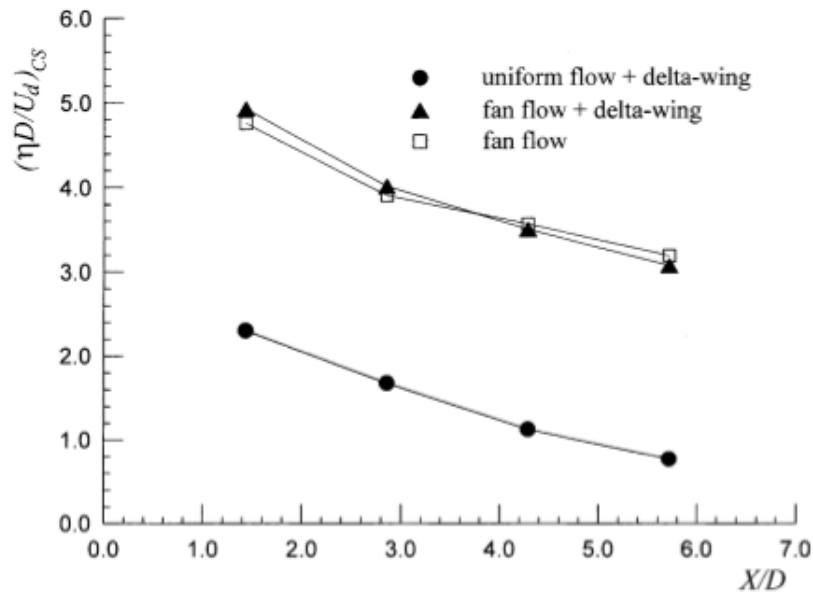
Figure 11: The cross-sectional normalized axial vorticity. Re= 11820, U_d= 2,67m/s (T.Y. Chen 2003)

Wachenfeldt analyzed the magnitude of the heat transfer coefficient in the intake duct at Grong primary school. The supply fan was believed to induce swirl and turbulence, and this would have an impact on the heat transfer conditions. Based on temperature measurements at the entrance and the exit section of the duct, he estimated the average air temperature. The surface temperature was estimated as mean of the surface temperatures in these two sections. The mass flow rate was predicted at the outlet, with outlet temperature as input.

He deduced values for the average heat transfer coefficients by setting up the first law of thermodynamics for the system and ignoring the effects of humidity transport and kinetic energy (Wachenfeldt 2003).

Equation 7: Average Heat Transfer Coefficient (Wachenfeldt 2003)

$$h = \frac{\dot{m}\, cp\left(T_{out} - T_{in}\right)}{\left(T_{surf} - T_{air}\right)A}$$
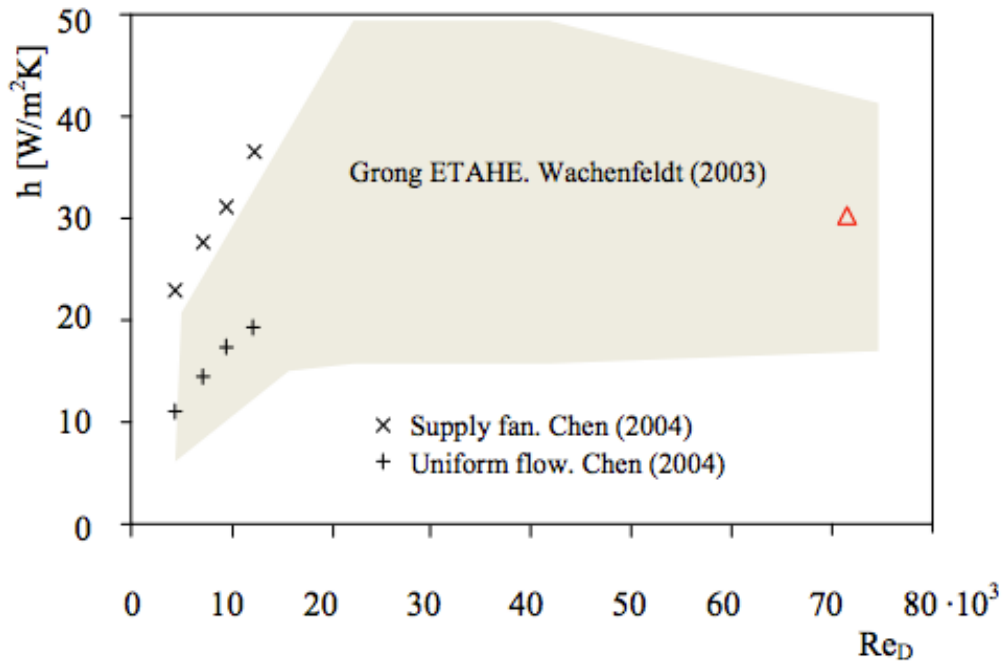
Figure 12: Overview Of Different Results For Heat Transfer Coefficient Between Airflow and duct wall (Per O. Tjelflaat 2011) for Wachenfeldt and Chen.

The model gave a huge variety for different measurements at different times, but the mean value of the average heat transfer coefficient seems to be around 30 W/m^2K as indicated in Figure 12. Most of his measurements were spread out within the gray area seen in the figure above.

A field experiment was conducted in 2005 in order to analyze the flow structures downstream of the supply fan situated at Grong. In this particular case the intake air was 22,8 °C and flow rate 1,39 m^3/s and Re= 52952. The velocity was measured along different spots along the height of the culvert at x/D_h= 2,6. The result can be seen in Figure 13. Here the highest speed is achieved in the area closest to the ceiling and the floor (Per O. Tjelflaat 2011). The high velocity close to walls was believed to enhance the heat transfer coefficient because the boundary layer will not be able to grow in this region.
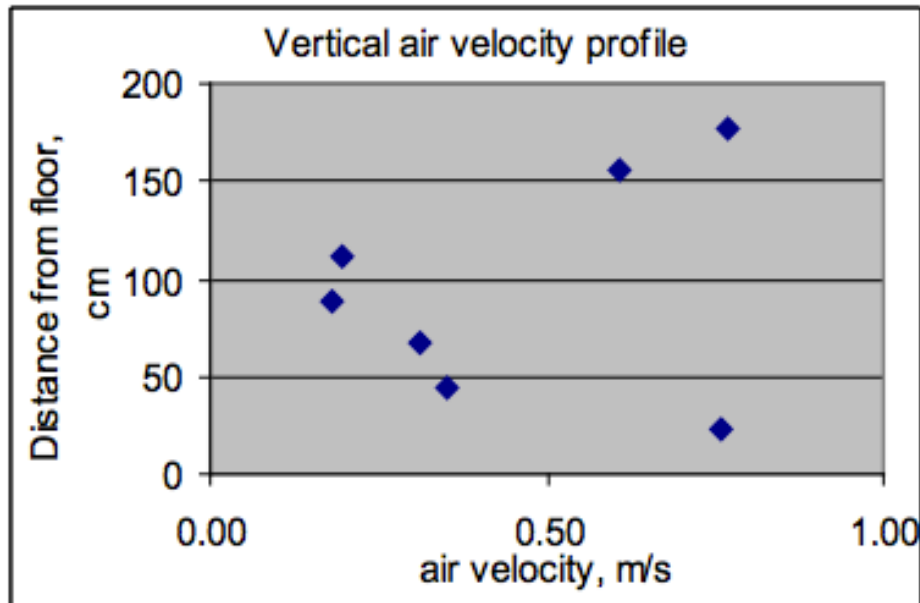
Figure 13: Velocity Profile With Supply Fan At Full Speed At x/D_h= 2,6 (Per O. Tjelflaat 2011)

For rectangular ducts with large cross section, the buoyancy force may play an important role (Zhang 2009). Buoyancy effects can cause the intensity of the heat convection on the walls to be highly non-uniform. Buoyancy forces are evident when there is a heat stratification accumulating at the floor or in the ceiling of the duct depending on the case. In a summer scenario with hot air and cold walls, the cold dense air will fall to floor and build up a thermal boundary layer there and thus inhibiting an efficient heat transfer to take place. Therefore a potential model should allow this effect.

3.2.1.3 Temperature Measurements Of A Hot Summer Week

In 2002, a measurement of the ambient and supply air temperature at Grong was recorded during a particular hot summer week in June that showed that the duct managed to cool the intake air by up to 8K during daytime (Figure 14). The supply fan was run constantly for these 5 days. The temperature difference during the nights is less with around 1-2K difference. The ground temperature was estimated to be around 7 °C. Also the airflow rate was estimated to 1,9 m³/s. (Per O. Tjelflaat 2011). The highest estimated cooling effect was measured to be 17kW on day 5.
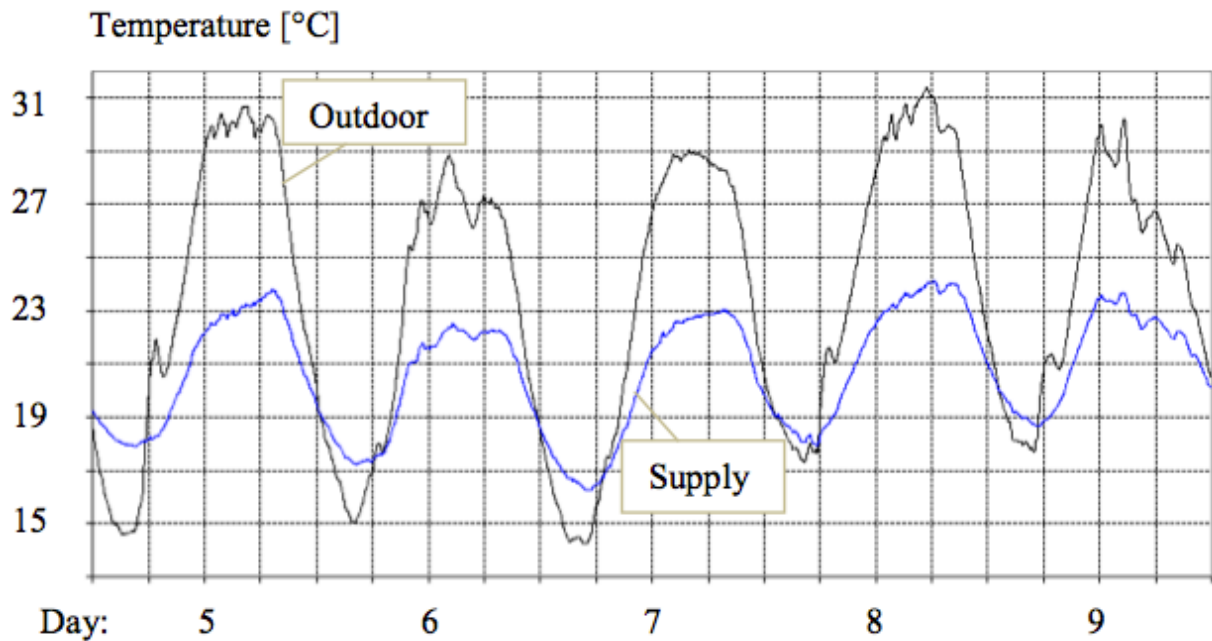
Figure 14: Measured Ambient (Outdoor) Temperature And Supply Temperature For A Hot Summer Week (Per O. Tjelflaat 2011)

3.2.2 Heat Transfer By Conduction

When a medium is subject to a temperature difference within itself, energy will flow from areas with high temperature to areas with low temperature. Heat flow within a medium is referred to as heat conduction. The rate at which the heat flows in a given direction, is given by Fourier's law. For a one-dimensional plane the heat transfer rate will be:

Equation 8: Conductive Heat Transfer Rate In X-Direction (Incropera and De Witt 1985)

$$q_{i,x} = -kA_i \left(\frac{dT}{dx} \right)$$

$$q''_{i,x} = \frac{q_{i,x}}{A_i} = -k \left(\frac{dT}{dx} \right)$$

$q_{i,x}$ = Heat transfer rate in x-direction [W]

$q''_{i,x}$ = Heat flux in x-direction per unit area [W/m²]

k = Thermal conductivity [W/mK]

$\dfrac{dT}{dx}$ = Temperature gradient in x-direction [K/m]
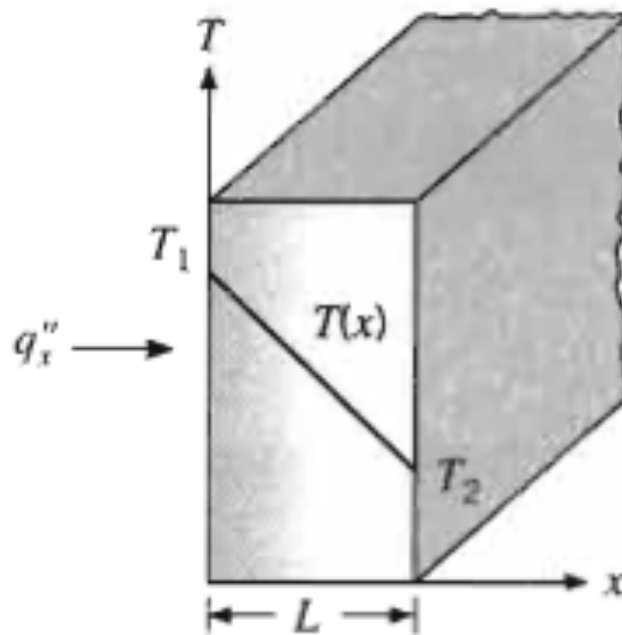
17

When trying to model heat conduction in the ground, a realistic approach would be to try to model a three-dimensional conduction model with appropriate boundary conditions. The disadvantage of such a model is that the solution would be very difficult (Zhang 2009).

Wachenfeldt arguments that due to high complexity, a one-dimensional approach is desirable. He points out that a highly detailed model would have to include a high number of different input data in order to make it realistic.

In his model he constructed a one-dimensional model, in which each surface of the culvert walls were connected to a boundary condition of undisturbed temperature after a certain length. From the walls to the undisturbed temperature, the construction included layers of concrete, gravel and clay. This is likely to be accurate within a certain depth into to the ground, since dominating direction of the heat transfer is perpendicular to the culvert wall. However deeper into the ground and close to edges, the direction of the heat flux can be far from perpendicular.

In a brief discussion he argues that the length between the wall surface and the undisturbed ground should be approximately one meter. In an example of a very high surface temperature, most of the surface flux will be directed outwards perpendicular, but deeper into the ground, more and more heat will be transported out of the one-dimensional domain. Setting the length to 10 meters would result in an underestimation of the heat flux at the boundary in the ground. It would also require a longer pre-simulation period due to big lag and storage effects, in order to obtain fully developed conditions.

And conversely, setting the length to short would induce to high temperature gradients with an overestimation of the heat flow and also cause an unrealistic prediction in the storage and lag effects (Wachenfeldt 2003).

Due to the ground's relatively high specific heat capacity and density, it will in transient conditions work as a thermal storage. When the ground is heated, it will take time for the earth to increase in temperature. This is due to the heat capacity and the density. It will oppose sudden changes.

If the air temperature on the culvert were to be much higher than the culvert surface, it would take time for this temperature rise and to propagate into the ground and be detectable there. This is referred to as lag effect of the ground.

In few words, the more ground and mass the model includes, the more apparent these effects will be.

4   CFD-modeling Of Air In A Square Duct

In order to investigate the heat transfer mechanism between intake air and the concrete surfaces inside a subterranean concrete duct, a simple model was made in Ansys Fluent. The real duct, from which a model has been made, is situated at Mediå School Grong in Nord-Trøndelag in Norway. Air enters through an intake tower and vertically down into a 12-meter long horizontal concrete duct. A supply fan is situated at the inlet of the horizontal section.

4.1   The program

ANSYS Fluent is a comprehensive simulation tool for CFD. It was chosen as a simulation tool in this thesis because of its capabilities to model flows, heat transfer and turbulence. It has an intuitive interface that seriously mitigates the obstacles of learning a new program fairly quickly, and yet still allowing the advanced user of making more intricate models.

4.2   CFD

Fluid flows and thermal fields can be described by three fundamental equations, namely the continuity, momentum and energy equation. The continuity equation takes care of mass conservation inside a control volume. The momentum equation describes a fluid motion, and is derived from Newton's second law. If heat transfer and temperature fields are to be evaluated, the energy equation must be solved. These equations can only be solved analytically in often very simplified cases where various assumptions have been made e.g. constant thermophysical properties of fluid or fluid flow in only certain directions. In order to avoid the difficulties of solving the partial differential, one can use algebraic approximations of the equations instead. The control volume is then divided into a finite number of discrete mesh points in which the approximations of these equations are solved (White 2006).

Equation 9: Continuity Equation (White 2006)

$$\frac{\partial \rho}{\partial t} + \frac{\partial}{\partial x_j}\left(\rho u_j\right) = 0$$

Equation 10: Momentum Equation (White 2006)

$$\rho \frac{Du_i}{Dt} = -\frac{\partial p}{\partial x_i} + \rho f_i + \frac{\partial \sigma'_{ij}}{\partial x_j}$$

Equation 11: Energy Equation (White 2006)

$$\rho \frac{D\mathrm{E}}{Dt} = \frac{\partial}{\partial x_j}\left(\sigma_{ij} u_i\right) + \rho u_i\, f_i - \frac{\partial \dot{q}_j}{\partial x_j}$$

$$p = \rho R T$$

ρ = Fluid density [kg/m³]
t = Time [s]
x = Length [m]
u = Fluid velocity [m/s]
p = Fluid pressure [Pa]
f = External force on system e.g. gravity [N]

$$\sigma'_{ij} = \mu\left(\frac{\partial u_i}{\partial x_j} + \frac{\partial u_j}{\partial x_i} - \frac{2}{3}\delta_{ij}\frac{\partial u_k}{\partial x_k}\right) = \text{Viscous stress tensor}$$

μ = Fluid viscosity [kg/ms]

$$E = e + \frac{1}{2}u^2 = \text{Specific total energy [J/kg]}$$

e = Specific internal energy [J/kg]

$\sigma_{ij} = -p\delta_{ij} + \sigma'_{ij} = \text{Total stress tensor [Pa]}$

$$\dot{q}_j = -K\frac{\partial T}{\partial x_j} = \text{Heat flux vector [W/m²]}$$

T = Temperature [K]
R = Gas Constant [J/kgK]

4.3   Model and meshing

Ansys includes a program called Designbuilder for making geometries. A simple rectangular geometry was created in the ZX –plane. Then a box was extruded from this rectangle with a depth of 12 meters. This box represents the airflow domain.

Meshes may have a various shapes. Here it was chosen to use prism cell shape mesh. An important thing to take into account in airflows along surfaces is the creation of boundary layers. Here the temperature and velocity gradients are bigger than in the rest of flow, hence the mesh must be denser in these regions. Therefore, the mesh was made from defining 5 number of inflation layers on the surfaces surrounding the inlet (i.e. the walls of culvert), and then sweep this mesh all the way through until the outlet. In the end a total of 25 160 nodes were created.

4.4   Coordinate System And Origin

In the model, the following system is used: The origin is situated in the lower left corner of the entrance. The width stretches in the x-direction and height in z-direction. The direction of the main flow will therefore be in y-direction.
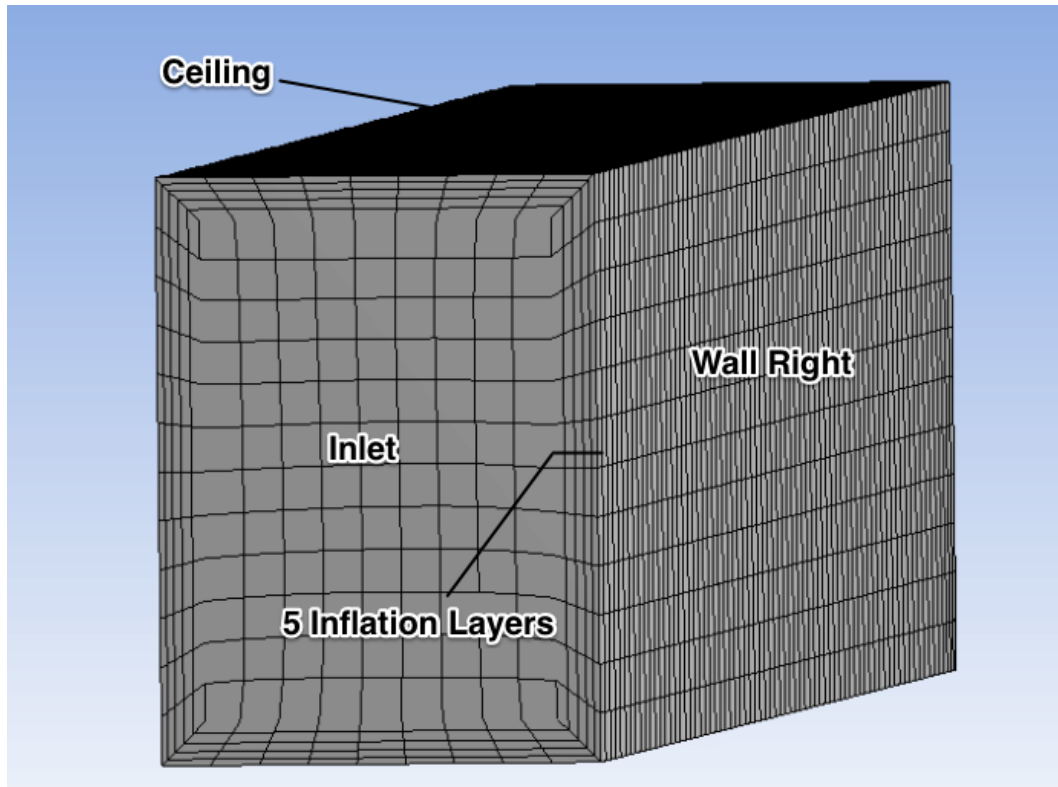
Figure 16: Generated Mesh For Airflow Domain

4.5   The choice of turbulence model

For the viscous model, the standard k-ε model was selected. This model contains several choices for near wall treatment. Fluent also has an option for «Enhanced Wall Treatment». This option was also activated. The k-ε model is valid in terms of thermal effects in fully turbulent regions away from any viscosity-dominated near walls (Ansys 2011). Ideally, one should apply two models in one, namely a model for the turbulent region (k-ε model) and an additional wall-function for the inner regions, such as the K-ω model (White 2006).

However, due to limitations in the candidate's knowledge of how to incorporate a two-turbulence model in Ansys Fluent, a model consisting solely of the k-ε was created.

4.6   Materials

Two materials were defined, air and heavy mix concrete. Due to relatively small variations in pressure in the duct, the air was modeled as being an incompressible ideal gas. This implies that the density will be a fuction of temperature, whereas the thermal conductivity and viscosity are considered constant. Since there were done winter simulations and summer simulation, air at 30 °C for summer and -10 °C were defined as shown in the following table.

	Density ρ	Specific heat cp	Conductivity k	Viscosity μ
Materials	[kg/m^3]	[J/kgK]	[W/mK]	[kg/ms]
Air (30 °C)	Ideal gas	1005	0,0264	1,380x10^{-5}
Air (-10°C)	Ideal gas	1005	0,0242	1,020x10^{-5}
Heavy mix* concrete	2100	653	1,40	-

*Taken from ESP-r standard library of material, since no other info was available.

In order to implement the effects of buoyancy with the ideal gas model, an acceleration of -9,81 m/s^2 downwards was imposed on the system to represent the gravitational field.

4.7 Boundary Conditions

The model created had six boundaries consisting of surfaces that are all subject to various boundary conditions. Four of these are walls defined in a similar manner. They are defined as stationary walls with no slip. No slip means that fluid close to the wall is not moving relatively to the wall surface.

Table 2: Boundary Conditions At The Wall Surfaces

Surface name	Ceiling	Floor	Wall left	Wall right
Material	Heavy mix concrete	Heavy mix concrete	Heavy mix concrete	Heavy mix concrete
Thickness [mm]	100	100	150	150
Thermal condition winter [°C]*	0	0	0	0
Thermal condition summer [°C]*	11	11	11	11

*The temperatures were based on the ground temperature profile of Grong at 2 meters depth in January and July.

The two remaining surfaces were inlet and outlet. The inlet has a constant mass flow rate 2,68 and 1,50 kg/s for summer and winter conditions respectively. Two different velocity profiles were tested: a uniform inflow and a rotational inflow. The rotational inflow was supposed to represent the velocity field created downstream of the axial supply fan.

The turbulence parameters were set to 10% turbulent intensity and a hydraulic diameter of 1,714 meters with 0 Pa gauge pressure at inlet and outlet.

4.8   Residuals And Convergence Criteria

Residuals are a measure of convergence in a simulation. A residual of an equation is the difference between two subsequent iterations. With every iteration the residuals will become smaller and smaller, until they reach the criteria defined by the user, if the solution converges.

The convergence criteria for the energy was set to 10^{-6}, while the rest were set to be 10^{-4}, except in the uniform winter calculations in which the continuity and epsilon equations had convergence criteria of 10^{-3}.

4.9   Solving Technique

For all the simulations, the SIMPLE algorithm is applied. Second-order upwind scheme was chosen for the discretization of the governing equations.

Initially the winter simulation was supposed to have a mass flow rate of 1,29 kg/s. Under this condition the solution didn't converge. However by increasing the mas flow rate to 1,50 kg/s and loosening the convergence criteria a bit, the solution finally converged.

5 Analysis Of The Heat Transfer In The Intake Duct

Different scenarios of flows were simulated in order to check its impact on the heat transfer coefficient. Firstly uniform flow in winter and summer condition are tested. Then the same scenarios are repeated with moderate rotation. In the end the summer scenario is repeated with a very strong rotation.

5.1 Calculation Of the Heat Transfer Coefficient

The heat transfer coefficient was found by area averaging of the local heat transfer coefficient found for each surface inside the culvert. The local heat flux is found in the flux report after each simulation. The surface temperature is evaluated as an area average for every surface. An average air temperature in the culvert is estimated as the average of the inlet and outlet air temperatures.

Equation 13: Estimated Air Temperature

$$T_{air} = \frac{(T_{inlet} + T_{outlet})}{2}$$

Equation 14: Local Heat Flux

$$\dot{Q}_i = A_i h_i \left(T_{air} - T_{surf} \right)$$

$\dot{Q}_i$ = Heat flux through surface i [W]
h_i = Local heat transfer coefficient for a surface i [W/m²K]
A_i = Area of surface i [m²]

Equation 15: Local Heat Transfer Coefficient

$$h_i = \frac{\dot{Q}_i}{A_i \left(T_{air} - T_{surf} \right)}$$

Equation 16: Average Heat Transfer Coefficient

$$h = \frac{1}{A_{tot}} \sum_{i=1}^{n} h_i A_i$$

h = Heat transfer coefficient of culvert [W/m²K]

5.2 Uniform Inlet Flow

An inlet flow is uniform if the entering velocity has one velocity magnitude and direction when entering the control volume. In this case the inlet flow was

always directed perpendicular on the inlet surface. As explained in section 3.2.1.1, the velocity at the walls will slow down and thermal and velocity boundary layers will build up further into the culvert.

5.2.1 Summer

In the summer case, the walls are colder than the incoming air, leading cold and dense air to accumulate on the culvert floor. The incoming air is 30 °C while the outer concrete walls are subject to a constant temperature of 11 °C. In the model the flow is directed in the y-direction. The mass flow rate is constantly kept at 2,68 kg/s (2,3 m³/s) during the summer.

As seen in the temperature plots, the thermal layer grows mostly on the floor, since cold air is denser.
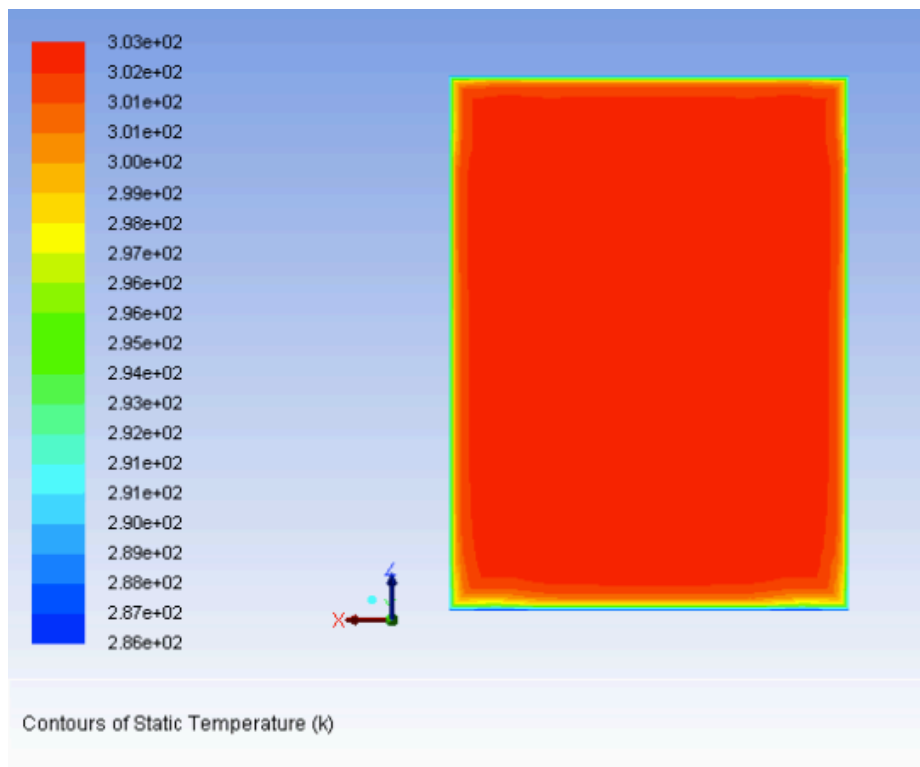
Figure 17: Static Temperature At Y= 3m
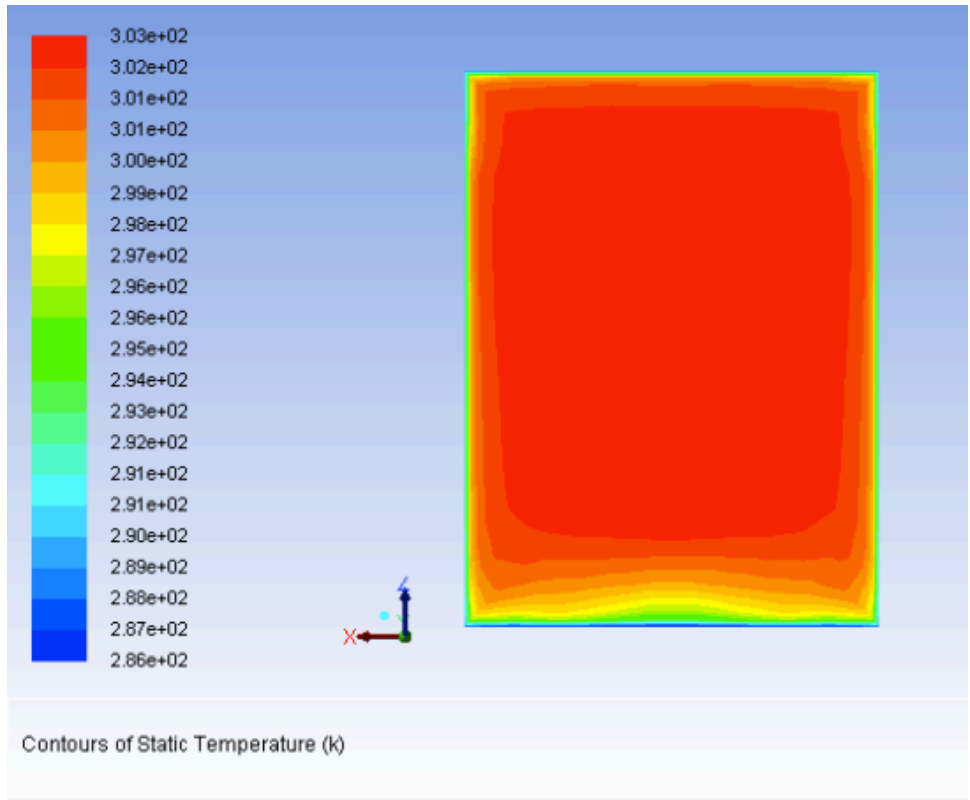
Figure 18: Static Temperature At Y= 6m
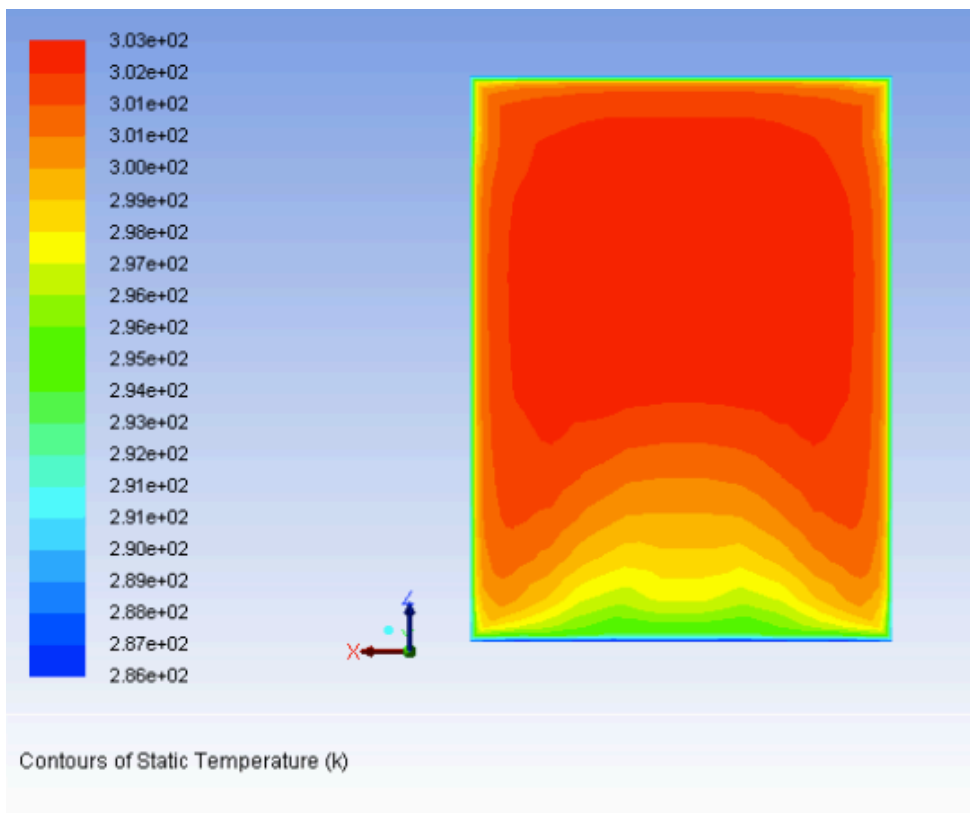
Figure 19: Static Temperature At Y= 11m

From the density plots (seen in appendix part B) a clear relation to the static temperature is seen. In the temperature plots the red color indicate high temperature and in the density plots red indicate high density. Since these two qualities are inverse of one another, the plots look very similar, only inverse.

In Figure 20, the velocity profile development can be seen, as the flow is moving throughout the duct. The z-coordinate indicates the height above the culvert floor (z=0). z= 2m is at the culvert ceiling. At y=2, the flow is still strongly uniform (the same velocity magnitude over the cross-section), but small effects of velocity retardation can be seen in the near wall section, especially at the
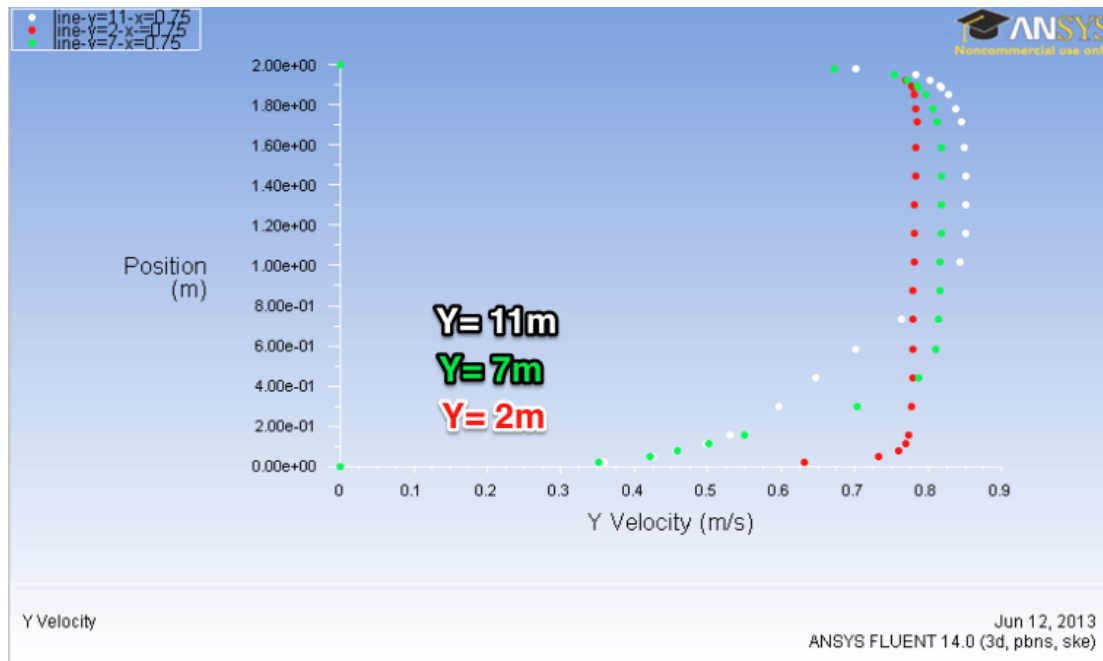
Figure 20: Velocity In Y-direction From Z= 0 To Z= 2m At X= 0,75m (midplane)

floor. Around the half way through the duct (y= 7m) these effects ever more striking. However the boundary layer at the floor is substantially larger. Close to the outlet at y= 11m, this velocity boundary layer is dominating and reaches to middle of the duct. The boundary layer in the ceiling is considerably smaller, only approximately 20cm.
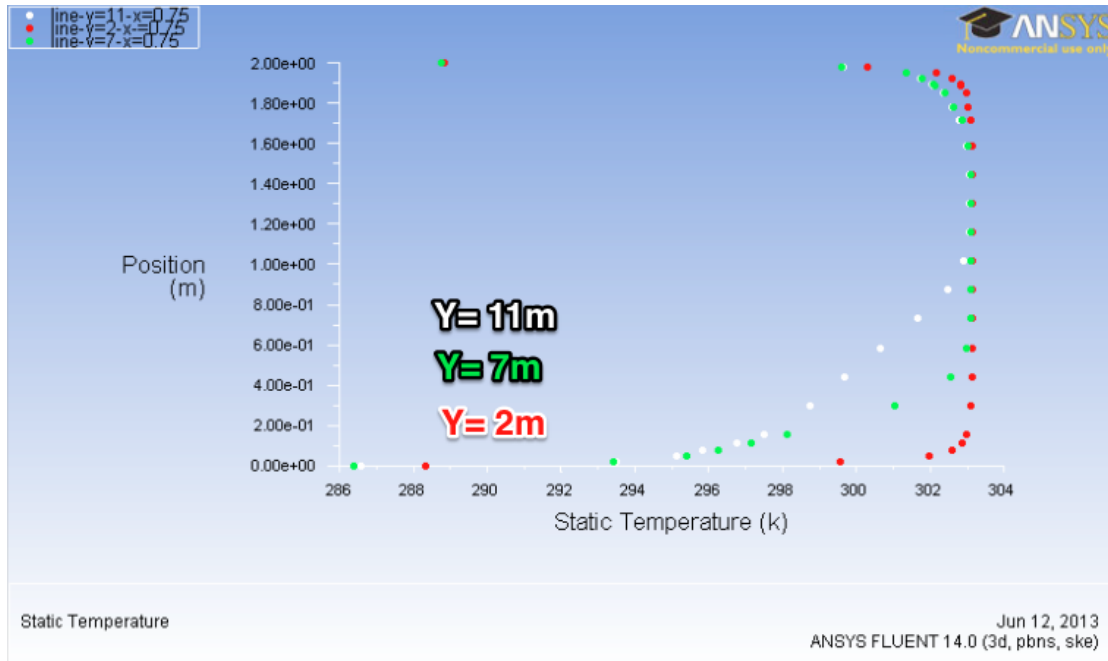
Figure 21: Static Temperature Profile From Z= 0 To Z= 2m At X= 0,75m (midplane)

Figure 21 illustrates the temperature profile of the flow in the same region as the velocity profile. A great similarity is seen between these to plots. It shows again how the cold dense air accumulates on the floor and how the boundary layer is struggling to build up in the ceiling.

5.2.2   Winter

In the winter case, the incoming air is -10 °C while the outer concrete walls are subject to a constant temperature of 0 °C. Now the cold air will be heated by the relatively warmer walls and buoyancy will lead warmer air to rise towards the ceiling. There the biggest boundary layer of warmer air will accumulate. This is shown in the temperature plots. The mass flow rate is constantly kept at 1,5 kg/s (2,3 m³/s) during the winter.

The density plots are can be seen appendix part B. Once again the temperature plots are inverse of the density plots.
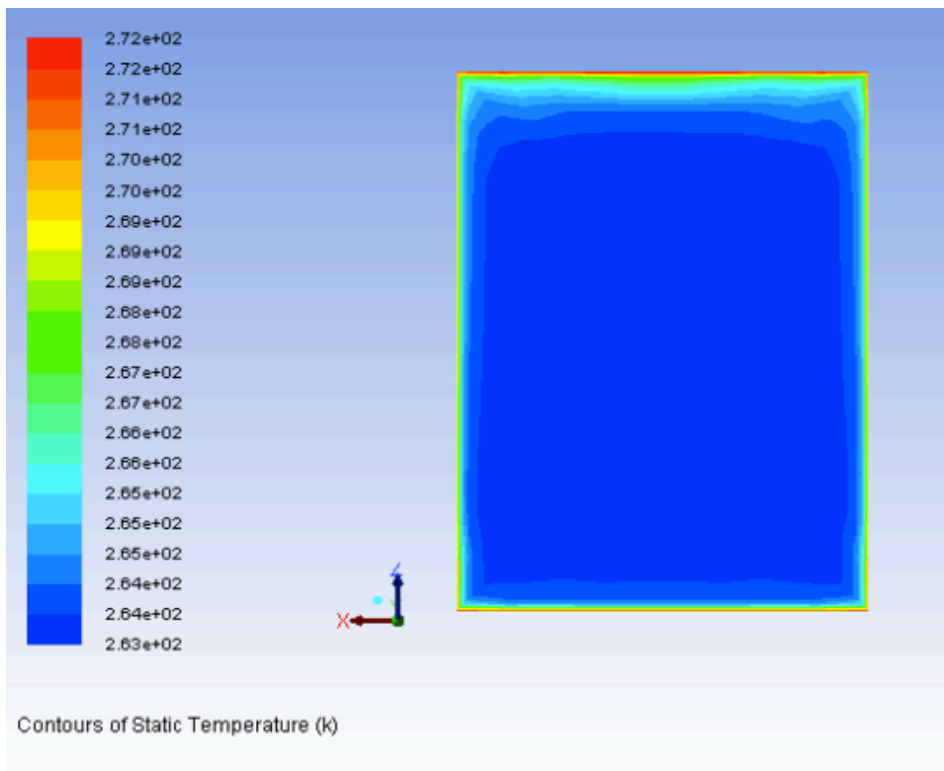
Figure 22: Static Temperature At Y= 3m
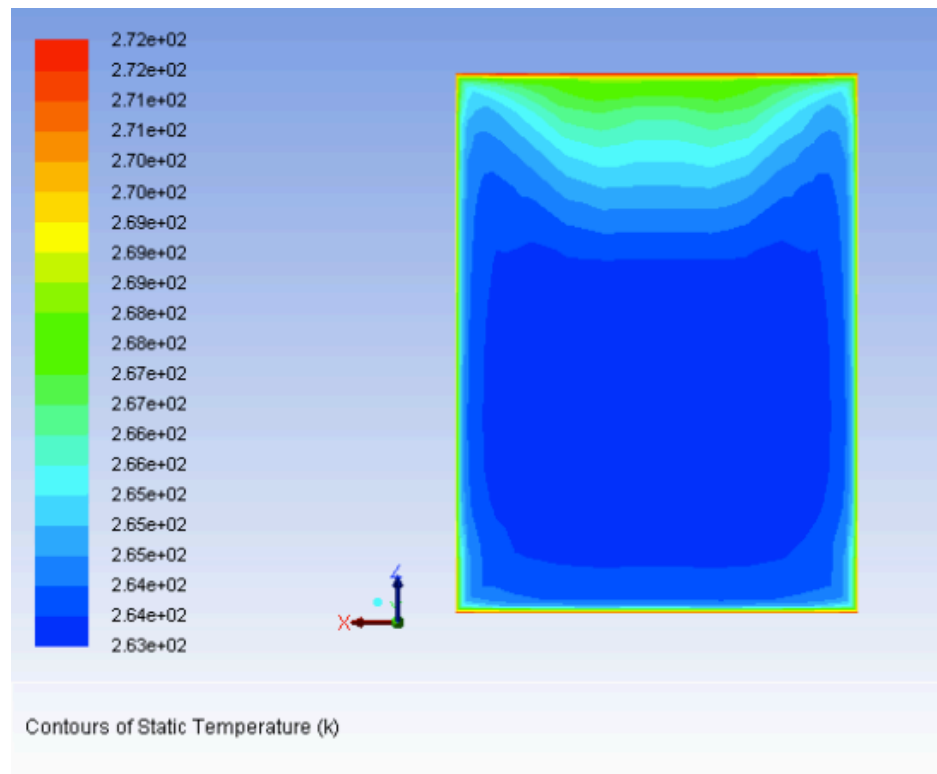
Figure 23: Static Temperature At Y= 6m
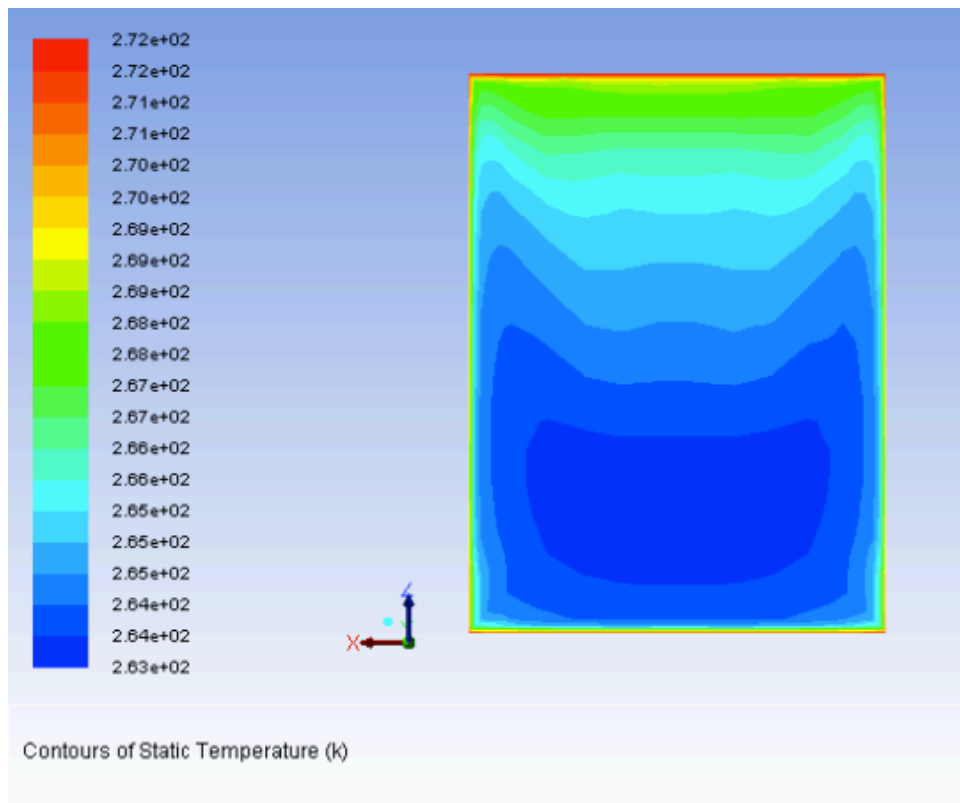
Figure 24: Static Temperature At Y= 11m

As for the uniform summer flow, the flow is very uniform in the areas close to the inlet, and at velocity boundary layer starts to grow in the ceiling. Towards the outlet at y= 11m, the velocity boundary layer dominates the most of the flow region. These boundary layers have grown more for the winter case, due to a lower mass flow rate; hence the buoyancy forces compared to momentum forces are bigger in the winter case. By inspecting the following velocity field and temperature plots these effects can easily be seen.
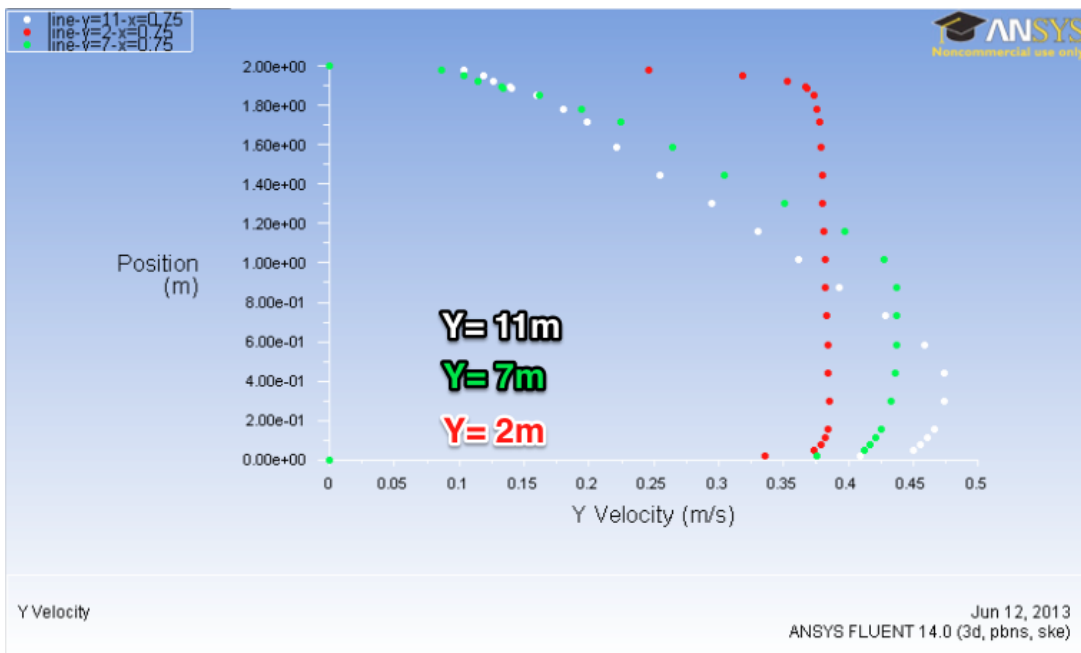
Figure 25: Velocity In Y-direction From Z= 0 To Z= 2m At X= 0,75m (midplane)
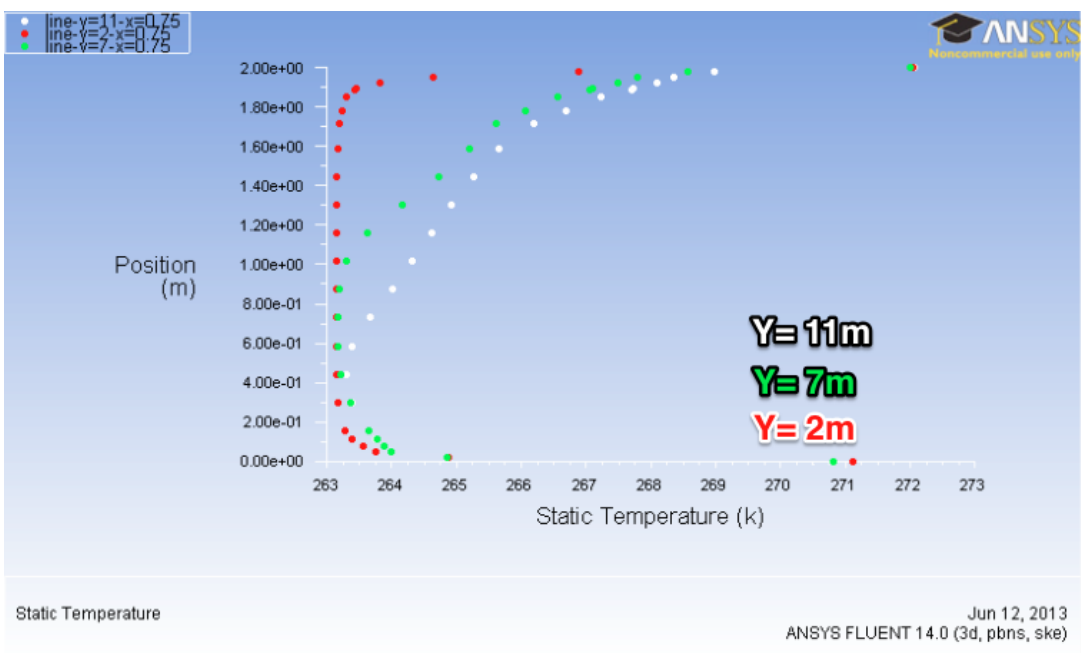
Figure 26: Static Temperature Profile From Z= 0 To Z= 2m At X= 0,75m (midplane)

32

5.2.3   Results Of Heat Transfer Calculation

The most important results of the uniform cases are summed up in Table 3.
For the entire tables of calculation, see Table 13 and Table 14 in appendix.

Two things are observed from these results. The first thing is that the heat
transfer coefficient for the ceiling and floor are very different in these two cases.
In the summer case the coefficient for the ceiling is 72% larger than for the floor.
Conversely in the winter, there the floor coefficient is 108% larger. This result is
a direct consequence of how the creation of boundary layers inhibits heat
transfer between the air and wall surfaces.

Another observation is that the heat transfer coefficients on either side of the
duct are equal, as expected in a uniform case.

Lastly, the overall heat transfer for the duct is seen to be lower for the winter
case. This is due to bigger momentum forces in the summer case as a result of a
bigger mass flow rate. An extra winter simulation with the same mass flow rate
as in the summer was run, and the heat transfer coefficient was increased to 4,20
W/m²K i.e. approximately the same as the summer case; for details see Table 15
in appendix.

Table 3: Heat Transfer Coefficients For Summer And Winter

	Units	**Summer**	**Winter**
$T_{out} - T_{in}$	K	-1,72	1,38
$\dot{m}$	kg/s	2,68	1,50
h_c	W/m²K	4,97	2,14
h_f	W/m²K	2,88	4,43
h_l	W/m²K	4,57	3,83
h_r	W/m²K	4,57	3,83
h	W/m²K	4,29	3,59

$T_{out} - T_{in}$ = Temperature increase [K]

$\dot{m}$ = Mass flow rate [kg/s]

h_c = Heat transfer coefficient ceiling [W/m²K]

h_f = Heat transfer coefficient floor [W/m²K]

h_l = Heat transfer coefficient wall left [W/m²K]

h_r = Heat transfer coefficient wall right [W/m²K]

h = Heat transfer coefficient duct [W/m²K]

5.3 Rotational Inlet Flow

At the entrance of the duct there is an axial supply fan. The flow past this fan is subject to the movements of the rotating blades giving the air immediately after the fan a rotation. The flow field downstream is believed to be somewhat similar to the one shown in Figure 9.

5.3.1 Inlet Flow Conditions

In order to simulate the rotational flow field past the supply fan, a cylindrical coordinate system was defined. Its axis origin is situated in the middle of the inlet cross-section and with axis direction in y-direction (the same as the flow direction).

Then a mass flow rate was specified with an axial and tangential component. When the tangential component is zero, the flow is uniform. For a larger tangential component the rotation becomes stronger.

5.3.1.1 *Axial Vorticity, A Measure Of Rotation Magnitude*

Vorticity is defined with respect to the axis it revolves around; in this case the y-axis. For this flow the cylindrical velocity components are v_r, v_θ and v_y, radial velocity, tangential velocity and axial velocity. The vorticity component of most interest is the one that tells us about rotation around the y-axis (η_y).

Equation 17: Axial Vorticity In Cylindrical Coordinates (White 2006)

$$\eta_y = \frac{1}{r}\frac{\partial}{\partial r}\left(r\, v_\theta\right) - \frac{1}{r}\frac{\partial v_r}{\partial \theta}$$

With $v_r = 0$ and $v_\theta = \text{constant}$ at the inlet, the vorticity component is then reduced to

Equation 18: Axial Vorticity At Inlet

$$\eta_y = \frac{r}{r}\frac{\partial}{\partial r}\left(v_\theta\right) + \frac{v_\theta}{r}\frac{\partial}{\partial r}\left(r\right) = \frac{v_\theta}{r} \ .$$

It can be seen how the tangential velocity is constant on the inlet surface with decreasing values close to the near wall regions. And from Equation 18 it is possible to see that the vorticity will be big for small radius and decrease with a growing radius. The two following plots confirm this.

Contours of Tangential Velocity (m/s)
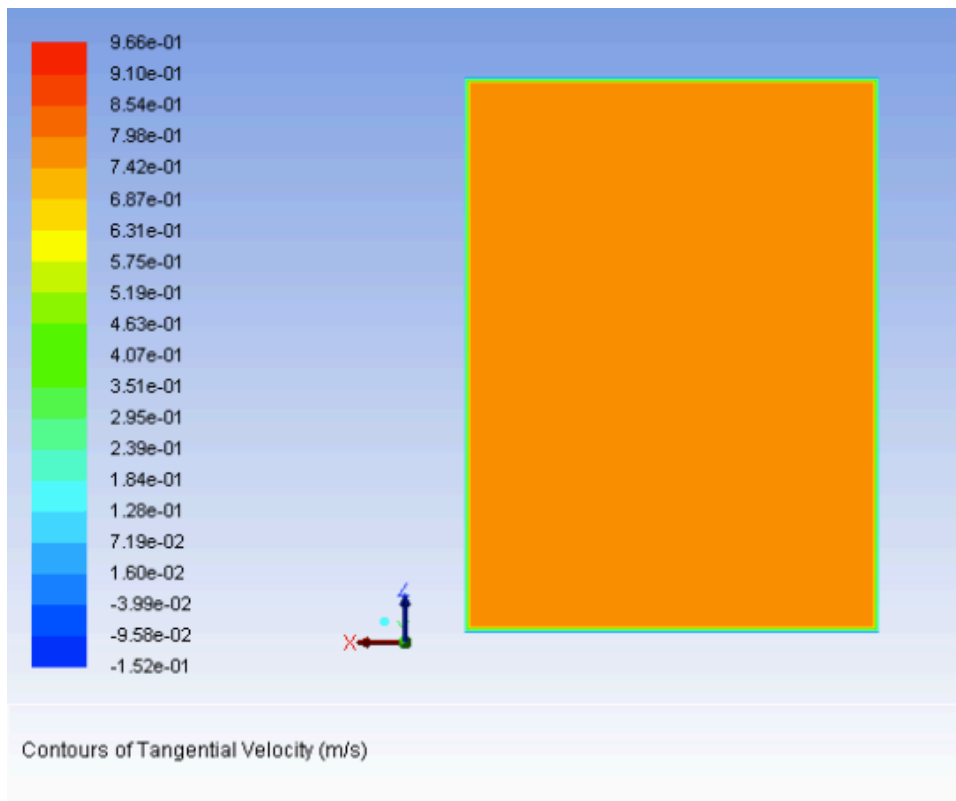
Figure 27: Tangential Component At Inlet (Tangential component= 33%)

Contours of Y-Vorticity (1/s)
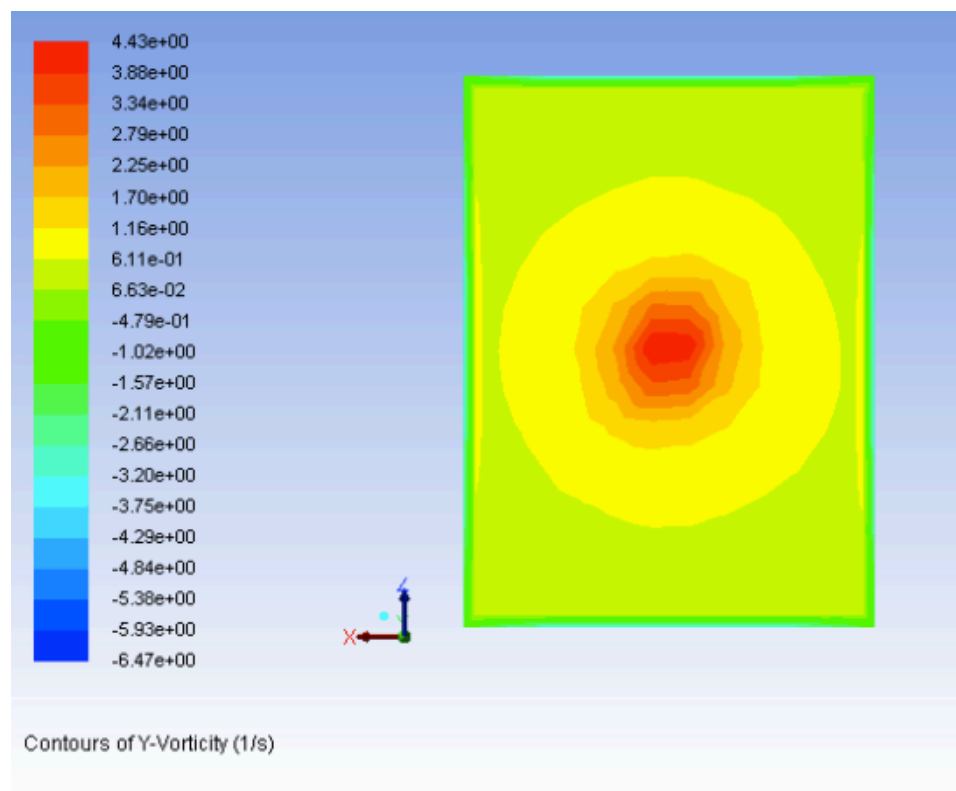
Figure 28: Axial Vorticity At Inlet (Tangential component= 33%)

5.3.2 Flow With Moderate Rotation

Since the magnitude of the tangential component was unknown for the real case, it was first tried to increase it step by step for the summer case. The two following plots show the difference in how the flow enters the inlet. The rotational case share similarities with the velocity field shown in Figure 9.

Velocity Vectors Colored By Static Temperature (k)
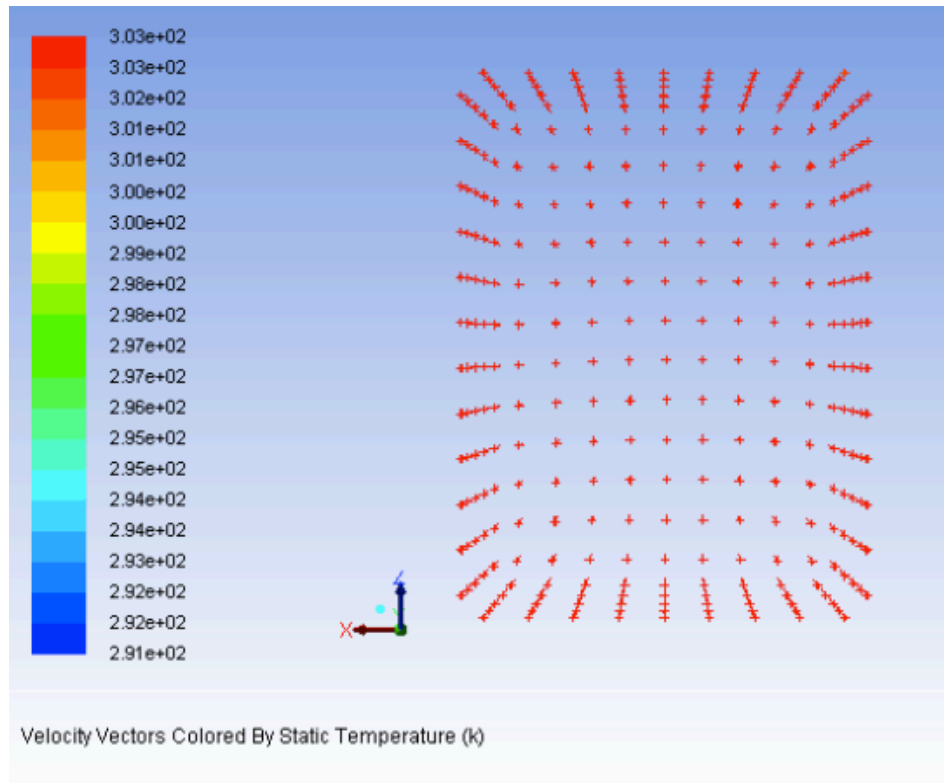
Figure 29: Uniform Flow At Inlet (Colors Indicate Static Temperature)

Velocity Vectors Colored By Static Temperature (k)
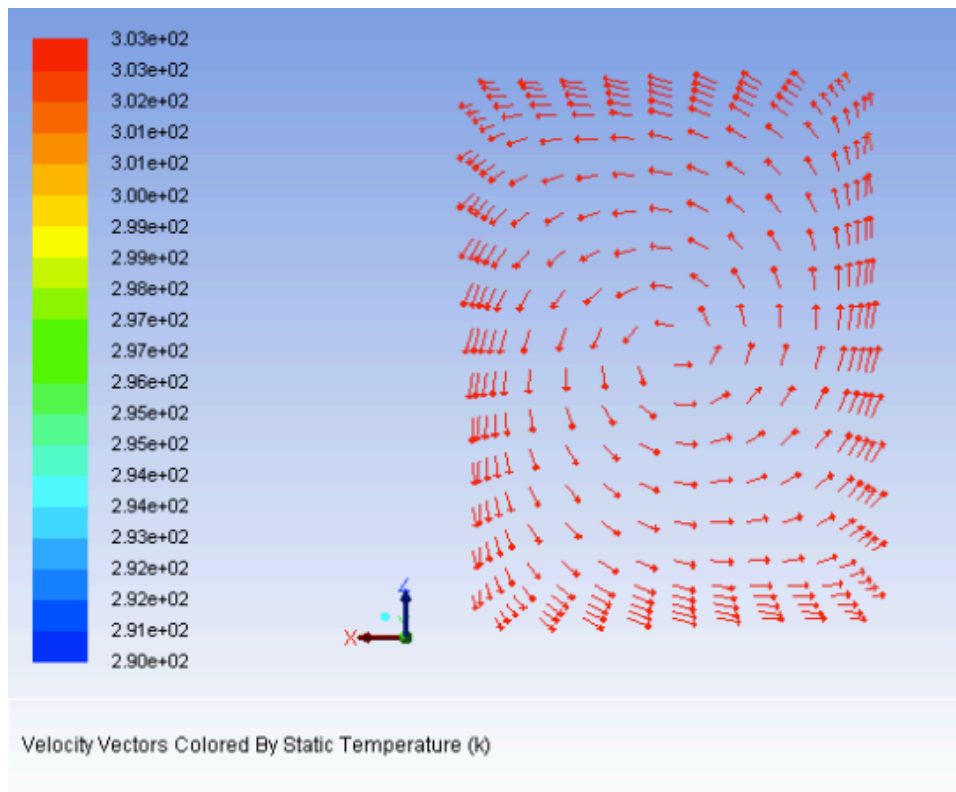
Figure 30: Rotational Inlet Flow, Tangential Component 33% (Colors Indicate Static Temperature) *

* The flow is clockwise, since the y-direction is up from paper.

5.3.2.1 Summer

In order to analyze the rotation's impact on the flow, a similar investigation was performed again for the summer rotational case. All boundary conditions are kept the same (surface temperature, mass flow rate, inlet air temperature) except for the tangential velocity component of the inlet flow, which is set to 33%.

The density plots are again very similar to the temperature plots (areas with high temperature has low density etc.), and are therefore omitted.

All the plots are shown with the y-direction, and therefore the flow direction up from paper, making the left wall appear on the right side, and vice versa.
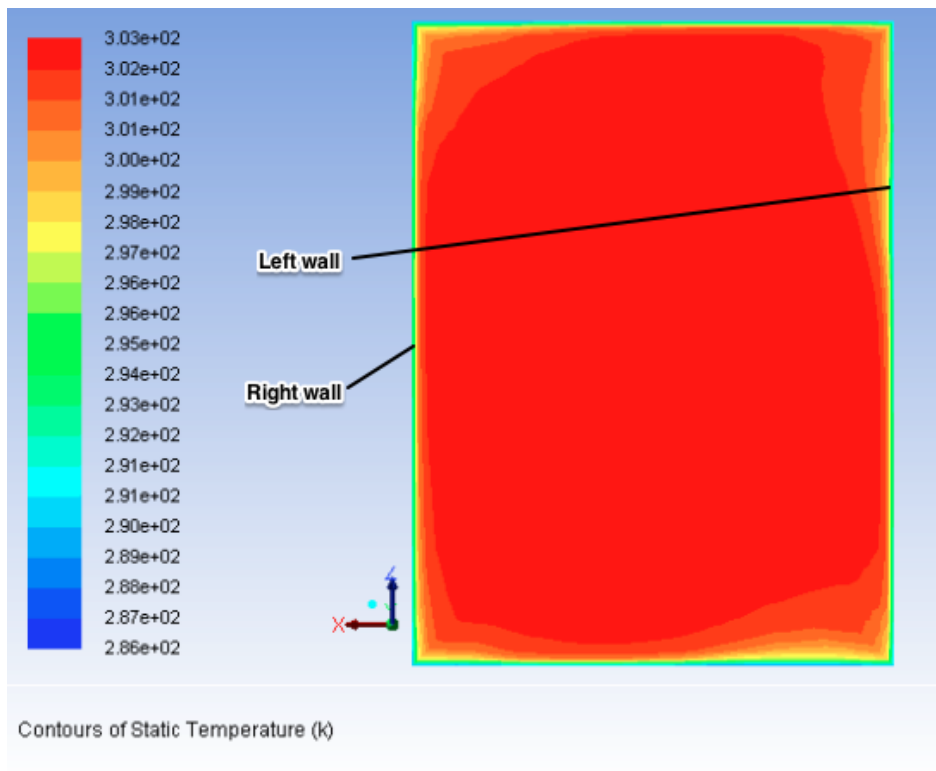
Figure 31: Static Temperature At Y= 3m
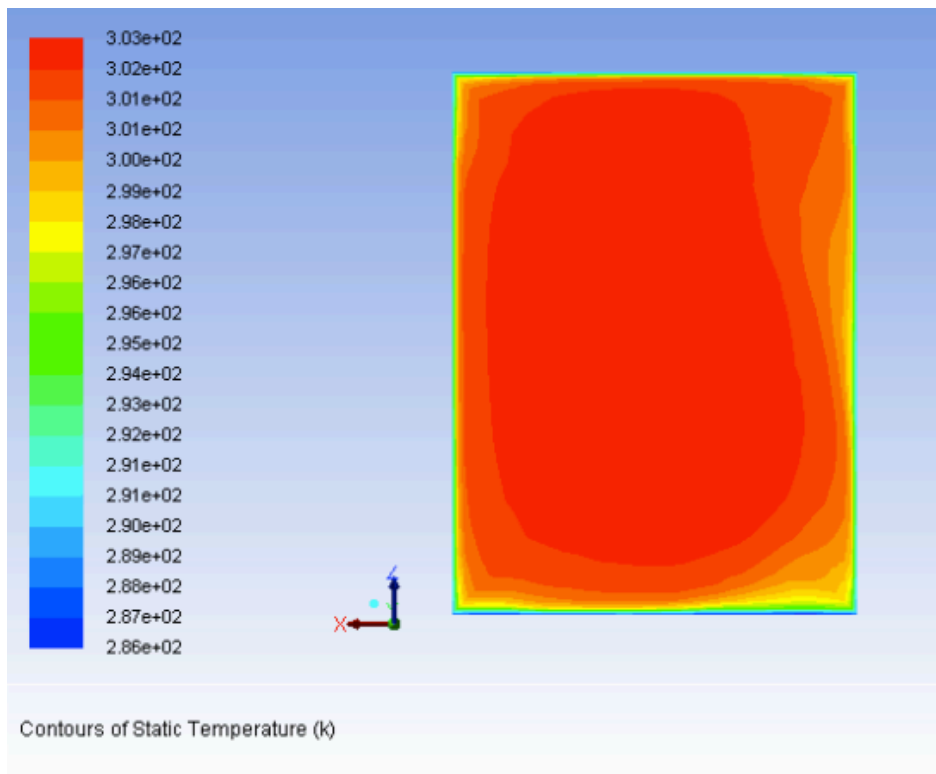

Figure 32: Static Temperature At Y= 6m
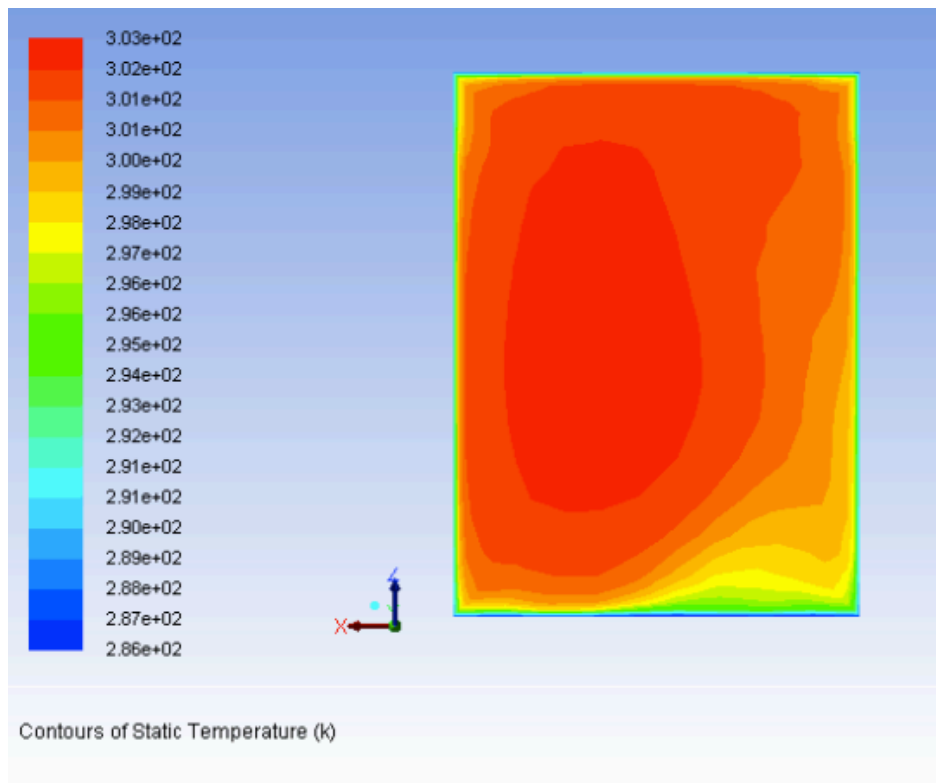
Figure 33: Static Temperature At Y= 11m

In the summer, cold air close to the culvert surfaces will fall to the floor due to higher density. Since the rotation of flow is clockwise, the flow will move upwards along the left wall and downward along the right wall. This is shown in the figure of the rotational flow at the inlet. As a result of that the falling air will contribute positively to an increase of the velocity on the right wall and negatively on the left wall.

In the region close to the entrance, the flow is mostly rotational. Closer to towards the outlet at y= 11m, a separation of the flow moving upwards is seen on the left wall. This is due to that the rotational effect wears off as the flow moves through the duct. At a certain point the buoyancy forces makes the cold air fall close to wall. A boundary layer is created along the left wall and on the floor, which again inhibits heat transfer in these areas relative to the other surfaces.

Velocity Vectors Colored By Static Temperature (k)
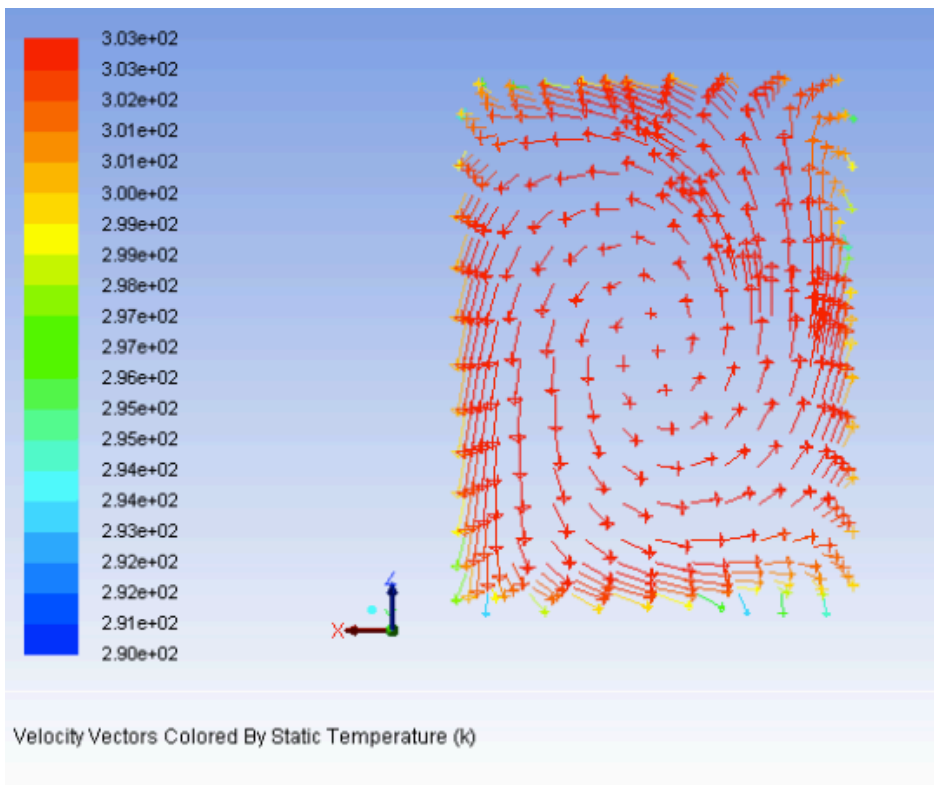
Figure 34: Velocity At Y= 3m. (Colors Indicate Static Temperature)

Velocity Vectors Colored By Static Temperature (k)
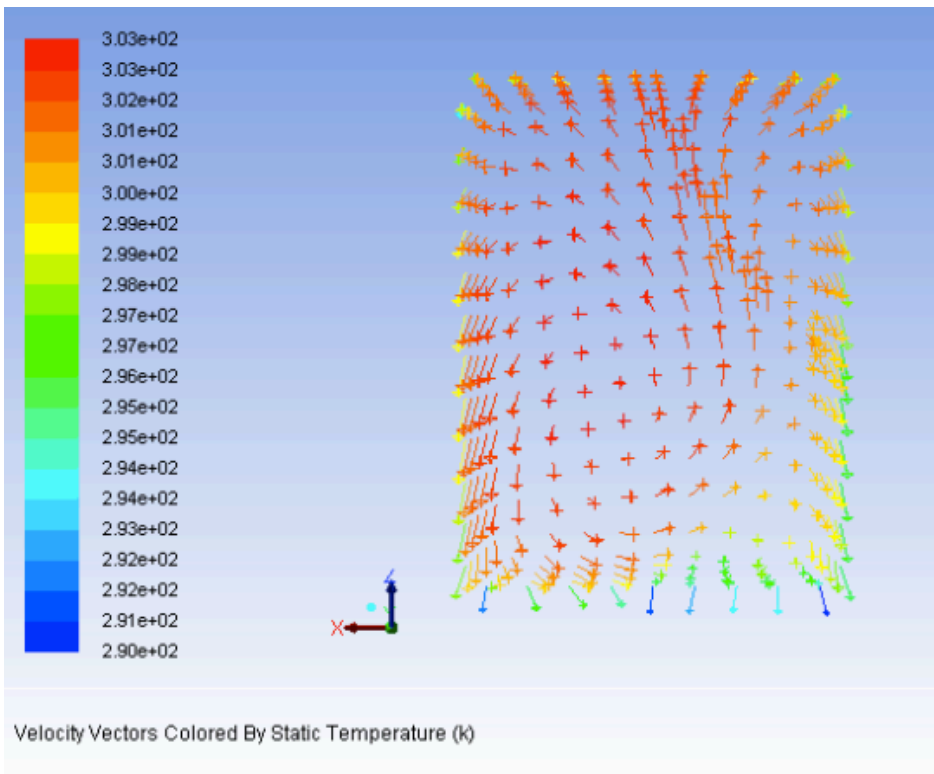
Figure 35: Velocity At Y= 11m. (Colors Indicate Static Temperature)

40
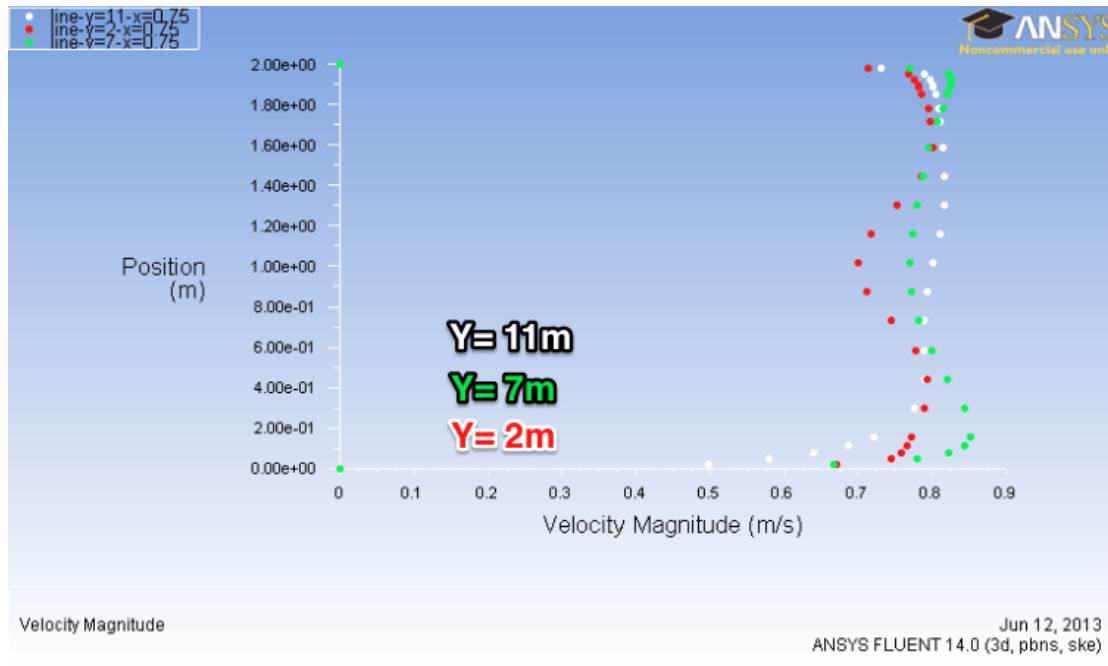
Figure 36: Velocity Magnitude From Z= 0 To Z= 2m At X= 0,75m (midplane)

What is interesting to notice here is that the velocities are higher towards the near wall regions at y= 2m, giving it a wave shape. This is the same tendency, which is seen in the profile measured at Grong according to Figure 13. The velocity transition from high to low is gentler here than in the measured results. Further into the duct, a velocity boundary builds up, but it is considerably smaller than for the uniform case. Towards the end, the wave shape is no longer noticeable.
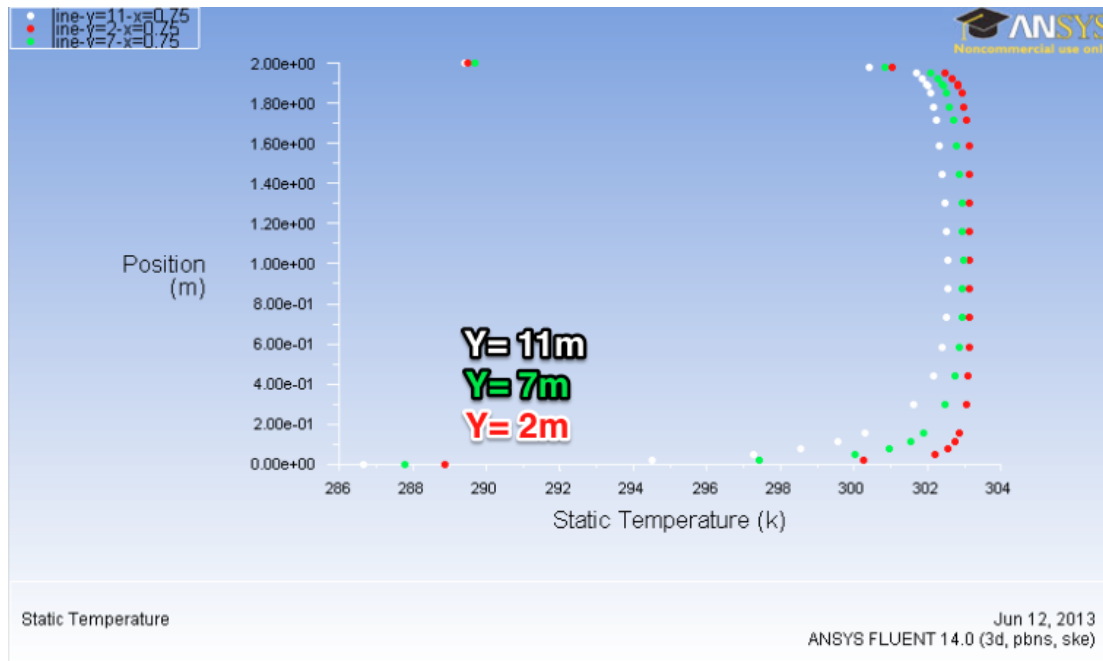
Figure 37: Static Temperature Profile From Z= 0 To Z= 2m At X= 0,75m (midplane)

The same wave shape is not seen for the temperature plot. The temperature boundary layers are considerably smaller for the rotational case compared to the uniform case. This means that there is a better temperature mixing in the flow, making it difficult for temperature stratification to be seen.

5.3.2.2 Winter

Again, same boundary conditions as for the winter case, only with the change of the tangential component, which was also set to 33%.

Due to big similarity with the summer case, only the temperature plot close to the outlet is given here.

In the winter case, warm air will rise along the sides of he duct. Now the air will contribute positively on the left where the air and the rotation of the flow move upwards, and on the right wall they will collide and create a separation of the rotational flow from the duct wall surface.
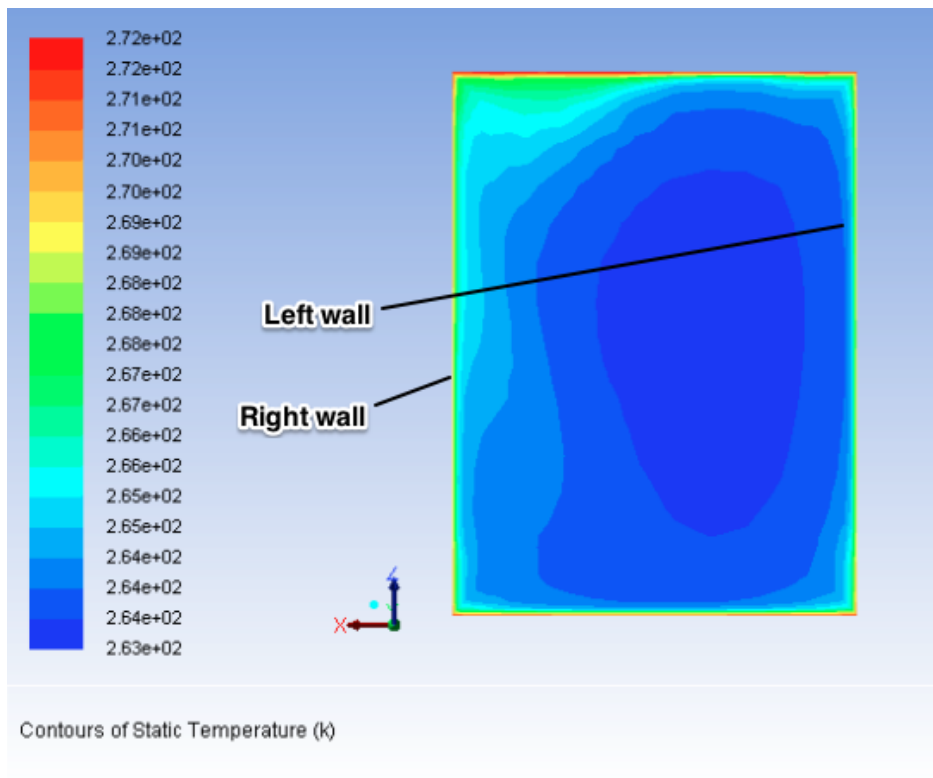
Figure 38: Static Temperature At Y= 11m
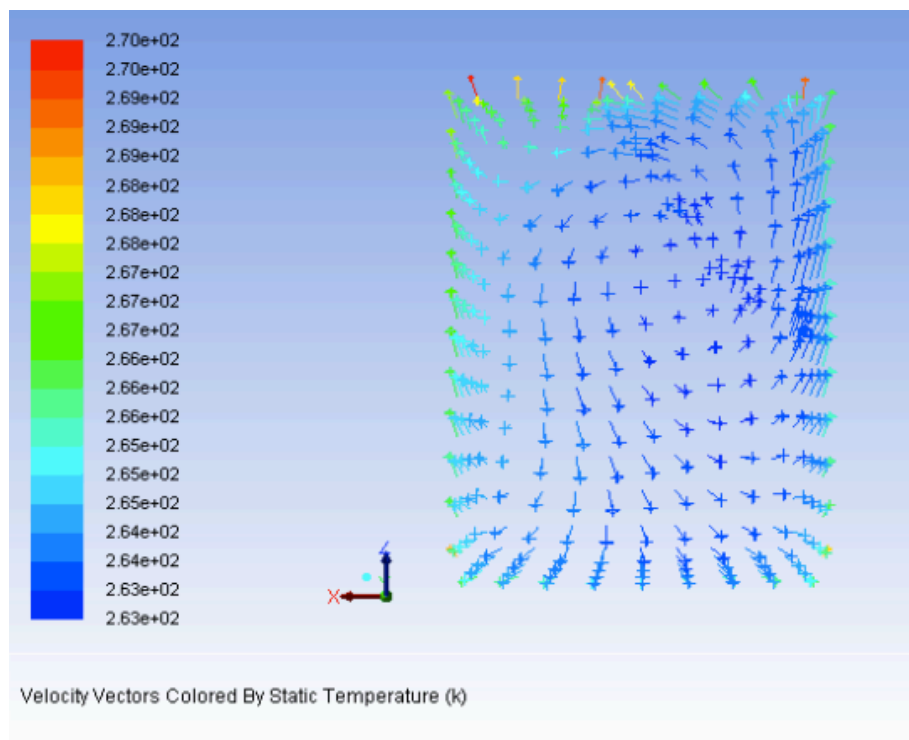
**Figure 39: Velocity At Y= 11m. (Colors Indicate Static Temperature)**
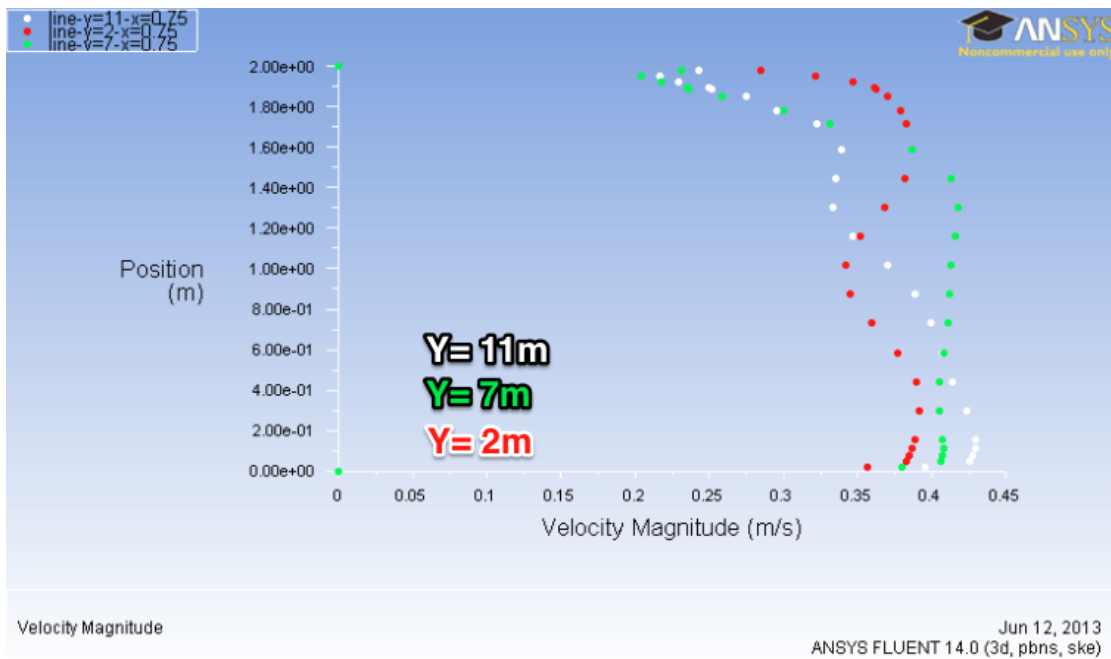
Figure 40: Velocity Magnitude From Z= 0 To Z= 2m At X= 0,75m (midplane)
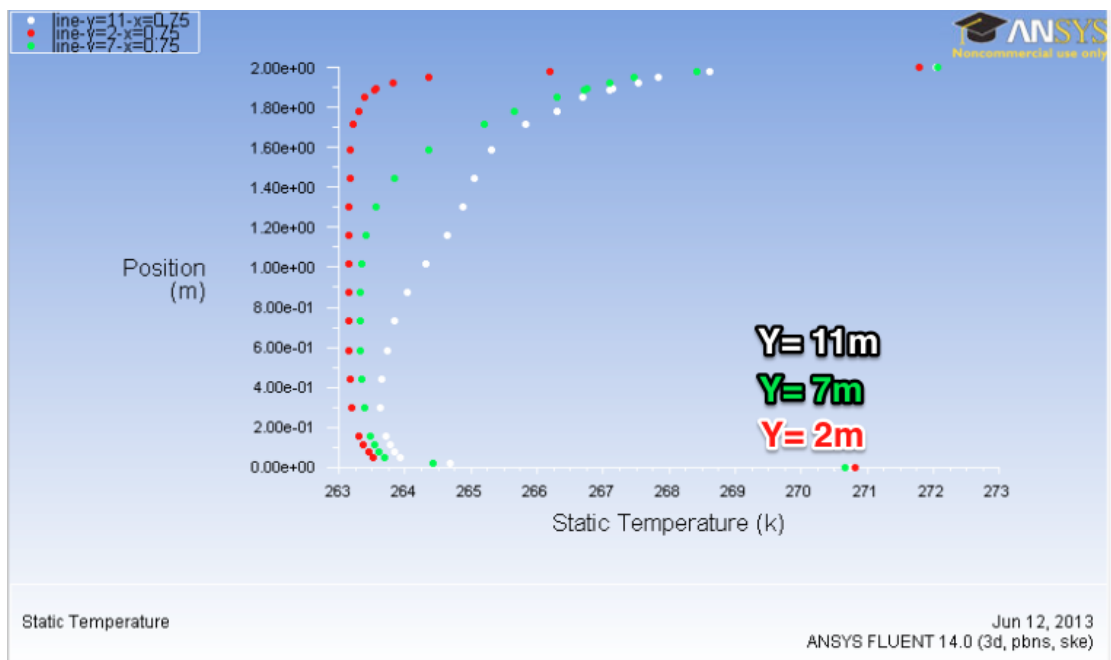
Figure 41: Static Temperature Profile From Z= 0 To Z= 2m At X= 0,75m (midplane)

Again there is a wave shape of the of the velocity profile of the air close to the inlet section. Due to a lower flow rate in the winter case, a clearly visible boundary layer builds up much sooner (already visible at y= 7m). This effect is also noticeable in the temperature plot as well. This indicates that the heat transfer will probably be higher for the summer case.

5.3.2.3 Results Of Heat Transfer Calculation

The most important results of the rotational cases are summed up in Table 4. For the entire tables, see Table 16 and Table 17 in appendix.

As for the uniform cases, there is still a significant difference in the in heat transfer coefficient in the ceiling and at the floor. In the summer case, the difference is now a 58% larger coefficient for the ceiling. In the winter the difference actually increased slightly to 109%. Still the effects the boundary layers are significant.

In terms of the walls, the situation is not longer symmetrical, as clearly shown in the temperature plots. The wall with the falling air or rising air that moves in the same direction of the rotational flow is seen to have the greatest heat transfer coefficient. For the summer case, this is the right wall, and the left wall for the winter case.

Again the overall heat transfer for the duct is lower for the winter case.

Table 4: Heat Transfer Coefficients For Summer And Winter With 33% Tangential Component Rotation

	Units	Summer	Winter
$T_{out} - T_{in}$	K	-1,89	1,45
$\dot{m}$	kg/s	2,68	1,50
h_c	W/m²K	5,69	2,28
h_f	W/m²K	3,59	4,77
h_l	W/m²K	4,69	4,23
h_r	W/m²K	5,32	3,71
h	W/m²K	4,85	3,78

In case of the velocity profiles, they became somewhat similar to what was measured at Grong according to Figure 13. In terms of the vorticity the results were like depicted in Figure 42.
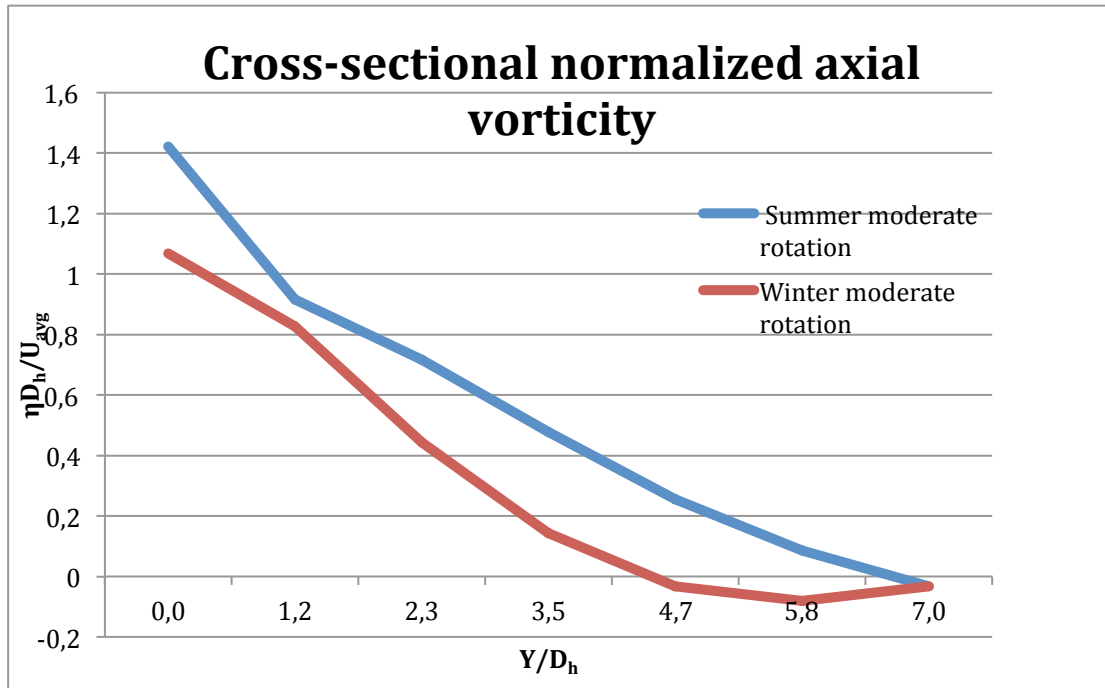
Figure 42: Normalized Axial Vorticity Throughout The Duct For Tangential Component= 33%

This result is considerably lower than for what was measured by Chen et al in Figure 11. One can observe how the vorticity decreases along the length of the culvert, and even faster for the winter case.

Therefore a last simulation was performed in which the tangential component was increased even more, in order to see how it would affect the flow. This time it was set to 83%.

5.4   Summer With Strong Rotational Flow

All the conditions for the summer were kept constant, except for the tangential component, which was enhanced considerably.

There is almost no distortion of the temperature profile due to buoyancy forces. The effect of the rotation is much stronger, even close to the outlet (y= 11m). There is little difference between the ceiling and the floor, nor between the right and the left side.
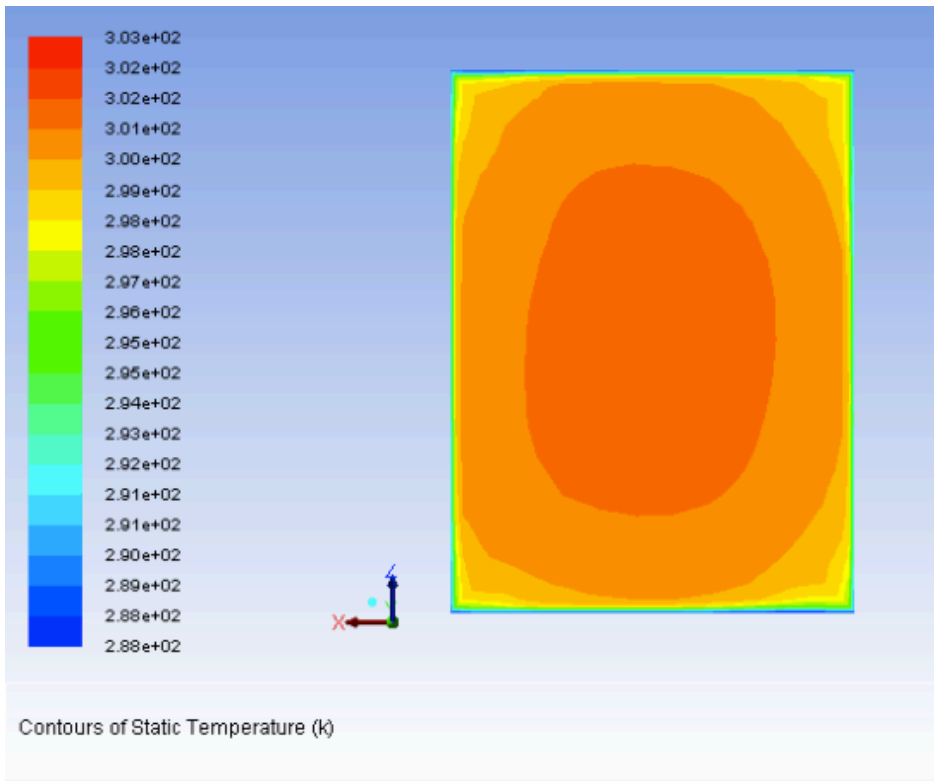
Figure 43: Static Temperature At Y= 11m
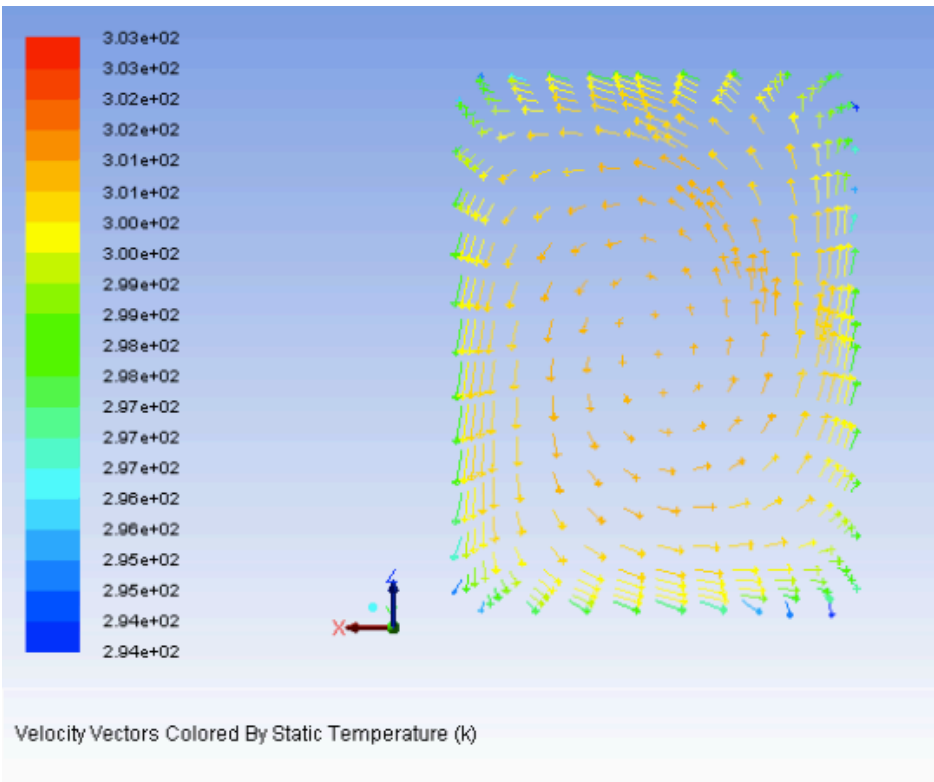
Figure 44: Velocity At Y= 11m. (Colors Indicate Static Temperature)
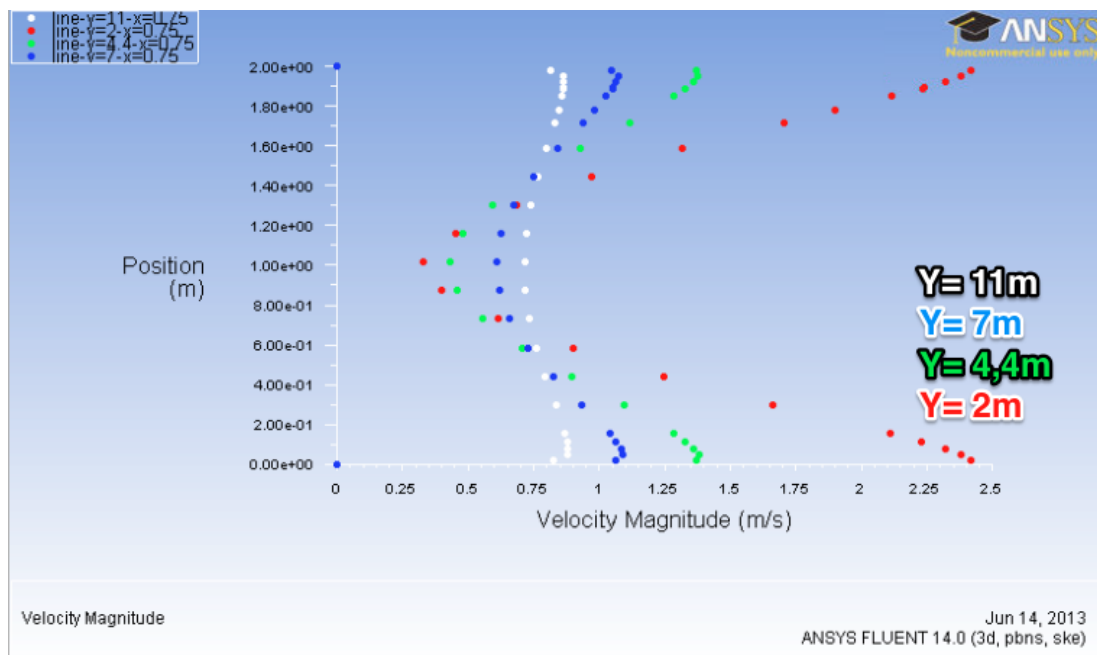
Figure 45: Velocity Magnitude From Z= 0 To Z= 2m At X= 0,75m (midplane)
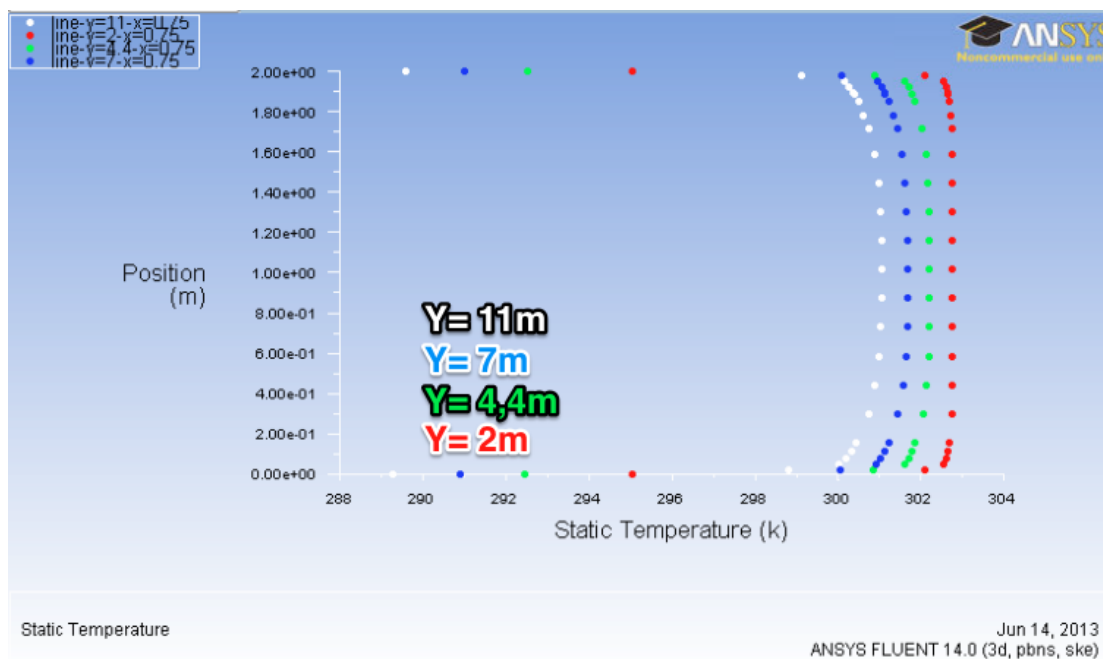
Figure 46: Static Temperature Profile From Z= 0 To Z= 2m At X= 0,75m (midplane)

This velocity profile shows what huge impact the increased rotation has on the flow. The velocity profile at y= 4,4m which is equal to the same distance x/D_h=2,6 in Figure 13, resembles the measured velocity profile even more, but with a higher velocity magnitude. From both of the plots, there are very few signs of a boundary layer creation.

The heat transfer characteristic leaves very few traces of buoyancy effects. The difference between ceiling and floor is merely 4% higher at the ceiling. And the difference between the right and left side is almost wiped out.

Table 5: Heat Transfer Coefficients For Summer With 83% Tangential Component Rotation

	Units	Summer (enhanced rotation)
$T_{out} - T_{in}$	K	-2,91
$\dot{m}$	kg/s	2,68
h_c	W/m²K	9,88
h_f	W/m²K	9,47
h_l	W/m²K	9,54
h_r	W/m²K	9,88
h	W/m²K	9,70
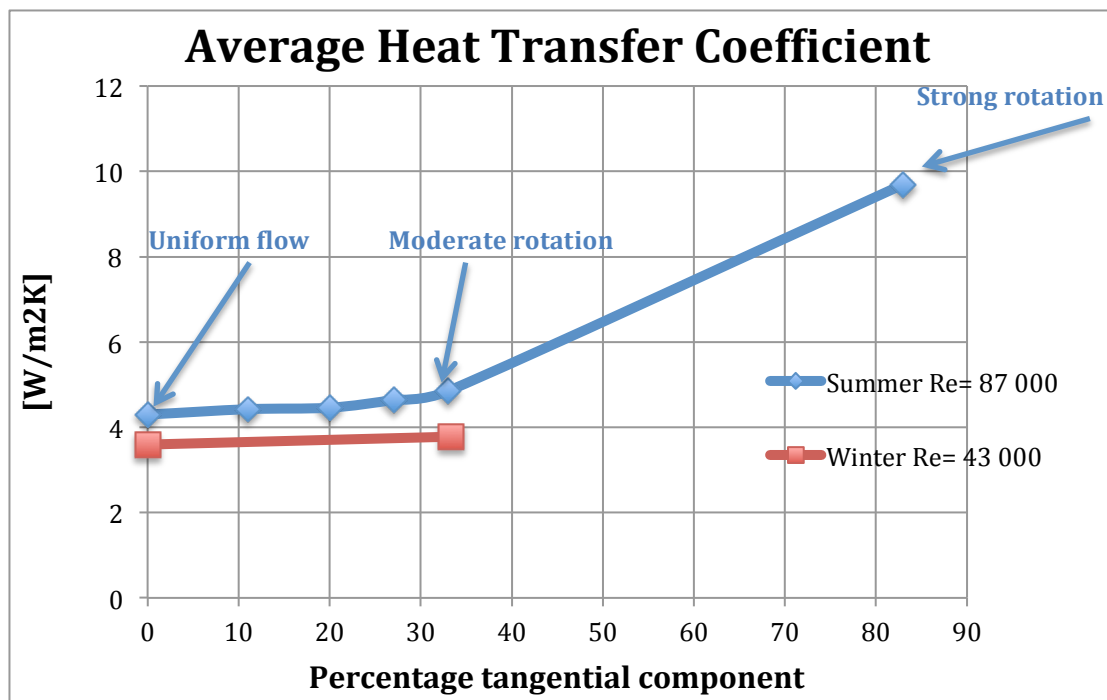
Figure 47: Average Heat Transfer Coefficient Results For Winter And Summer

All the results of average heat transfer coefficients are presented in Figure 47. The increased rotation to boosted the heat transfer coefficient by 126% from the uniform summer case. This is not far from the enhancement Chen et al. reported in their findings (117%) on the difference in heat transfer coefficient for uniform vs. rotational flow.
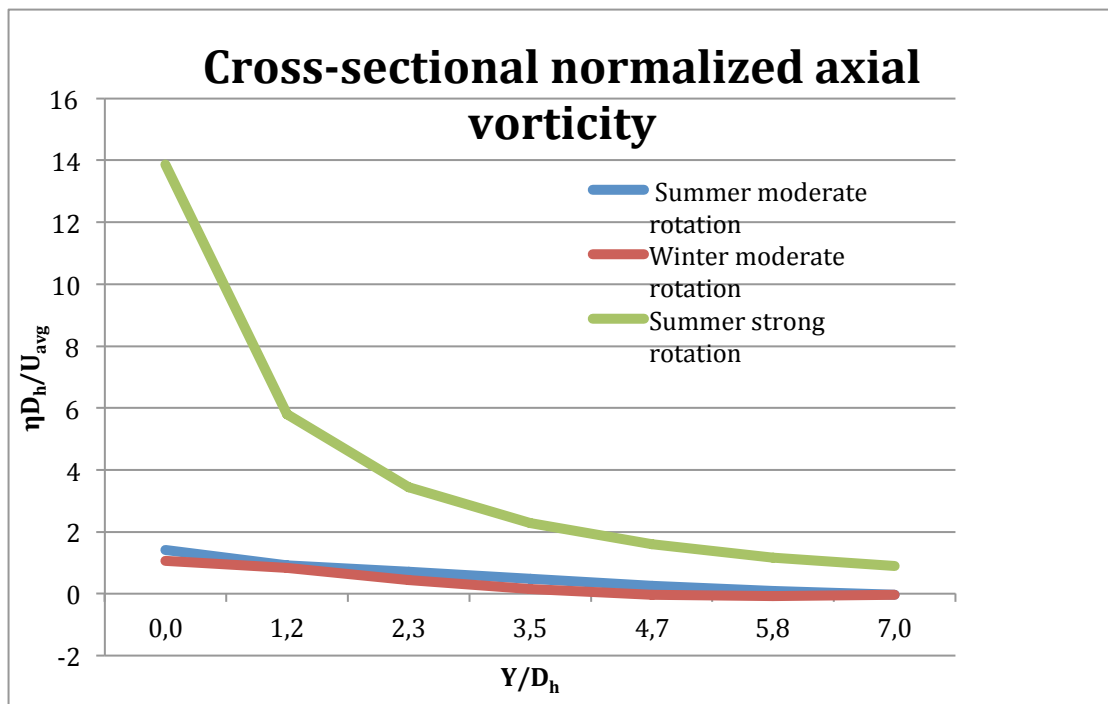
Figure 48: Normalized Axial Vorticity Throughout The Duct

In terms of the cross-sectional normalized axial velocity, the last simulation shares more similarities with what Chen et al. had in their experimental setup. With the strong rotation the effects of rotation last all the way through the duct according to Figure 48.

5.4.1 Result

As the tangential component was increased, it increased the heat transfer coefficient, as expected. But all in all the coefficient was found to be very low.

5.5 Choice Of Heat Transfer Coefficient For ESP-r

As seen in the results, the evaluated heat transfer coefficient found in Ansys are substantially lower than the ones reported by Chen et al. or Wachenfeldt and Zhang who made direct measurements at Grong. It is therefore decided to use a value of 30 W/m^{2}K on the culvert surfaces in the next analysis in ESP-r, in order to evaluate the preheating and precooling potential of the culvert.

6   Modeling An Intake Air Culvert In ESP-r

The heat transfer between the ground and the intake air is to be modeled and analyzed as a whole. This will be done in order to evaluate the cooling and heating capacity of leading the air through the duct. Therefore a model of duct has been created in ESP-r.

The intake air for a school is being led through the intake duct before entering the zones of occupancy. Inside the culvert, the two most important thermodynamic processes going on are convection between air and the duct surface and heat conduction between the duct surface and the surrounding ground. Also long wave radiation and humidity play a minor role, but their effects have been neglected here.

6.1   The Program

ESP-r is an open-source program developed at University of Stratchclyde in Glasgow, used for building energy performance modeling. It has been continuously developed since 1974. The program allows the user to implement his own values specific for his case, instead of using default values already integrated in ESP-r (ESP-r).

6.2   Location And Climate

Since local weather conditions and ground temperatures influence the performance of the culvert, a local climate file for Grong has been used. This file includes calculated monthly average temperatures at various depths.

6.3   Materials and Constructions

Defining materials is a crucial part of the modeling. There are already included standard libraries in ESP-r, and most of the materials where chosen from there, since no other information was available at this point. The materials used in the model are summed up in the following table.

Table 6: Material Properties

	Conductivity	Density	Specific Heat Capacity	Diffusivity
Material	[W/mK]	[kg/m^3]	[J/kgK]	10^6[m^2/s]
Clay 1	1,28	879	1460	0,99
Gravel 1	0,52	2050	184	1,38
Heavy mix concrete	1,40	2100	653	1,02
PVC – insulation	0,160	1379	1004	0,12

6.4 Dimensions Of The Culvert And Zones

The part of the culvert that is to be inspected is the horizontal section from the fan after the vertical intake section, until the filter. This section is approximately 12 meters long, 2 meters high and 1,5 meters wide. It was decided to divide this section of the model into 6 zones with an additional zone *intake* in the end. The *intake* zone does not affect the rest of the model, and ultimately it was not used. Each zone is exactly 2 meters long.
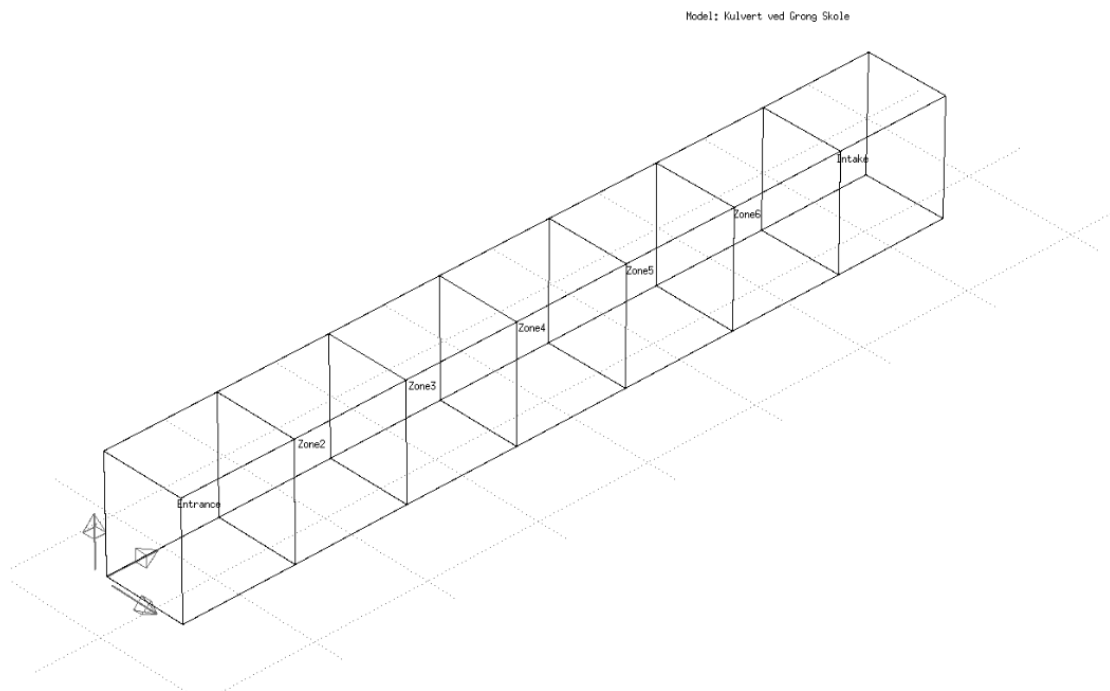
Figure 49: Zones In The Model, ESP-r

6.5 Ground

ESP-r has several options on how to simulate the boundary conditions at the ground. Among them are static temperature, monthly temperature profile, user defined profile or 3D conduction model (ESP-r). Since the culvert is exposed to ground on four surfaces of its surfaces, the choice of model of ground will be

important. Ideally, a two or three-dimensional model should be chosen, placing an adiabatic layer far away from the inner duct surfaces and imposing ground temperatures on the boundaries. Due to its complexity, and lack of extensive climate data, a one-dimensional representation was chosen.

In a real situation with a high temperature difference between the duct air and the undisturbed ground, one will expect the heat flow through a given duct surface, to be mostly perpendicular on the surface. But as the heat is led out into the surrounding soil, the heat flux becomes more and more lateral. Far away from the wall, the heat flux is no longer perpendicular to the surface. Wall surfaces with one meter earth were chosen in this model, since the heat flux is still mostly perpendicular on the surface at this distance. Another effect provided by the earth is the storage and lag effects. The bigger earth, the bigger these effects become (Wachenfeldt 2003).
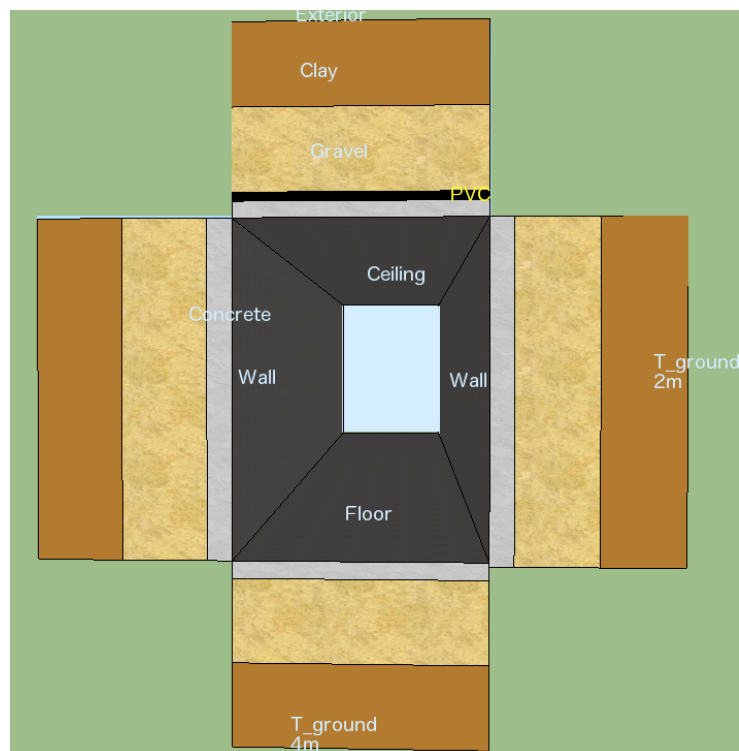
Figure 50: 1-D Model Of Ground In Model Seen From The Front

6.6 Surfaces And Boundary Conditions

In ESP-r one defines surfaces and these can be divided into different zones. Each surface must consist of a construction. All the zones in the model are equal, with the respect to constructions.

An adiabatic construction called fictitious is used to divide the zones. This layer does not represent any real construction, only air. This was chosen to be adiabatic, because air is the main transporter of heat in this model.

53

Each surface must be imposed a boundary condition. In *entrance* the surface *inlet* has an adiabatic condition. This was chosen, since the heat into the zone is mainly brought with the air. Firstly the condition "exterior" was chosen, but this was changed at later point. This is because "exterior" also includes direct solar radiation, which is not present at in the horizontal part of the culvert. To compensate for this in periods of no fan, a small amount of air infiltration was added.

The surface of the ceiling is approximately situated one meter under ground, and the roof construction with ground is 1,15 meters. Therefore the exterior was chosen as boundary condition. The culvert walls on both sides are situated at an average depth of two meters, hence ground temperature of two meters were used. For the culvert floor, ground temperature at four meters depth was imposed. In *zone6,* the last zone, the surface leading into the intake chamber is set to be adiabatic, for the same reason as the *inlet* surface in *entrance.*

Table 7: Constructions Properties And Boundary Conditions

Construction	Description	Material	Thickness [mm]	Boundary condition
Inlet	Opening area where air enters	Fictitious	-	Adiabatic
Wall _A1/B1	Culvert wall on each side	Heavy mix concrete	150	Ground temperature at 2 meter
		Gravel 1	500	
		Clay 1	500	
Roof1	Culvert ceiling	Heavy mix concrete	100	Exterior
		PVC (insulation)	50	
		Gravel 1	500	
		Clay 1	500	
Floor1	Culvert floor	Heavy mix concrete	100	Ground temperature at 4 meter
		Gravel 1	500	
		Clay 1	500	
0_in	Open area between the zones	Fictitious	-	Adiabatic
0_out	Open area between the zones	Fictitious	-	Adiabatic

6.7   Flow Network

A basic flow network was designed to simulate the air movement through the model. The internal nodes are nodes of measurement. They measure the temperature and flow of air. There is one node included in each zone.
One external node is used to impose ambient air conditions. The nodes are connected together by components. Only two components were necessary to define for this model. A fan connects the external node to the node in *entrance.* And air openings connect the remaining nodes. The network itself is connected together like this.

```
Connections

     Node +ve       |dHght|to| Node -ve    |dHght|via Component
a ex                0.0 --> Entrance        0.0  fan
b Entrance          0.0 --> Zone2           0.0  Opening
c Zone2             0.0 --> Zone3           0.0  Opening
d Zone3             0.0 --> Zone4           0.0  Opening
e Zone4             0.0 --> Zone5           0.0  Opening
f Zone5             0.0 --> Zone6           0.0  Opening
g Zone6             0.0 --> Intake          0.0  Opening
h Intake            0.0 --> ex              0.0  Opening
```

Figure 51: Flow Network, ESP-r

The *intake* node was connected to the external node. This connection's purpose is to extract the air injected in the *entrance* zone.

For more details on the model, see appendix part D.

7 Calculation Of Culvert Performance For Precooling And Preheating

7.1 Ambient And Ground Temperatures

Two very important parameters that are expected to affect the performance greatly are the ambient temperature and the ground temperatures.

Figure 52 shows how the ground temperatures at the different depths and ambient temperature vary over a year. The simplification of monthly ground profiles is also quite evident in the plot. One clearly sees that the amplitudes of the ground temperatures are lower with respect to the ambient. At greater depths there are smaller amplitudes and the peak values are shifted more to the right. The peak of ambient temperature is around week 28, and around week 37 for 4 meters.

Due to that the culvert is expected to be able to perform better in the fall compared to the spring. During the weeks 44-46 and 10-12 the ambient temperatures are somewhat similar. But the ground temperatures are approximately 6K lower in the latter case, due to winter that passed.
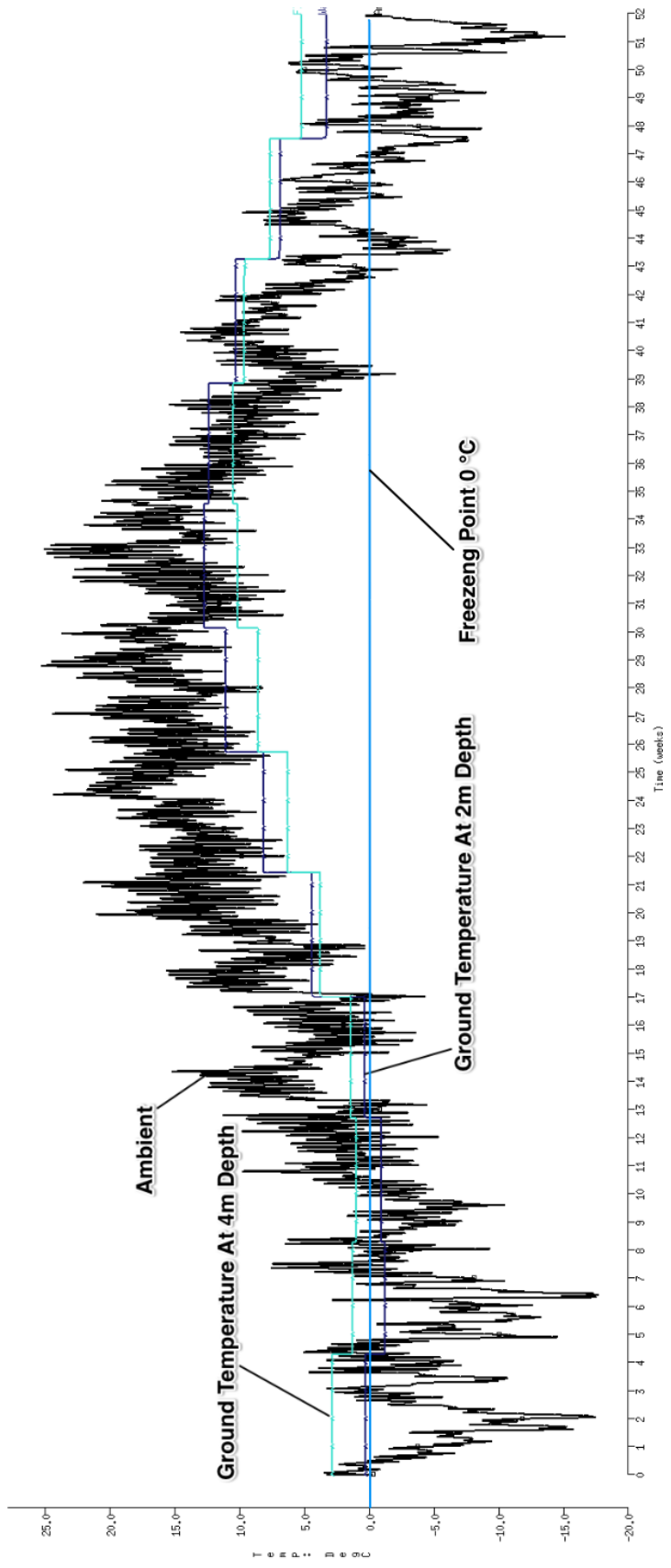
Figure 52: Ambient And Ground Temperatures At 2 And 4 Meters Depth, 1 Jan – 31 Dec

57

7.2 Ground Temperature Plots

The culvert has been tested at four different periods during the year, to get an idea of how it will perform under different conditions. These are:

- Winter: 11-16 January
- Spring: 14-19 March
- Summer: 18-23 July
- Fall: 1-6 November

For each season, the fan was set to operate under two different conditions, on and off. Since people are expected to be present at the school between 8 and 16 o'clock, the fan was always kept on during these hours in order to keep a necessary flow of air for the occupants and thus maintaining the concentration of bad air under a satisfying level. For the condition of variable fan, the fan was shut off outside time of occupancy (TOO) during the colder seasons fall, winter and spring. For the summer, when cooling of the air is expected to be desirable, the fan was started at 4 o'clock and kept running until 16 o'clock, since cold night air can help removing some of the heat accumulated in the concrete walls during the day. These modes are summed up the following table.

Table 8: Seasonal Fan Modes

	Mass flow rate with fan on [kg/s]	Variable fan hours	Constant fan hours
Fall	1,3	8-16	0-24
Winter	1,3	8-16	0-24
Spring	1,3	8-16	0-24
Summer	2,7	4-16	0-24

Like mentioned before, the ESP-r model was updated with an enhanced heat transfer coefficients on the wall surfaces. It was to decided to investigate the impact of the update by simulating the temperature profile in the ground. This was done from the 1st to the 3rd of November.
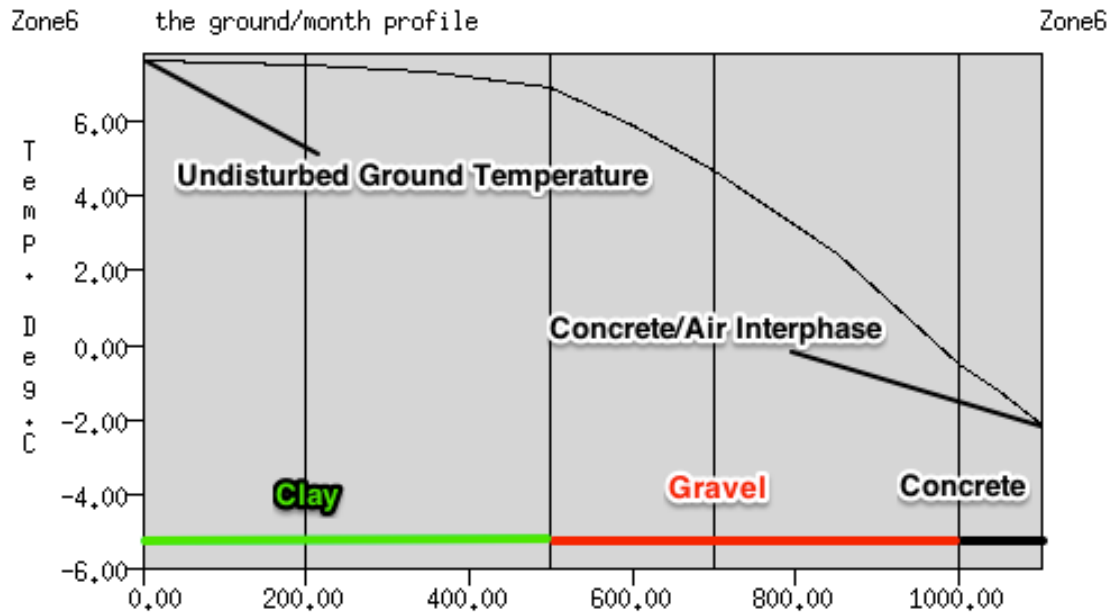
Figure 53: Instantaneous Temperature Plot For Floor1, Zone6, 1 November 18.25. Abscissa units in millimeter

In Figure 53 one can see how the temperature distribution is at a certain moment in the November. The surface element Floor1 is subject to monthly ground temperature profile at 4 meters deep of 7,6 °C (see appendix part D for monthly ground temperature profiles over the whole year) in November outside of the clay region. This is seen to the left in the figure. The outer element at 0 mm consists of clay, and then gravel is the next layer before a concrete layer closest to the air. At this moment the air is colder then the ground temperature, roughly -2 °C. Through the concrete and the gravel the temperature rises steadily until it reaches the clay layer. However, this is just a momentary snapshot. And one cannot deduct very much from just looking at this moment. Therefore plots like this one were sampled every 10 minutes over 3 days to see the changes, using the old and the new model, creating accumulated temperature plots shown next.

7.2.1 Floor Element Comparison With Old And New Model

These two figures show how the temperature various in the different layers of the ground over a period of three days in November. It is obvious how the stable ground temperature on the left changes the temperature of the clay very little. In the gravel and the concrete layer, the variations grow substantially. In the old model the temperature range on the concrete surface is between -1 and 5 °C (Figure 54). For the new model, this range has grown to -5 to 4 °C (Figure 55). The temperature range has grown with 3K from the old to the new model. This is expected, since the new model has a bigger heat exchange with the fluctuating air temperature, whereas the old model will have lower heat exchange, thus making it less affected by the air temperature inside the duct.
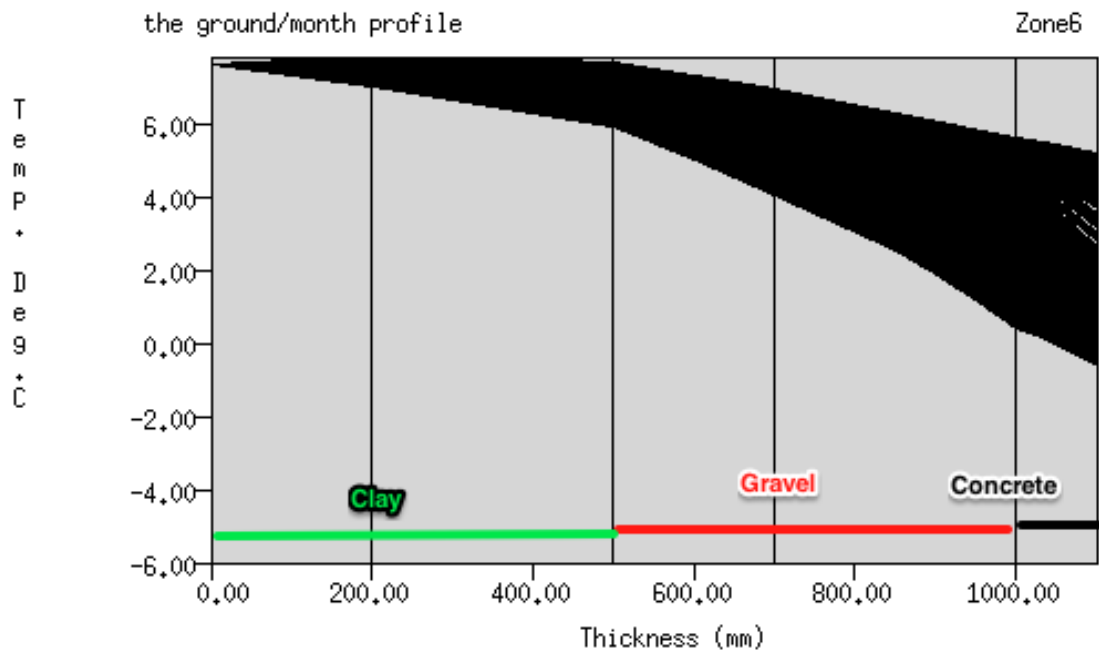
Figure 54: Accumulated Ground Temperature Plot For Floor1, Zone6, 1-3 November, Old Model, Constant Fan
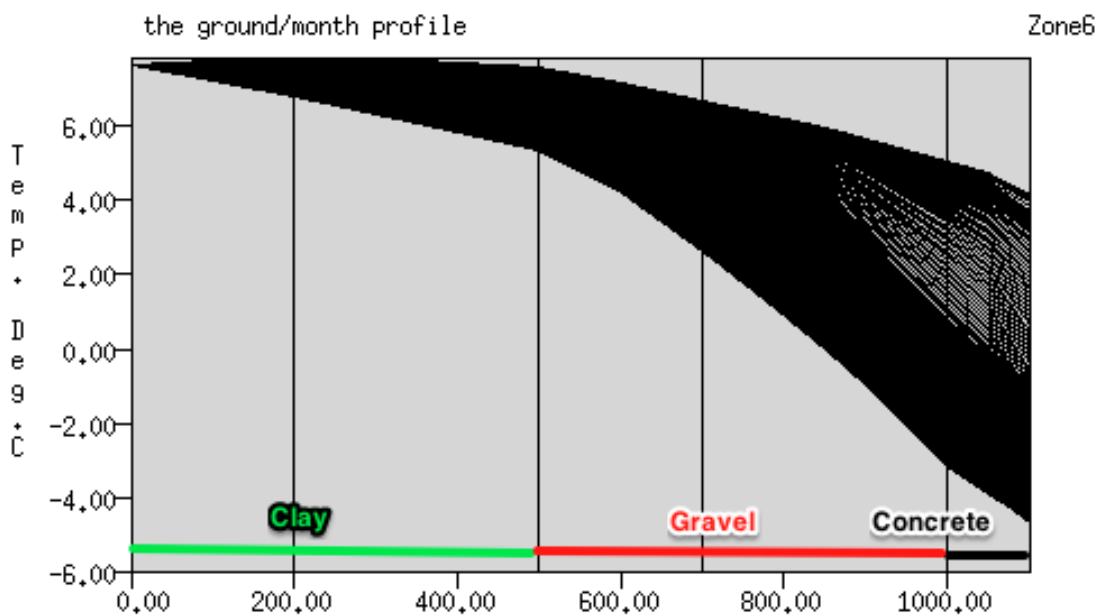
Figure 55: Accumulated Ground Temperature Plot For Floor1, 1-3 November, New Model, Constant Fan

The same simulations were also done for the variable fan mode. The fan was on only during 8 and 16 o'clock, and shut off the rest of the time.
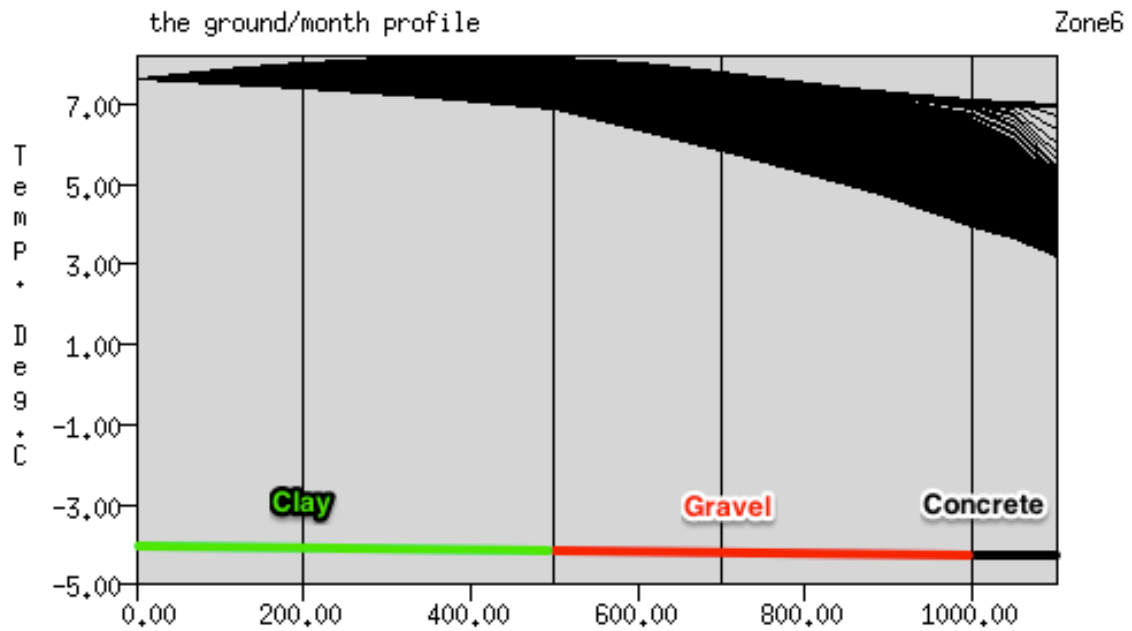
Figure 56: Accumulated Ground Temperature For Floor1, Plot 1-3 November, Old Model, Fan 8-16
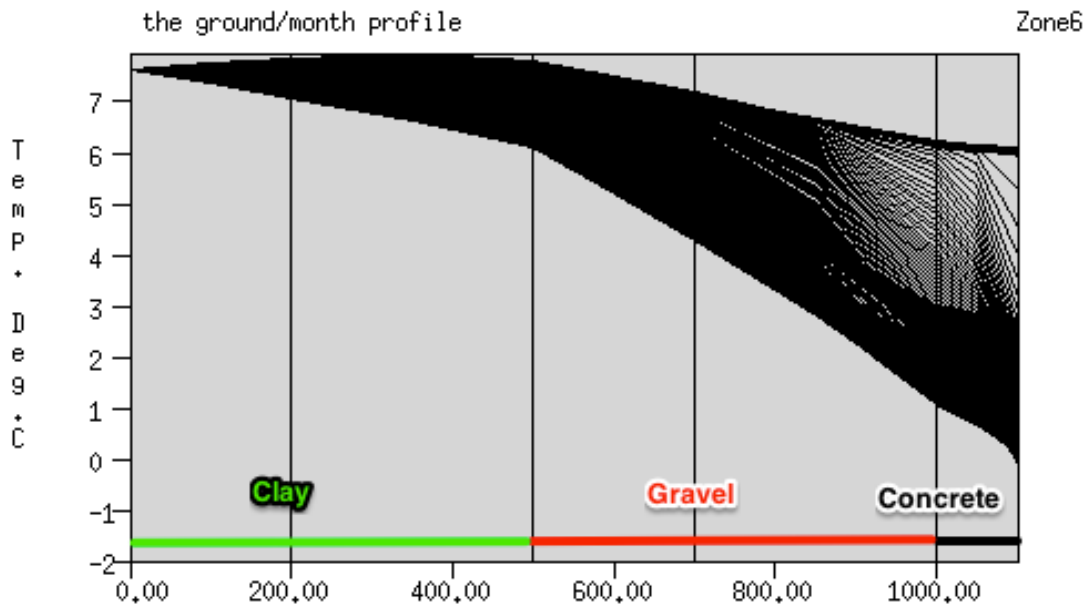
Figure 57: Accumulated Ground Temperature For Floor1, Plot 1-3 November, New Model, Fan 8-16

Since the fan is switched off during the colder period of the day, the temperatures are expected to be higher. The concrete region has generally a

higher temperature compared to the constant fan simulations. The temperature range is now 3 to 7 and 0 to 6 °C for the old and the new model respectively. Both ranges have diminished by 2-3K and the lowest temperatures have risen with several degrees. The difference between the old and the new model is still quite noticeable.

The same procedure was done for the wall element WallA1, and compared in the same way. The wall element is subject to a constant monthly temperature of 6,9 °C in the ground and varying intake air temperature on the other side. The results are similar, with bigger temperature range for the new model, and higher temperatures when the fan is shut off during time of no occupancy. The results can be seen in appendix part C.

7.3   Culvert Performance Under Different Seasons

The culvert performance is measured in terms of how much the air receives or looses energy when passing through it. The main focus here is the hours in which occupants are present in the school building i.e. between 8 and 16 o'clock. This period of time is situated between two blue lines for every day in the temperature graphs. Every season has been evaluated for six continuous days. The time of no occupancy is denoted as NO in the following graphs.

For all the seasons it is desirable to have a temperature inside the school building between 19 and 22 °C. When the ambient is below 19 °C there is a preheating potential and above the 22 °C there is a potential for precooling.

Like in the previous section, a comparison was done for the fall season. From ESP-r, the temperature of *zone6* is defined as the supply temperature.

7.3.1 Comparison: Old Vs. New Model During Fall

Figure 58 and Figure 59 show how the ambient temperature and the supply air at the end of the duct vary over a period of six days. The main purpose of these figures is to show how the new model supply air (green) has been changed compared to the old model supply air (black).

In the case of constant mass flow rate, there is a very good correspondence between the ambient and the supply temperature for both models. Since the old model has a lower heat transfer coefficient, the influence of the ambient temperature is very profound. This is due to a lower heat exchange between the ground and the intake air. Actually, in the old model, the effect of the ground on the intake air is rarely bigger than 0,5K (temperature difference between ambient and supply air). The biggest difference is soon on the night after the first day around midnight where the difference is around 1K.

There is a phase change between the supply air and the ambient air temperatures that can be observed by looking at the peaks. The peaks of the supply air occur after the one of the ambient air. This phase change grows from barely half an hour for the old model to approximately two hours for the new model.

In the model with variable fan, the fan is switched off in the period of no occupancy. This is clearly seen in Figure 59. Whenever the fan is switched off, the mass flow rate falls to zero and the supply air temperature tells the temperature of the air in *zone6*. In November, the outer ground elements on the walls and the floor are subject to undisturbed temperatures of 6,9 and 7,6 °C respectively. By looking at the temperature plots for the ground, it is seen that the new model has lower temperatures in the concrete region close to the surface, than the old model. This explains the higher temperature in *zone6* for the old model compared to the new model.

As soon as the fan is turned on in the morning at 8 o'clock, the old model has a rather quick transition towards the ambient temperature, whereas the new model has a slower transition, because the ground is influencing the supply air more over a longer period of time. For the old model, the heat exchange between the culvert walls and the intake air is too small to be noticeable.
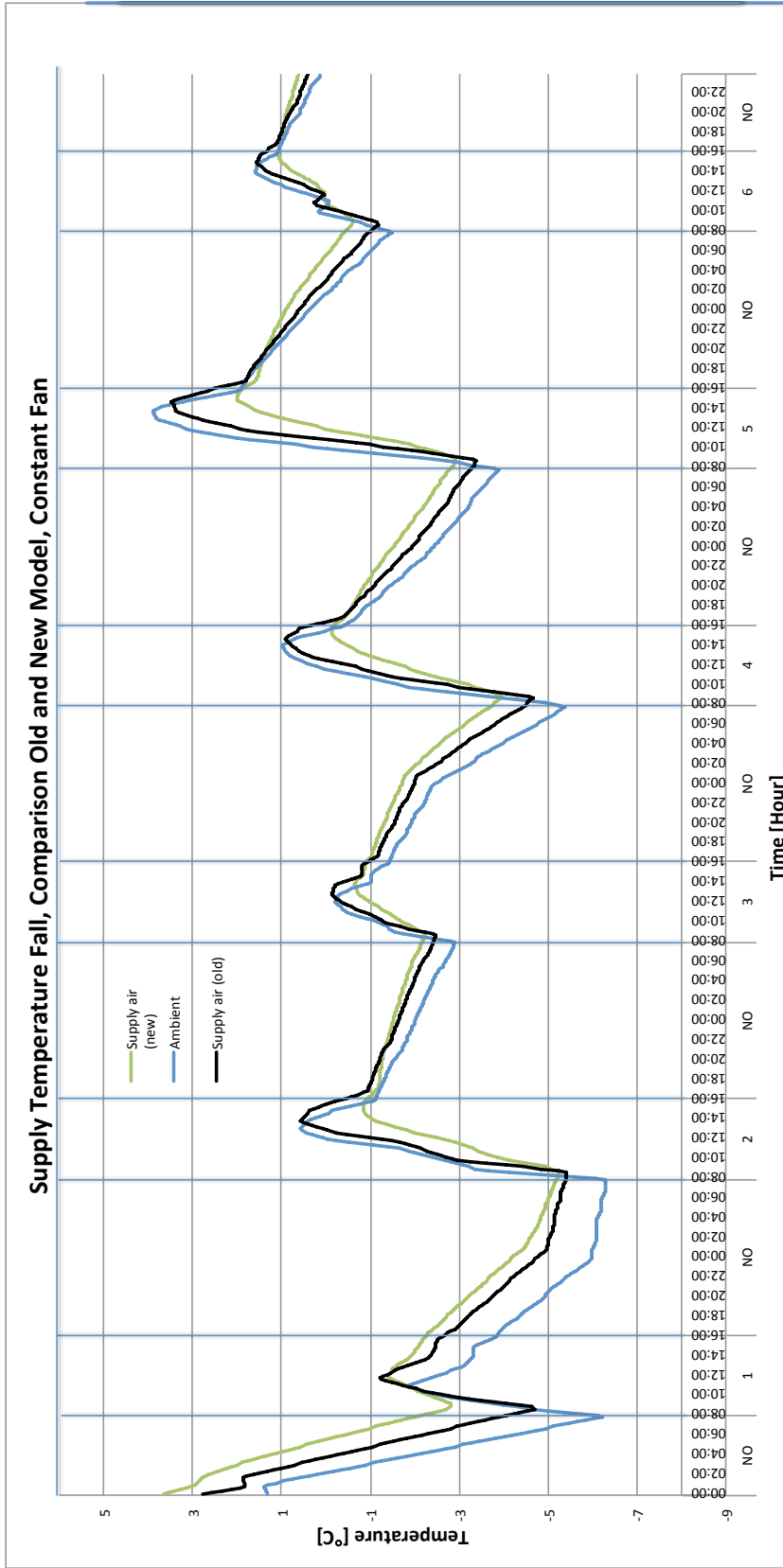
Figure 58: Temperature 1-6 November. Comparison Old Vs. New Model
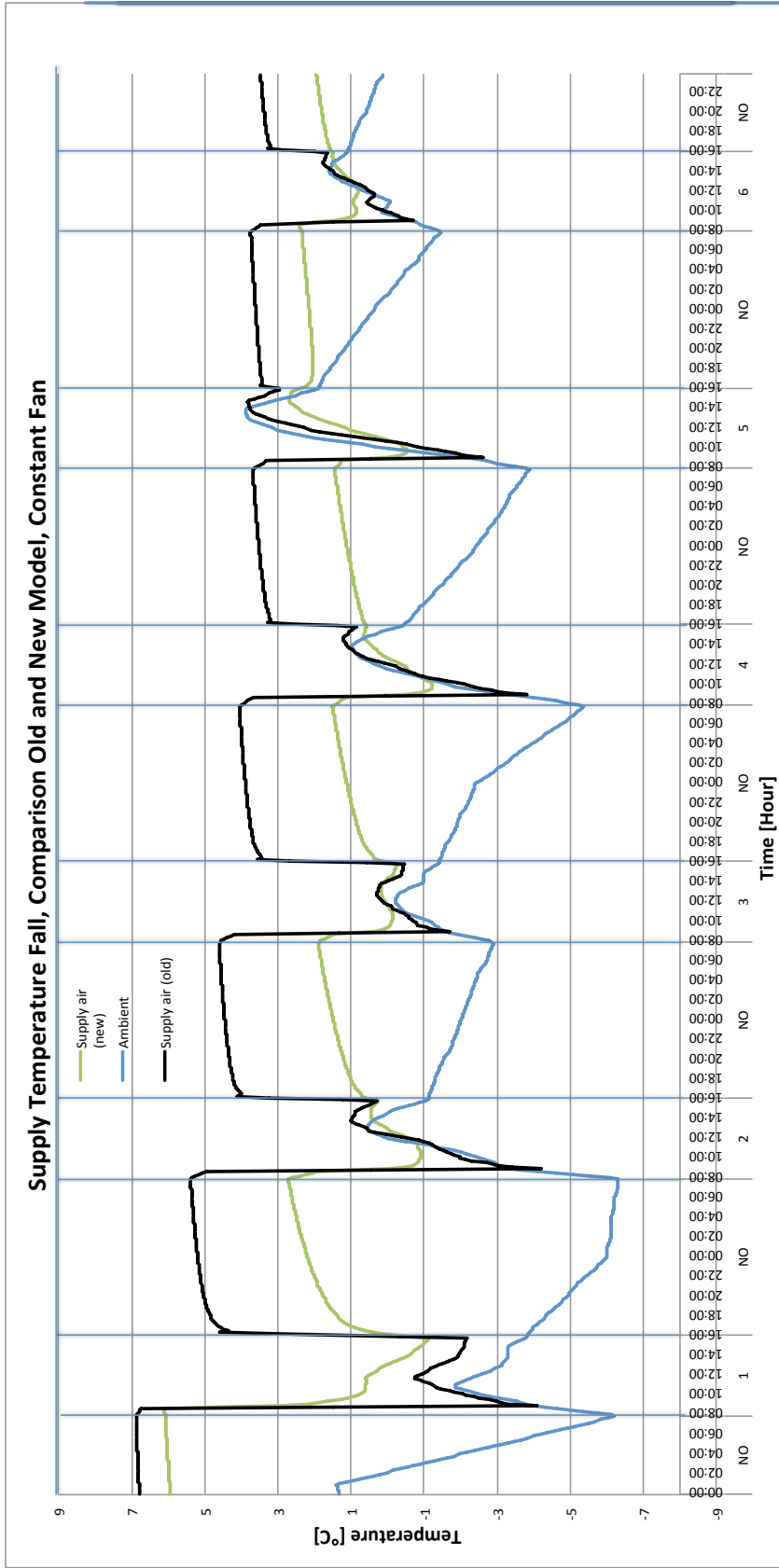
Figure 59: Temperature 1-6 November. Comparison Old Vs. New Model

7.3.2   Preheating Seasons

For every season, three graphs have been developed for a case with constant and variable fan. The first one depicts the supply temperature vs. the ambient temperature. After this a graph displays the preheating potential in terms of degrees Celsius during the hours of occupancy. The hours outside of this interval is called heating potential. Lastly a graph displays the preheating effect during the time of the day when the fan is turned on and the mass flow is non-zero. When the supply fan is on, the mass flow rate is constantly kept at 1,3kg/s.

$$Heating\ Potential = T_{supply\ air} - T_{ambient}\ [°\mathrm{C}]$$

$$Temperature\ Difference\ (NO) = T_{supply\ air} - T_{ambient}\ {}^{*}[°\mathrm{C}]$$

$$Heating\ Power = \dot{m}\,cp\!\left(T_{supply\ air} - T_{ambient}\right)[\mathrm{kW}]$$

$$Heating\ Power\ (NO) = \dot{m}\,cp\!\left(T_{supply\ air} - T_{ambient}\right)[\mathrm{kW}]$$

$\dot{m}$ = Mass flow rate air [kg/s]
cp = Specific heat capacity air [J/kgK]
* NO = No occupancy

7.3.2.1   Fall: 1-6 November

Once again, the ground temperatures are 6,9 and 7,6 °C outside the walls and the floor.

Figure 60 shows the temperature variations from 1st to 6th of November. The ambient temperature falls very much from the last day of October to the first day of November. This thermal energy is stored in the layers of the culvert and released during most of the first day. After this the daytime temperature rises steadily until day 5. Day 6 is slightly colder again. This gives a bad performance of the duct during the time of occupancy. Generally the duct is seen to heat the air when ambient temperature is falling, and conversely. Typically during the night the air gets heated, and cooled down during the day when the fan is running constantly.

From Figure 61 shows that there is only a heating potential on day 1 during the time of occupancy and on the other days only during the first hour. The other days, the duct contributes at cooling the intake air instead most days.

When the fan is running constantly, the heating potential and the heating power will be proportional.

In Figure 62 the periods in which the fan is turned off are easy to spot. Now the cold night air is not cooling the culvert walls when the ambient temperature is at its lowest. The ground layers manage to recharge for a while, and this energy is mostly released at the beginning of each day (Figure 64 and Figure 65). The heating potential is seen to be least on day 5. This is a result of the sudden rise of the ambient day temperature compared to the day before.

Lastly Figure 65 shows how the heating power is non-zero during the time of occupancy. Otherwise it is proportional to the heating potential.
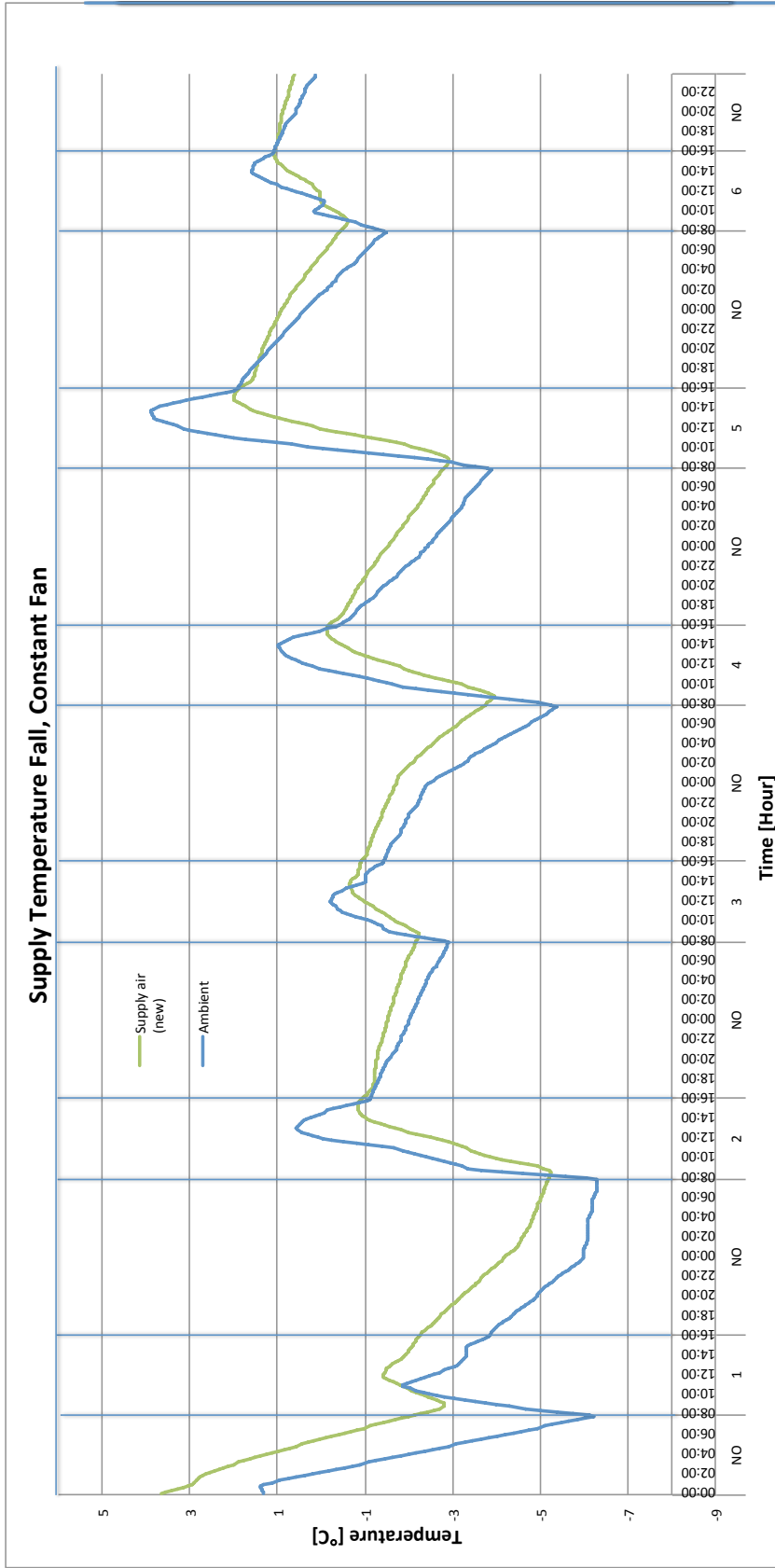
Figure 60: Supply Air And Ambient Air 1-6 November, Constant Fan
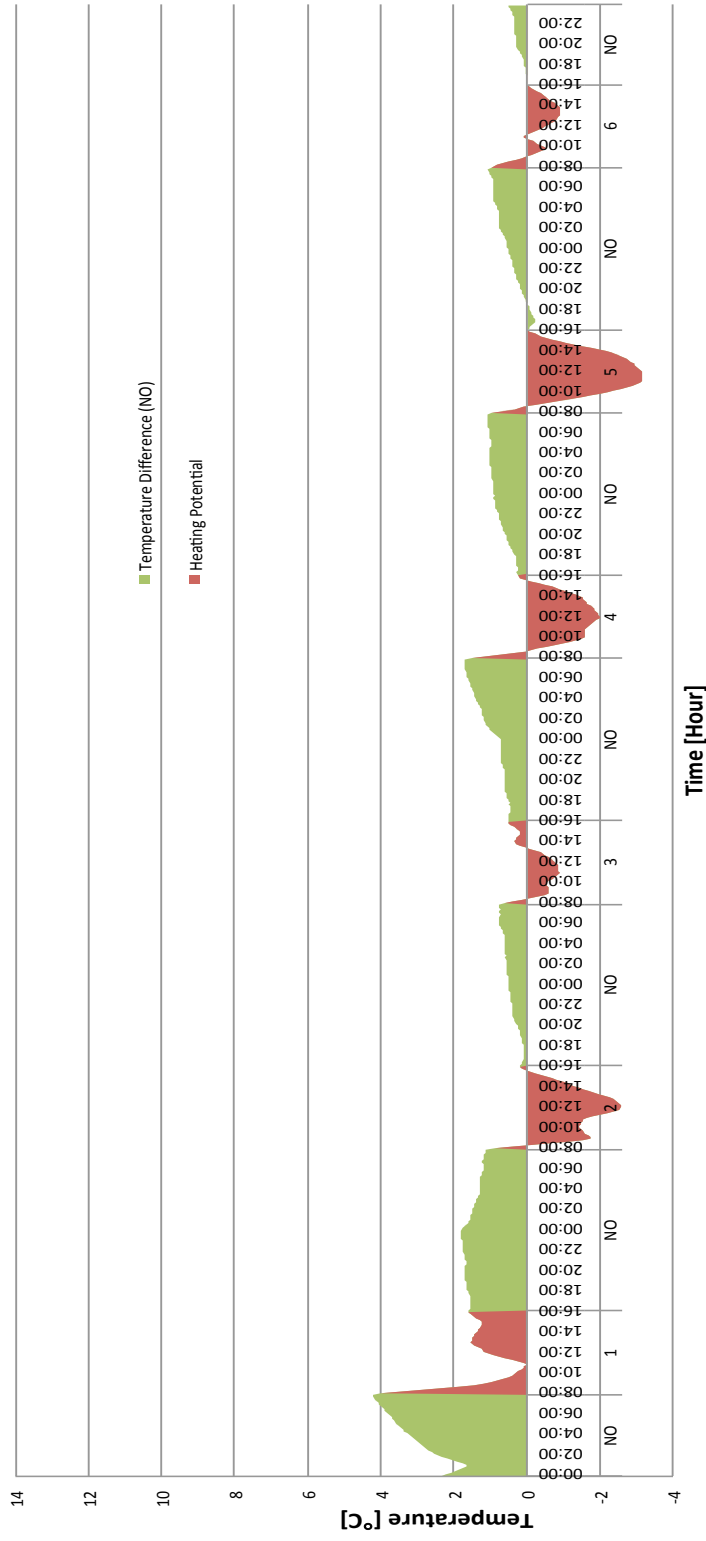
Figure 61: Heating Potential 1-6 November, Constant Fan
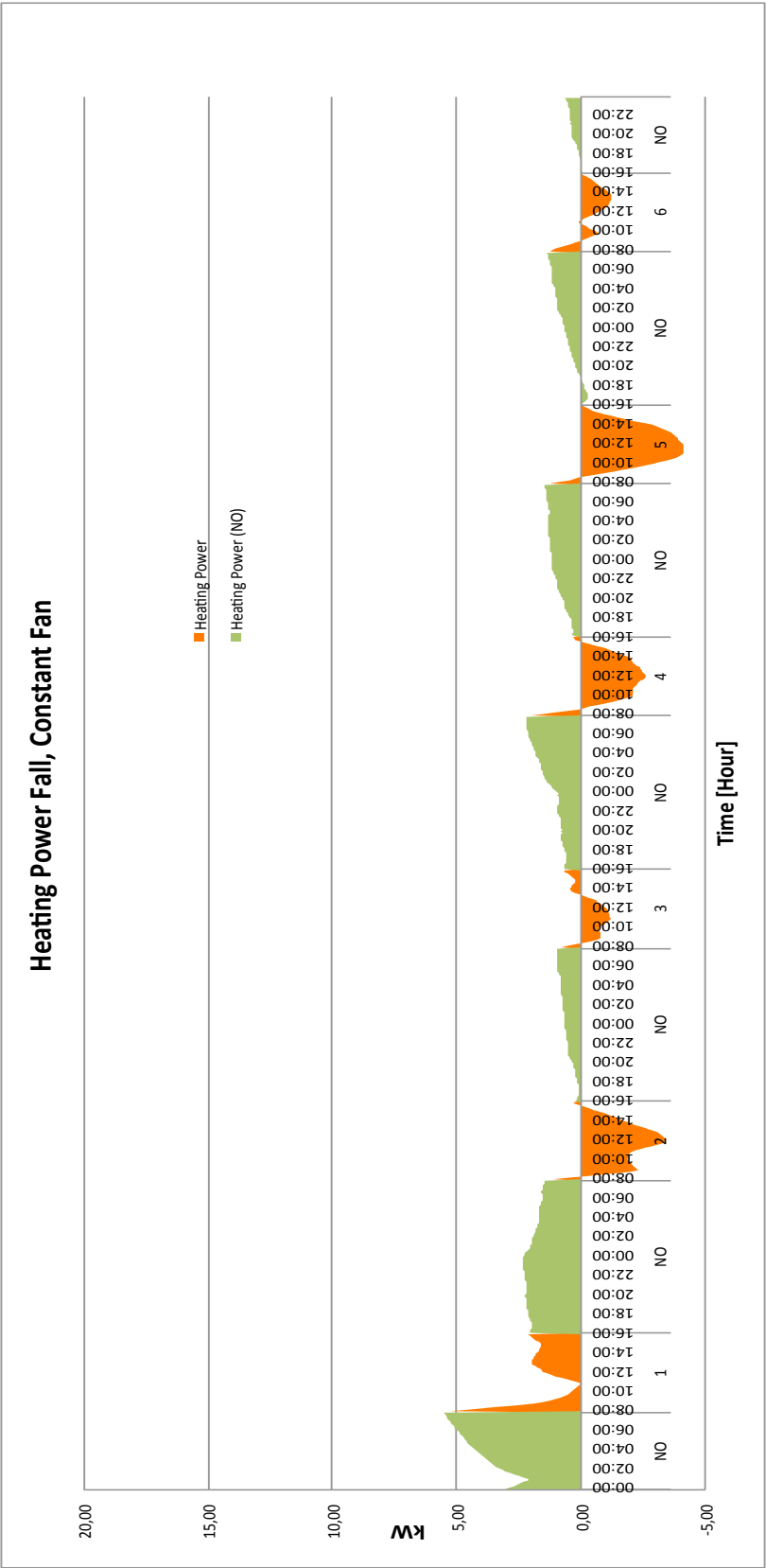
Figure 62: Heating Power 1-6 November, Constant Fan
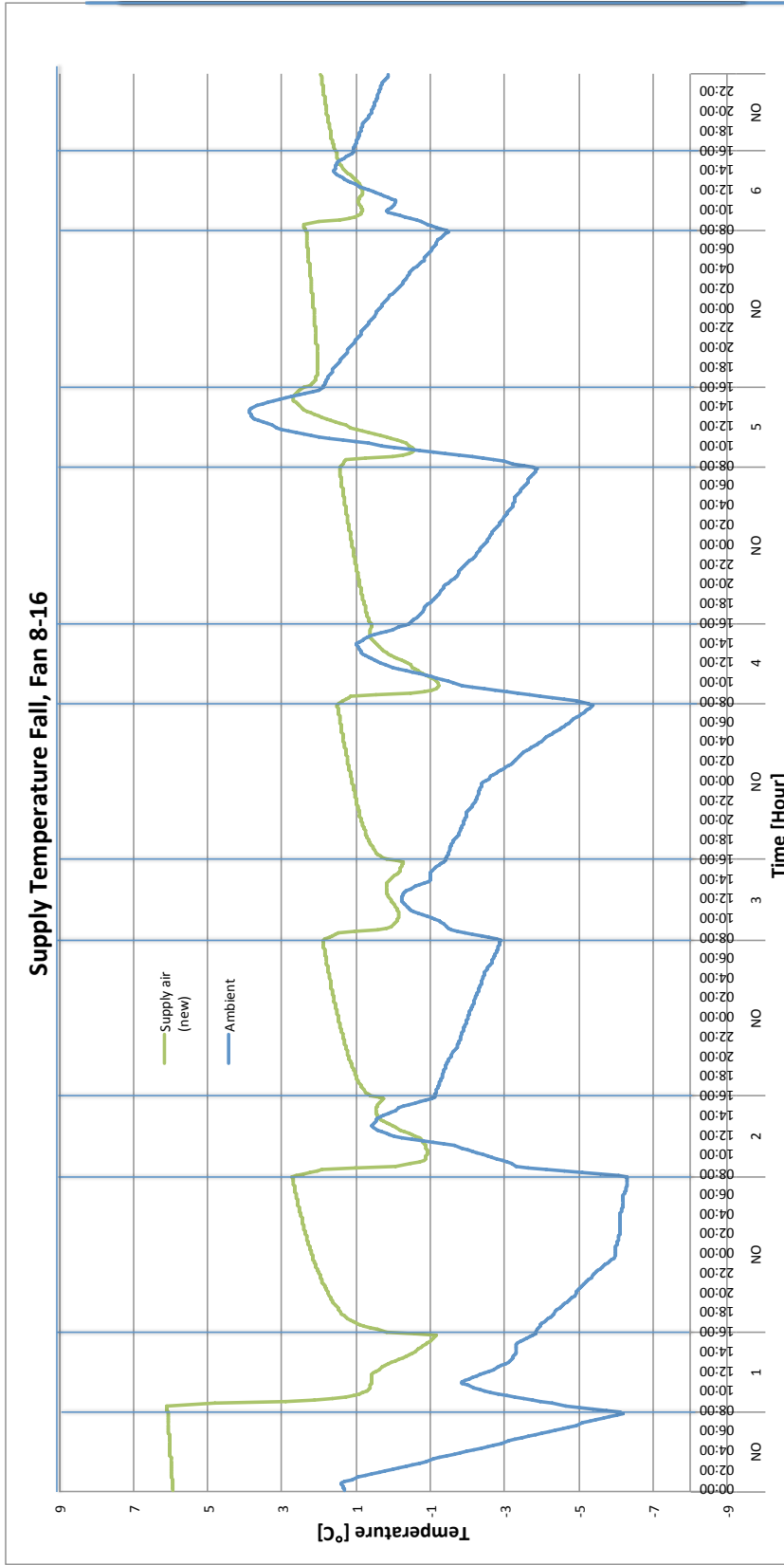
Figure 63: Supply Air And Ambient Air 1-6 November, Fan 8-16
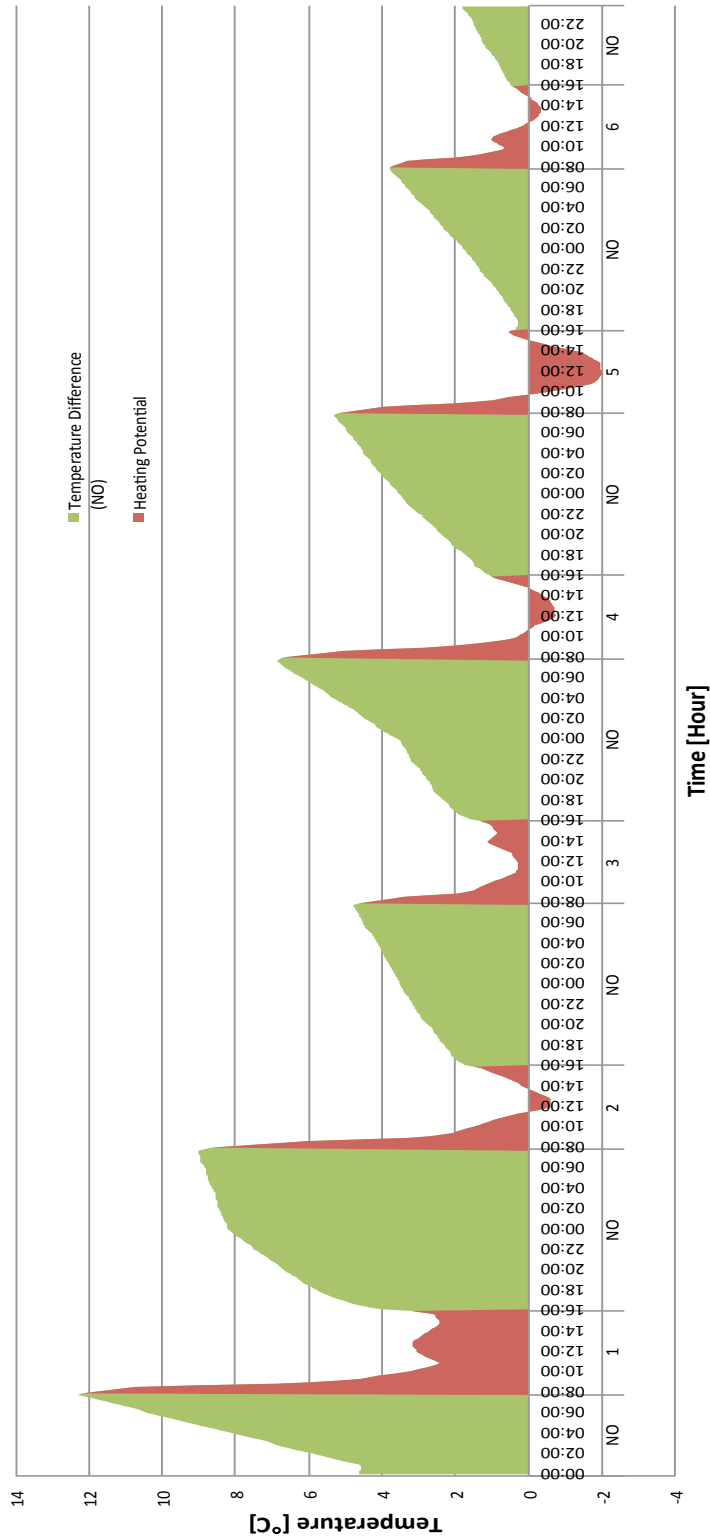
Figure 64: Heating Potential 1-6 November, Fan 8-16
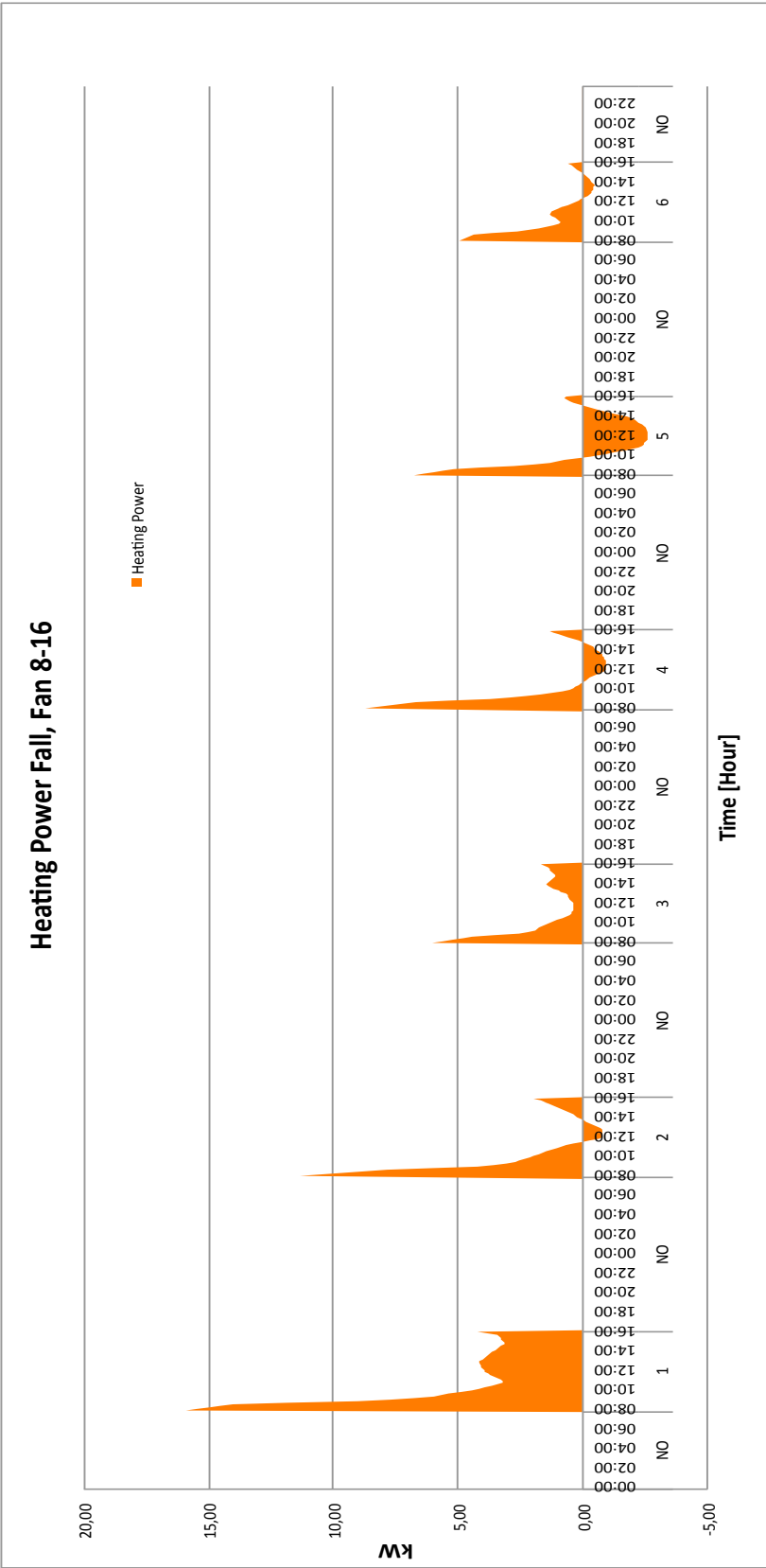
Figure 65: Heating Power 1-6 November, Fan 8-16

73

The result of the average heating power for every day is summed up in the following table. For the constant fan mode the duct is cooling the intake air instead of heating it most days, which is clearly an undesirable result. With a variable fan the result becomes much better, were only day 5 has a slight net cooling.

Figure 65 shows how the peaks of the heating power reaches levels of 15 and 10 kW during the first hours of operation for the variable fan case on day 1 and 2. However the average heating power during the 8 hours of operation lands on 5,35 and 1,83 kW for these two days as shown in Table 9. For the constant fan case, the heating power barely reaches 5 kW on the day 1.

Table 9: Average Heating Power Fall

Fall	Constant Fan	Variable Fan
Day	Avg. Heating Power (TOO*)[kW]	Avg. Heating Power (TOO)[kW]
1	1,57	5,35
2	-1,78	1,83
3	-0,33	1,55
4	-1,39	0,98
5	-2,35	-0,33
6	-0,43	0,97
Average period	-0,78	1,72

* TOO= During time of occupancy, 8-16 o'clock.

7.3.2.2 Winter: 11-16 January

The next season to be evaluated is the winter. In January the monthly ground temperatures are 0,3 and 2,8 °C outside the walls and the floor respectively.

Figure 66 shows how day 2 and day 5 experience colder day temperatures than the other days. The relatively warmer days before makes the duct heat the intake air these days. For the other days, the heating potential is mostly negative when the fan is running constantly.

Shutting off the fan outside the time of occupancy is seen to ameliorate the temperature characteristics substantially as seen in Figure 69. This gives a more positive heating potential on the others days, except for day 6 when there is a sudden rise in the daytime ambient temperatures.
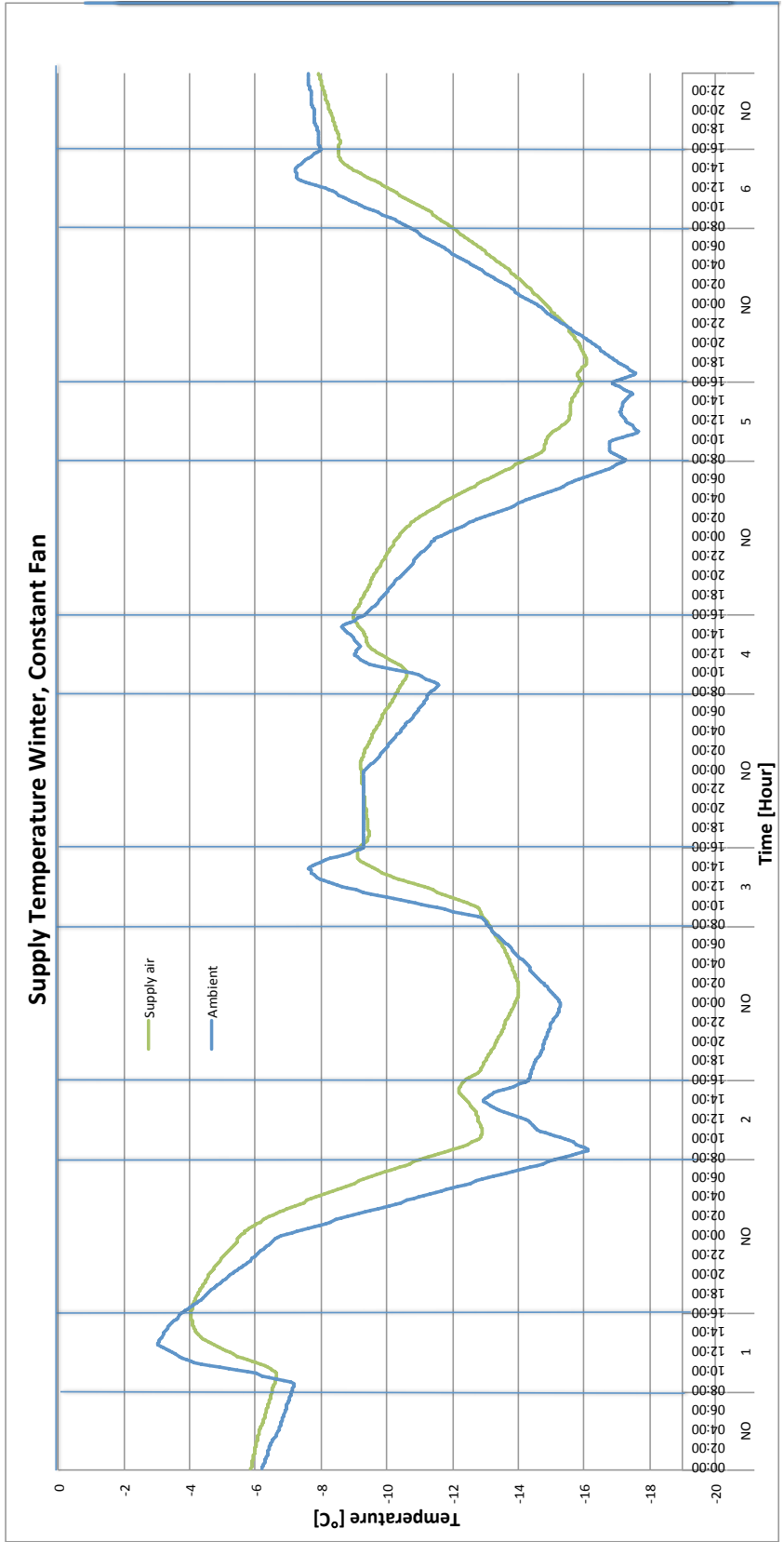
Figure 66: Supply Air And Ambient Air 11-16 January, Constant Fan
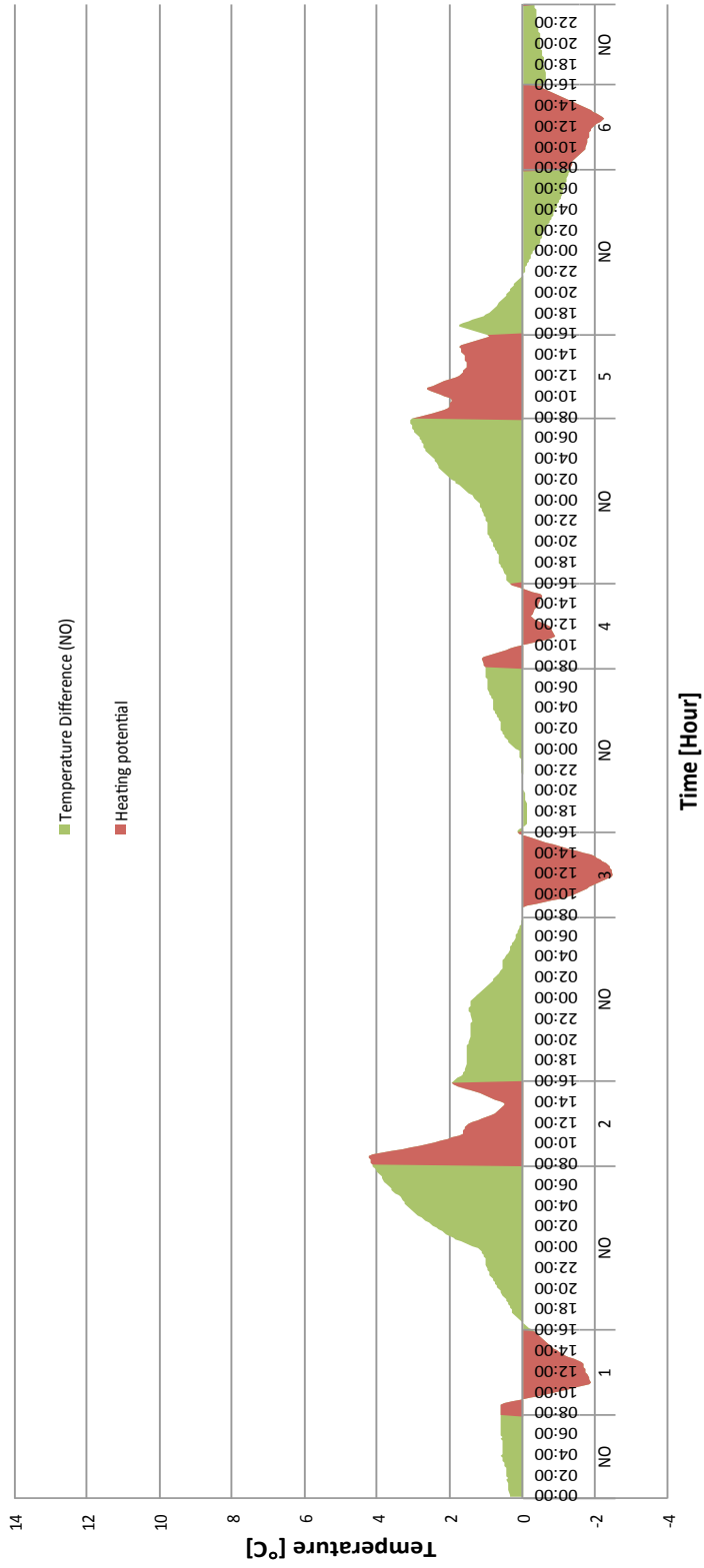
Figure 67: Heating Potential 11-16 January, Constant Fan
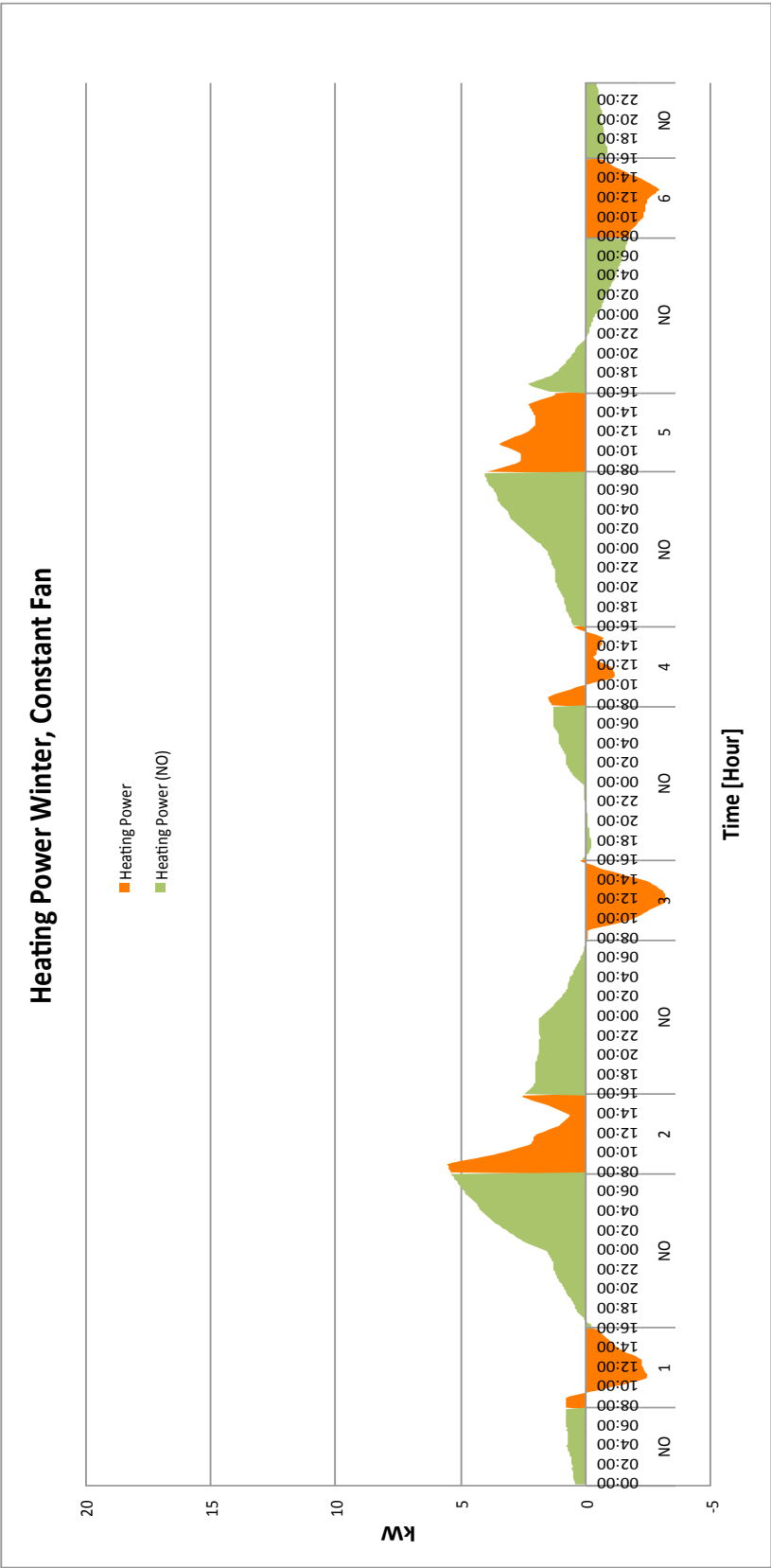
Figure 68: Heating Power 11-16 January, Constant Fan

77
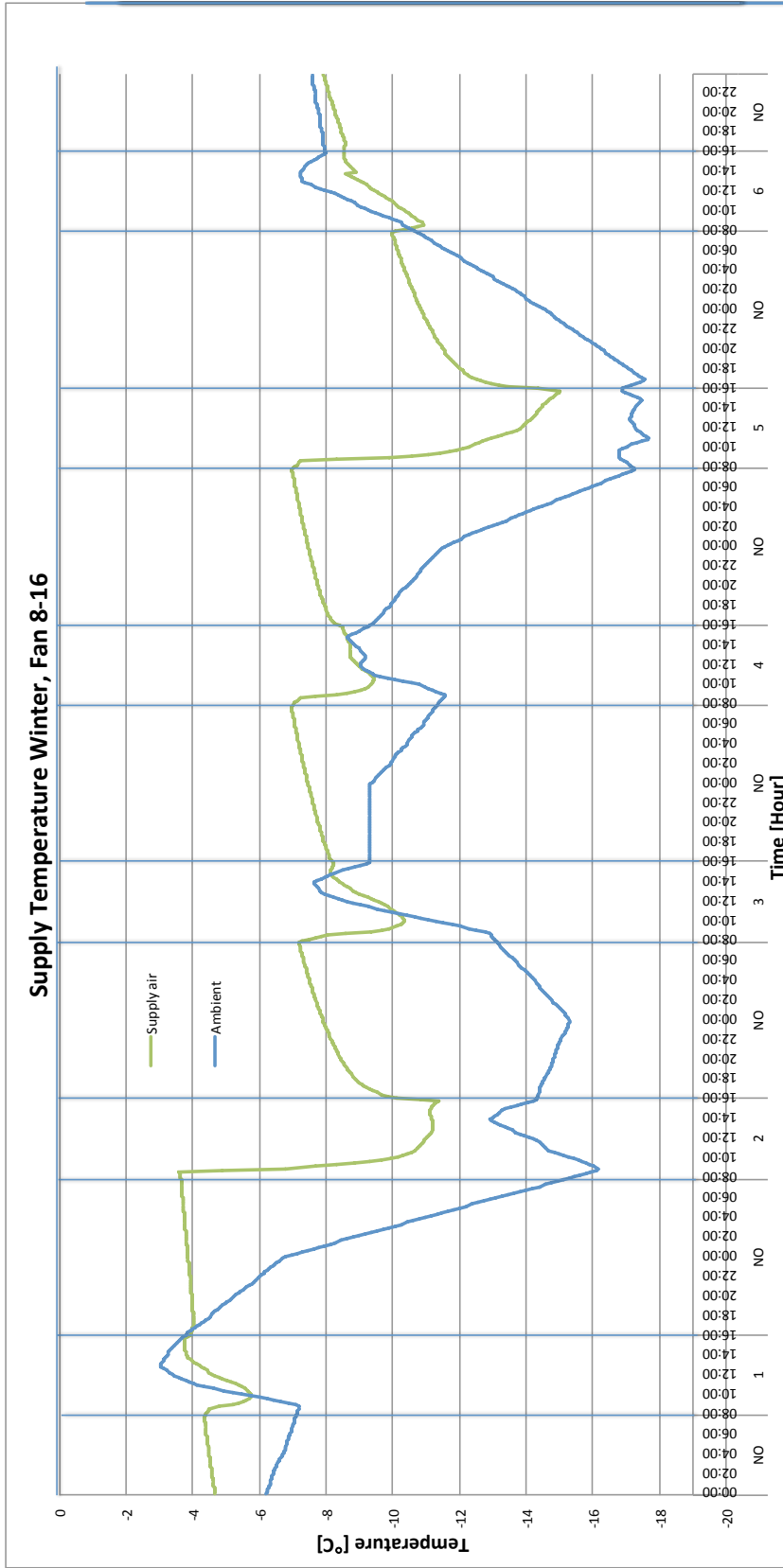
Figure 69: Supply Air And Ambient Air 11-16 January, Fan 8-16
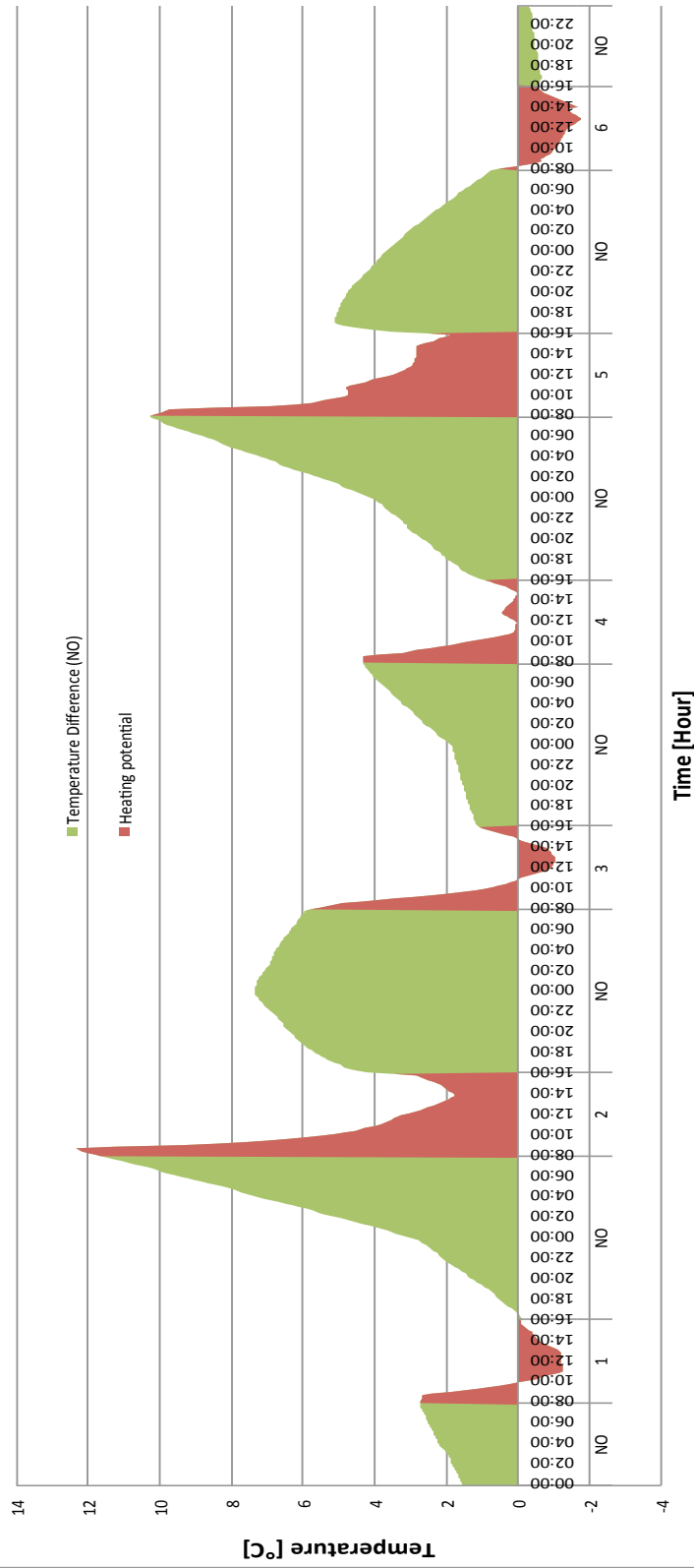
Figure 70: Heating Potential 11-16 January, Fan 8-16
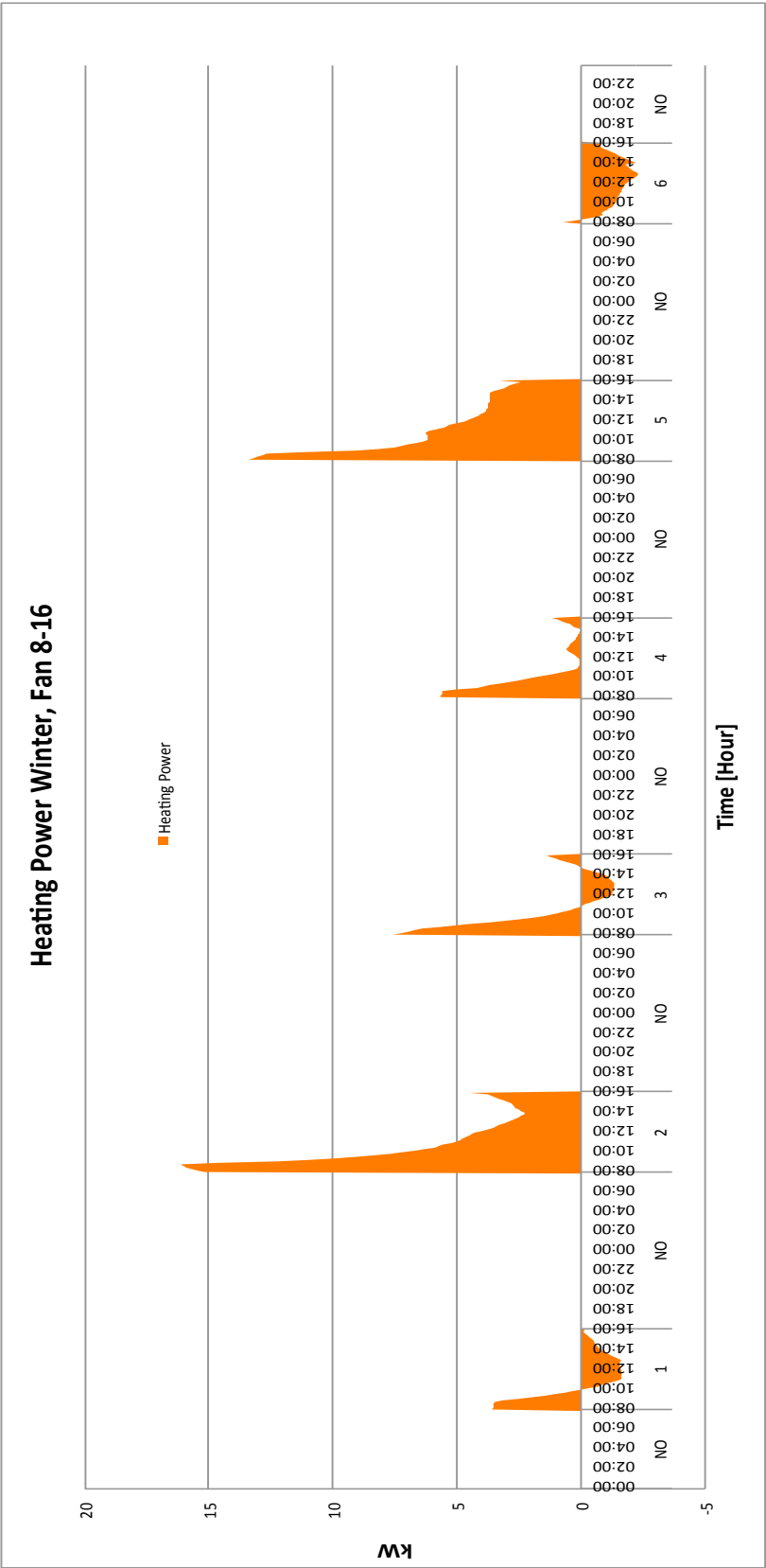
Figure 71: Heating Power 11-16 January, Fan 8-16

For the constant fan mode, the duct gives a heating effect on the two coldest days and cooling on the remaining ones. Once again, by varying the fan, this negative trend turns to a situation where the duct heats 4 out of 6 days.

The constant fan mode barely reaches an effect of 5kW in day 2, whereas in the variable fan case this number climbs to 15 kW on day 2 and 14 kW on day 5 as being the maximum effect observed in that period, according to Figure 68 and Figure 71.

Table 10: Average Heating Power Winter

Winter	Constant Fan	Variable Fan
Day	Avg. Heating Power (TOO)[kW]	Avg. Heating Power (TOO)[kW]
1	-1,14	-0,16
2	2,54	6,00
3	-1,76	0,93
4	-0,13	1,39
5	2,47	5,75
6	-2,07	-1,41
Average period	-0,01	2,08

7.3.2.3 Spring: 14-19 March

In March the monthly ground temperatures are -0,9 and 1,4 °C outside the walls and the floor respectively. This is a few degrees less than for the winter and the ambient temperature is generally higher. This makes the ground less suited for preheating in this period, which is confirmed by both of the graphs with the supply air vs. ambient air temperature.

Figure 75 shows how the temperature falls also when the fan is turned off. The reason for this is because in this period the ambient temperature is higher than the ground temperatures.
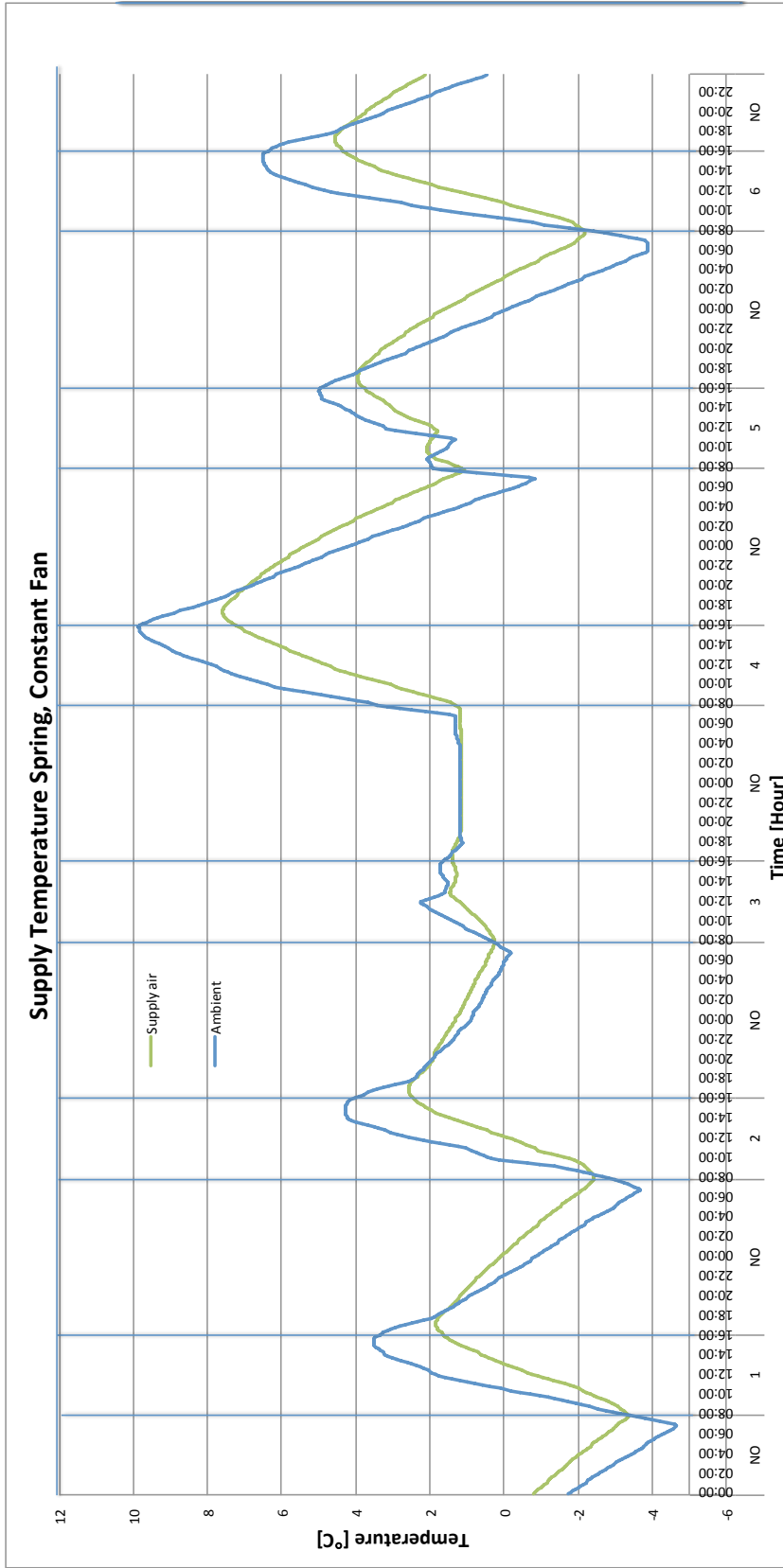
Figure 72: Supply Air And Ambient Air 14-19 March, Constant Fan
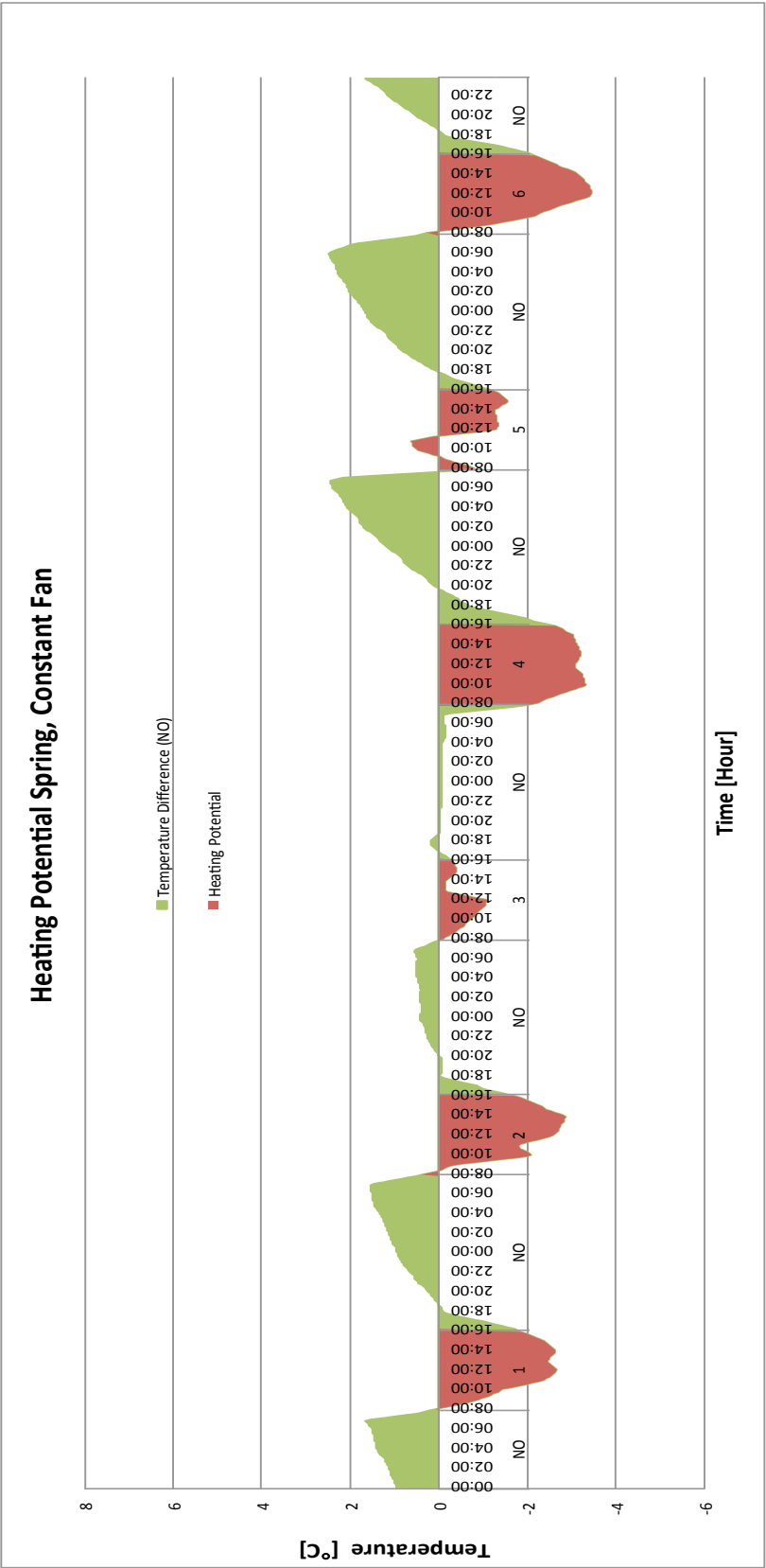
Figure 73: Heating Potential 14-19 March, Constant Fan
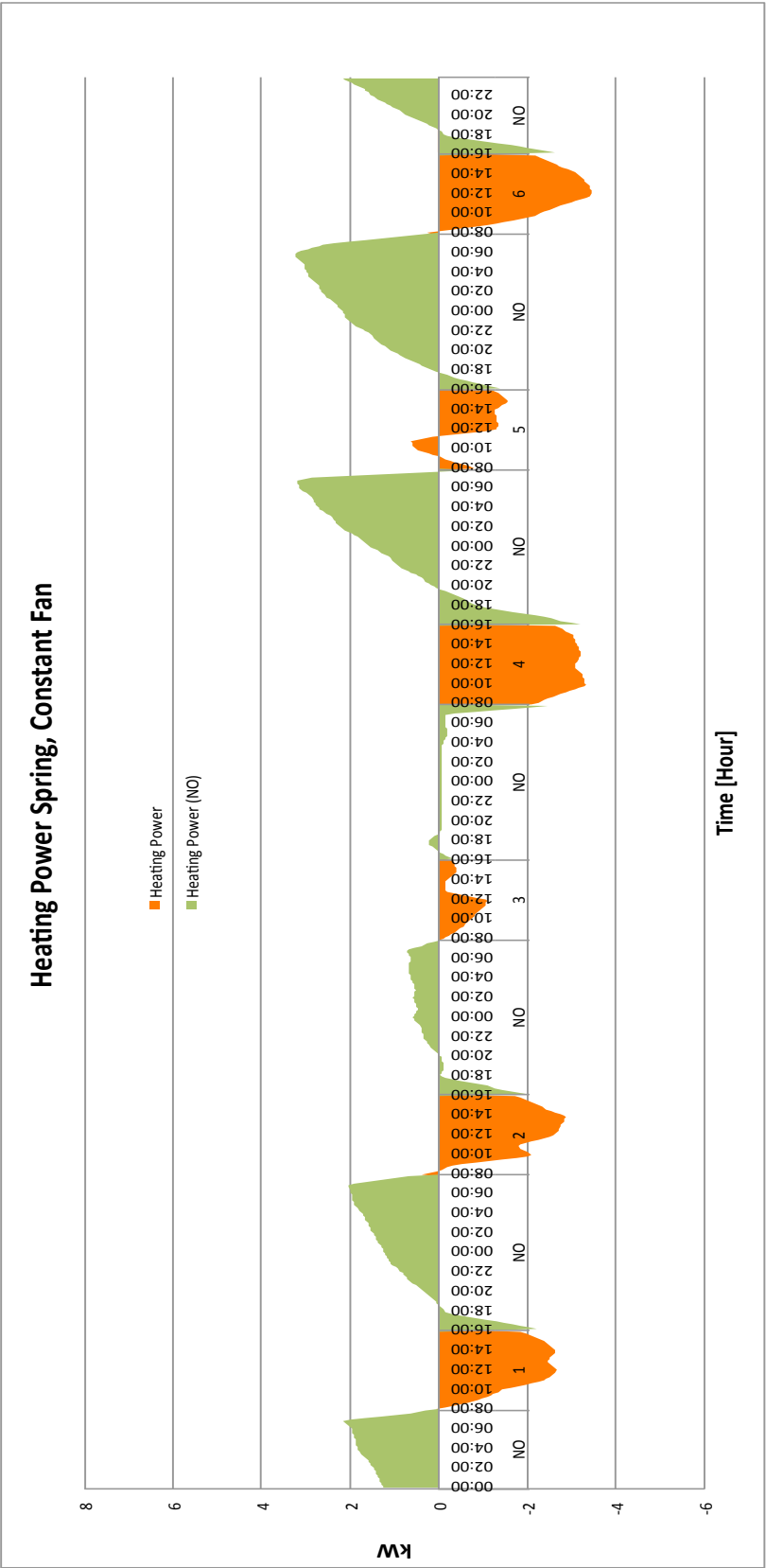
Figure 74: Heating Power 14-19 March, Constant Fan
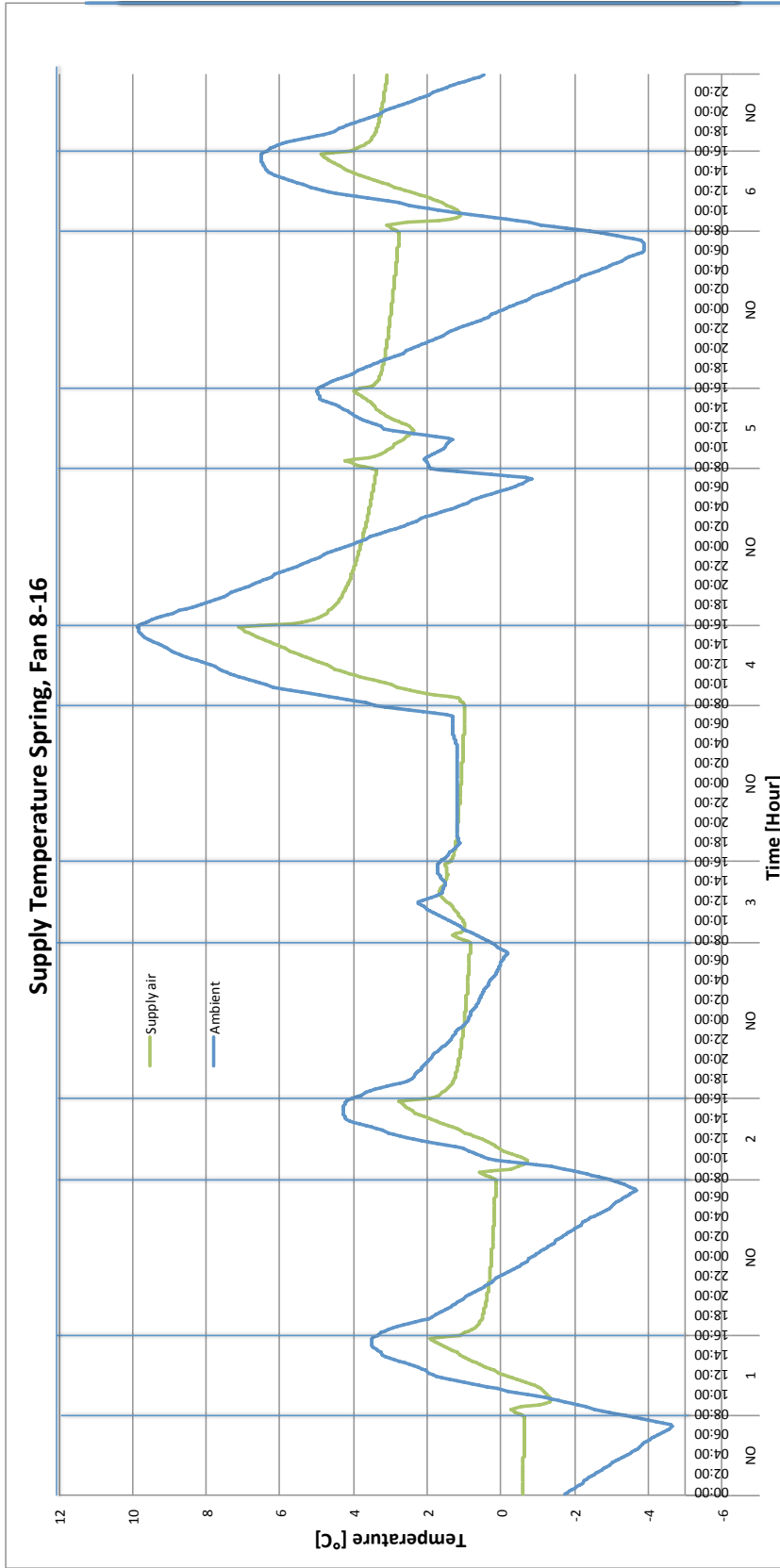
Figure 75: Supply Air And Ambient Air 14-19 March, Fan 8-16

85

Figure 76: Heating Potential 14-19 March, Fan 8-16
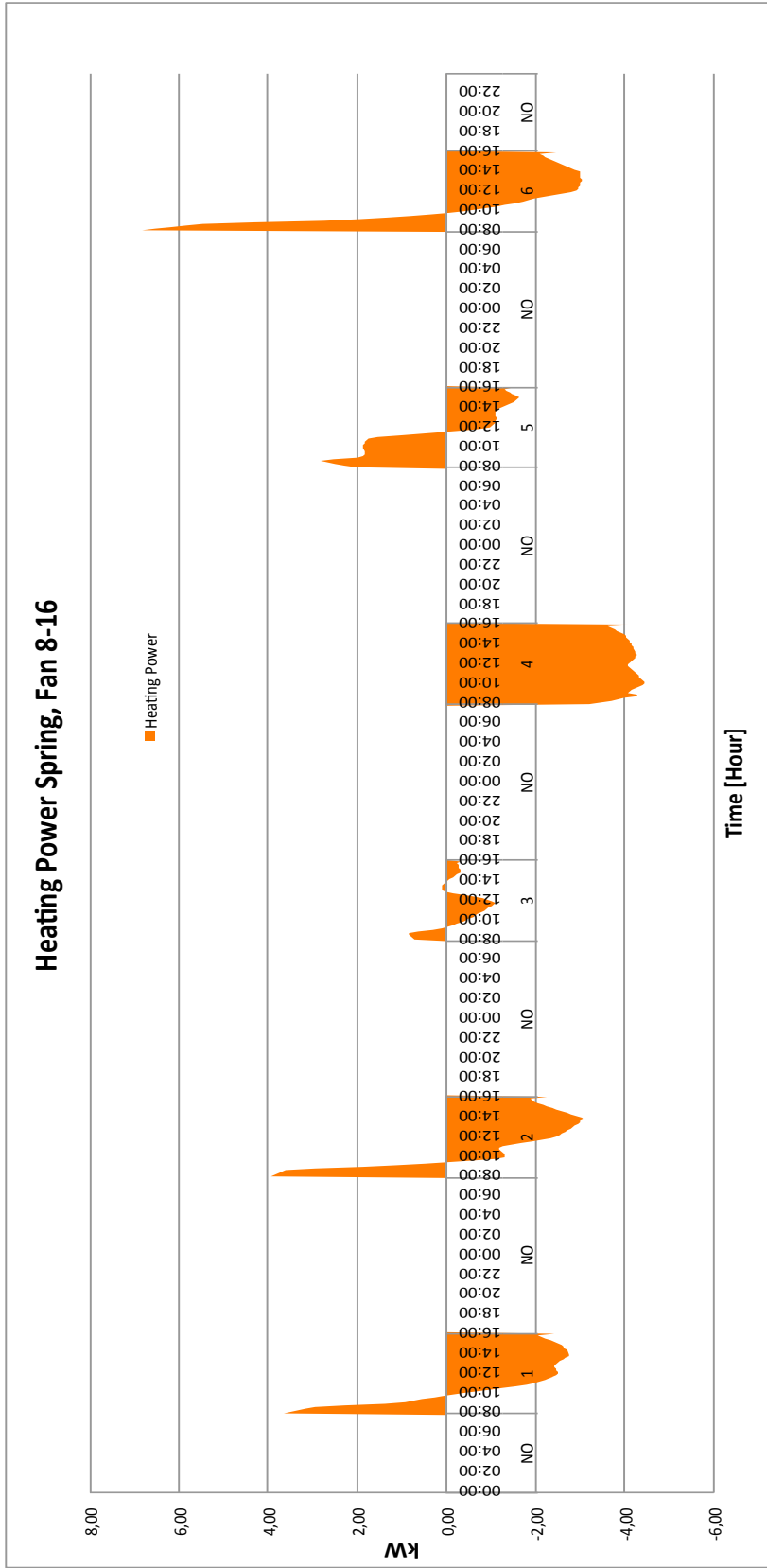
Figure 77: Heating Power 14-19 March, Fan 8-16

For both of the modes the culvert is cooling the intake air almost every single day. Turning off the fan is still beneficial, because it prevents further cooling of the culvert walls. But the overall contribution of heating is negative.

For both of the cases the culvert gives a negative net heat flow for the period. For the variable fan, the heat loss is 83% less, by comparing the numbers in the table below.

Table 11: Average Heating Power Spring

Spring	Constant Fan	Variable Fan
Day	Avg. Heating Power (TOO)[kW]	Avg. Heating Power (TOO)[kW]
1	-2,55	-1,24
2	-2,53	-1,22
3	-0,66	-0,22
4	-3,93	-4,11
5	-0,93	0,16
6	-3,25	-0,94
Average period	-2,31	-1,26

7.3.3 Precooling Season

In the precooling season, the main objective should be to cool the air down if the ambient temperature is sufficiently high i.e. higher than 22 °C. However, the highest temperatures found in the climate file for Grong are in the period chosen for the summer. These ambient temperatures are much lower than the ones measured for the summer 2002 presented in Figure 14.

The mass flow rate is increased during the summer to 2,7kg/s whenever the fan is turned on. For the variable fan, it is on between 4 and 16 o'clock. The reason for extending the fan hours to start at 4 instead of 8 o'clock was to benefit from the low nocturnal ambient temperature.

$$Cooling\ Potential = T_{ambient} - T_{supply\ air}\ [°C]$$

$$Temperature\ Difference\ (NO) = T_{ambient} - T_{supply\ air}\ In\ time\ of\ no\ occupancy\ [°C]$$

$$Cooling\ Power = \dot{m}\,cp\left(T_{ambient} - T_{supply\ air}\right)\ [kW]$$

$$Cooling\ Power\ (NO) = \dot{m}\,cp\left(T_{ambient} - T_{supply\ air}\right)\ [kW]$$

7.3.3.1 Summer: 18-23 July

Two extra lines have been drawn in Figure 78 and Figure 81 to show the temperature range (19 to 22 °C) in which the temperature is considered to be on a comfortable level. Any ambient temperature above 22 °C should be cooled

down during the time of occupancy. Only on day 4 and 5 the ambient temperature is more than 2K above the above the comfortable temperature range. In other words, the potential for necessary precooling is naturally very reduced. In the measurement from 2002 the potential for precooling was much higher (Figure 14) due to a much higher daytime temperature.

The undisturbed ground temperatures outside the walls and the floor are 11,1 and 8,5 °C, i.e. quite good for cooling the ambient air during hot summer days. This can be seen in Figure 81 when the temperature sinks when the fan is shut down. However the nights are quite cool, so keeping the fan running the whole time contributes to more cooling in the time of occupancy, as seen in Table 12.

However, due to the low ambient temperature in the beginning of day 1,2,3 and 6 the culvert contributes in an undesirable cooling, since the culvert walls are even colder due the previous night, and the start of the fan at an earlier point.
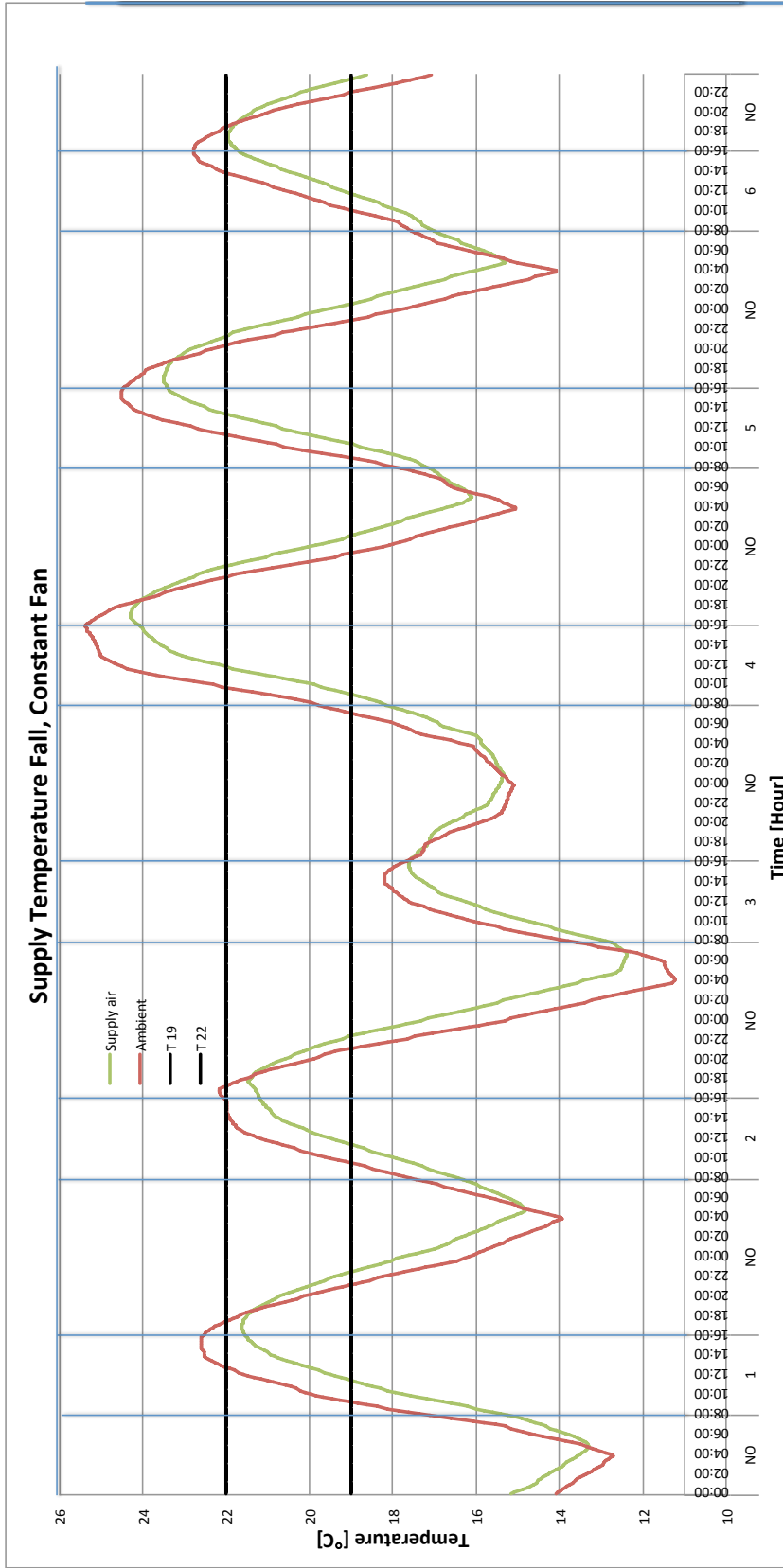
Figure 78: Supply Air And Ambient Air 18-23 July, Constant Fan

90
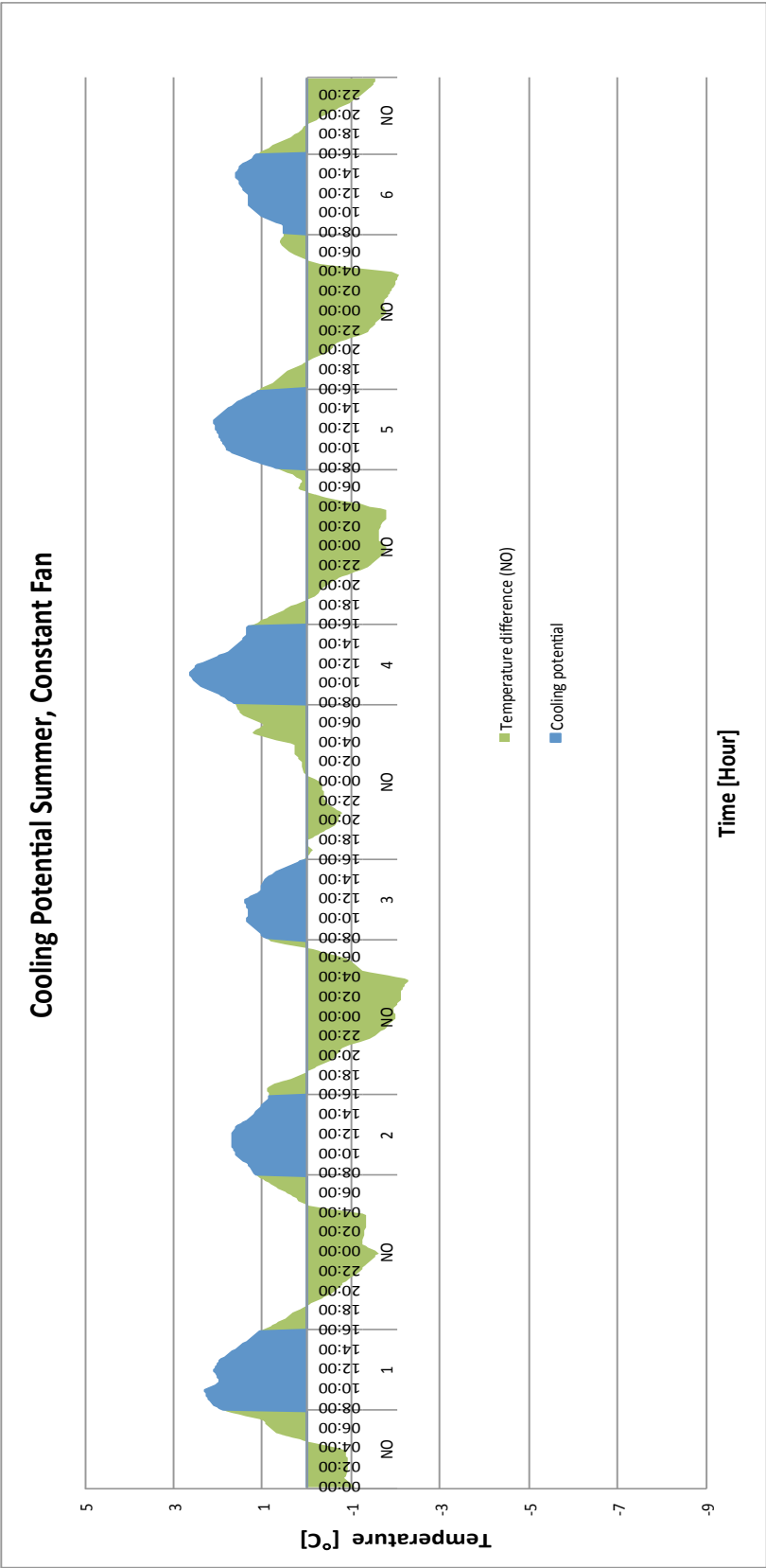
Figure 79: Cooling Potential 18-23 July, Constant Fan
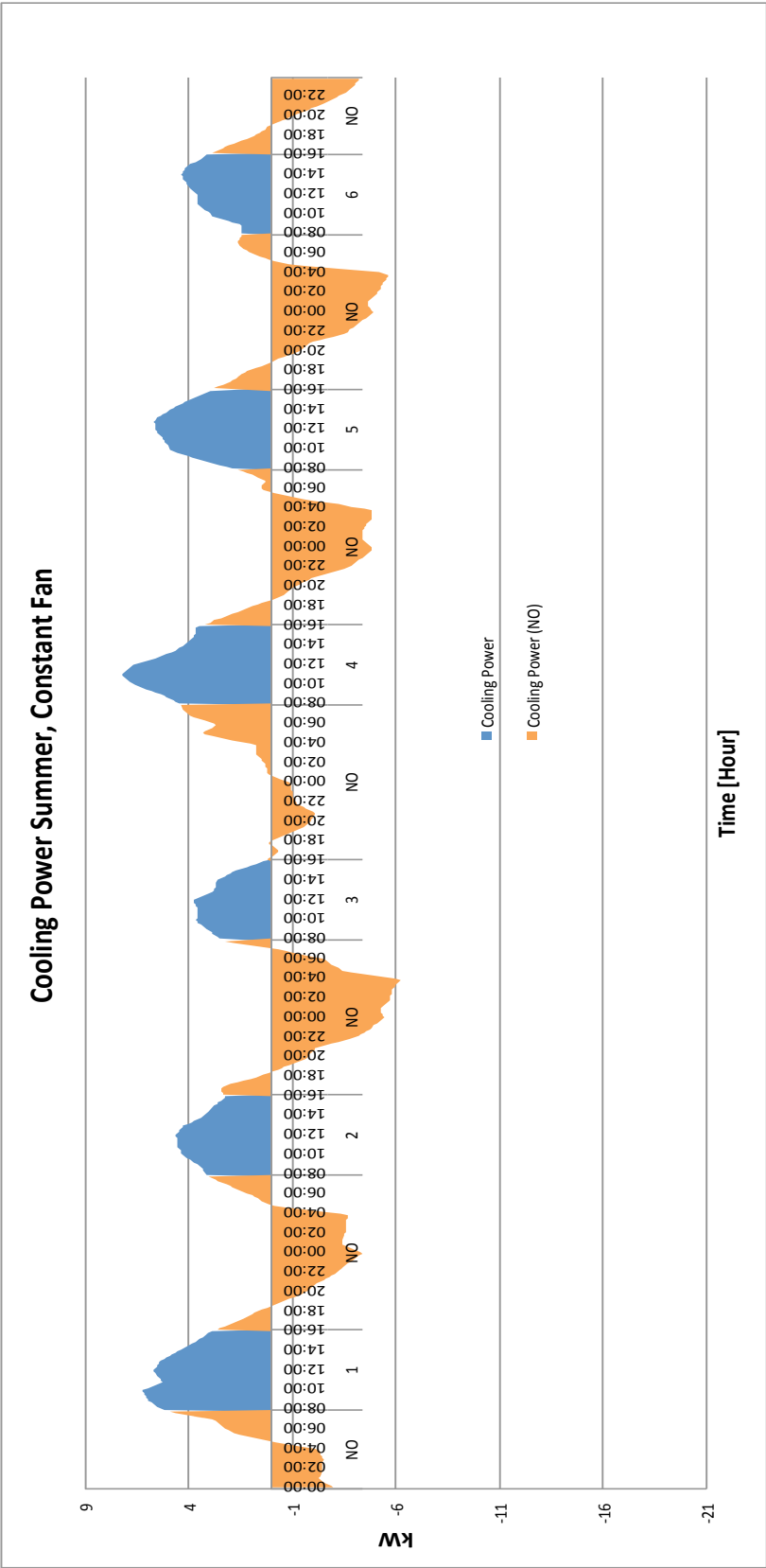
Figure 80: Cooling Power 18-23 July, Constant Fan
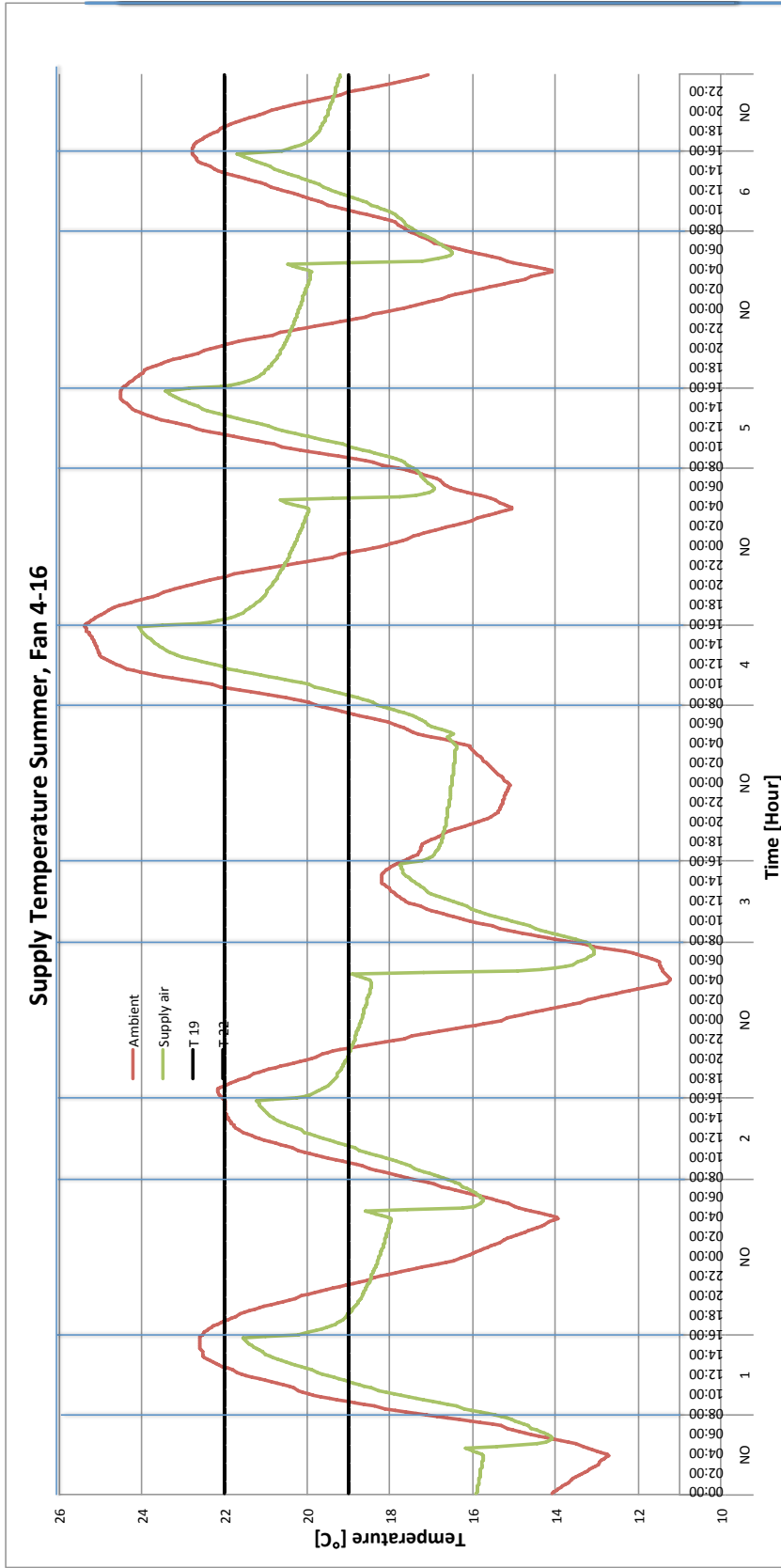
Figure 81: Supply Air And Ambient Air 18-23 July, Fan 4-16

93
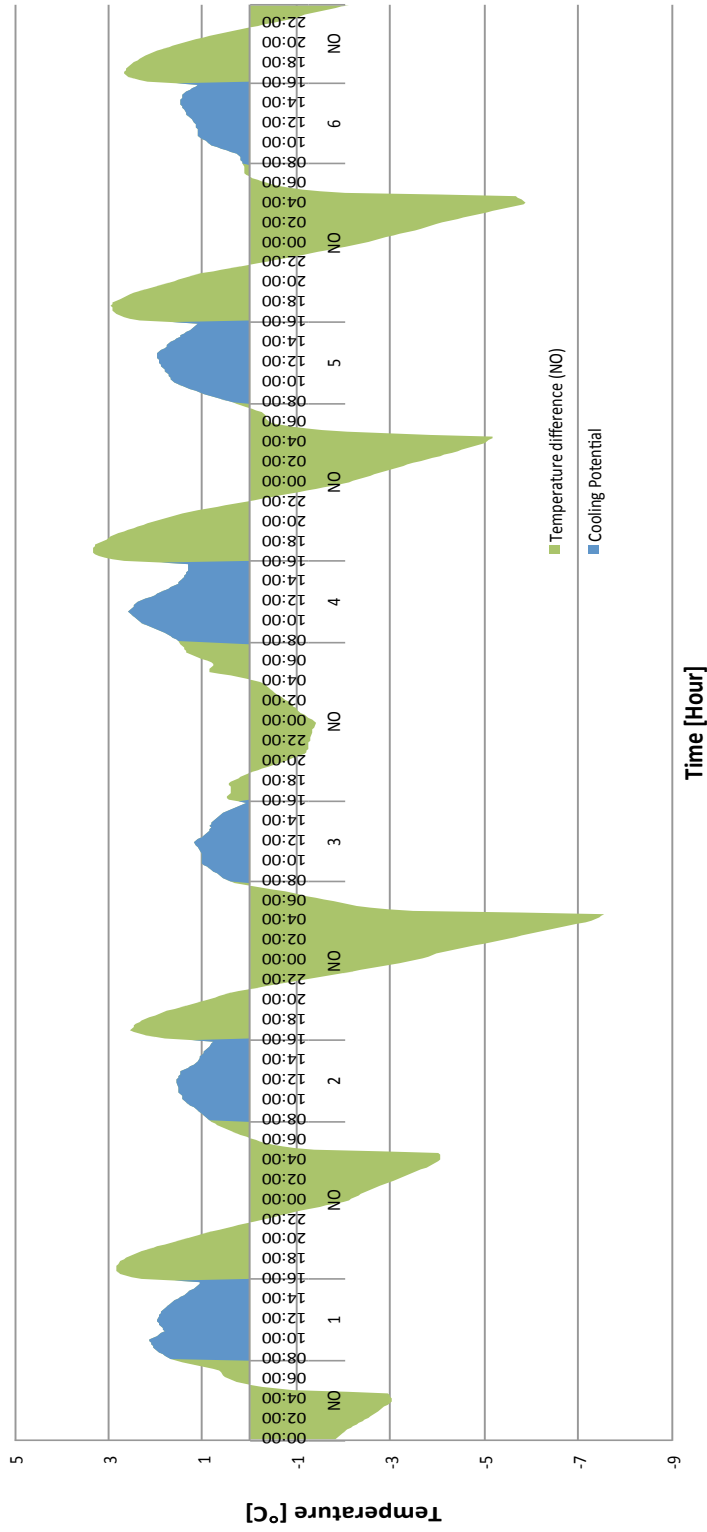
Figure 82: Cooling Potential 18-23 July, Fan 4-16
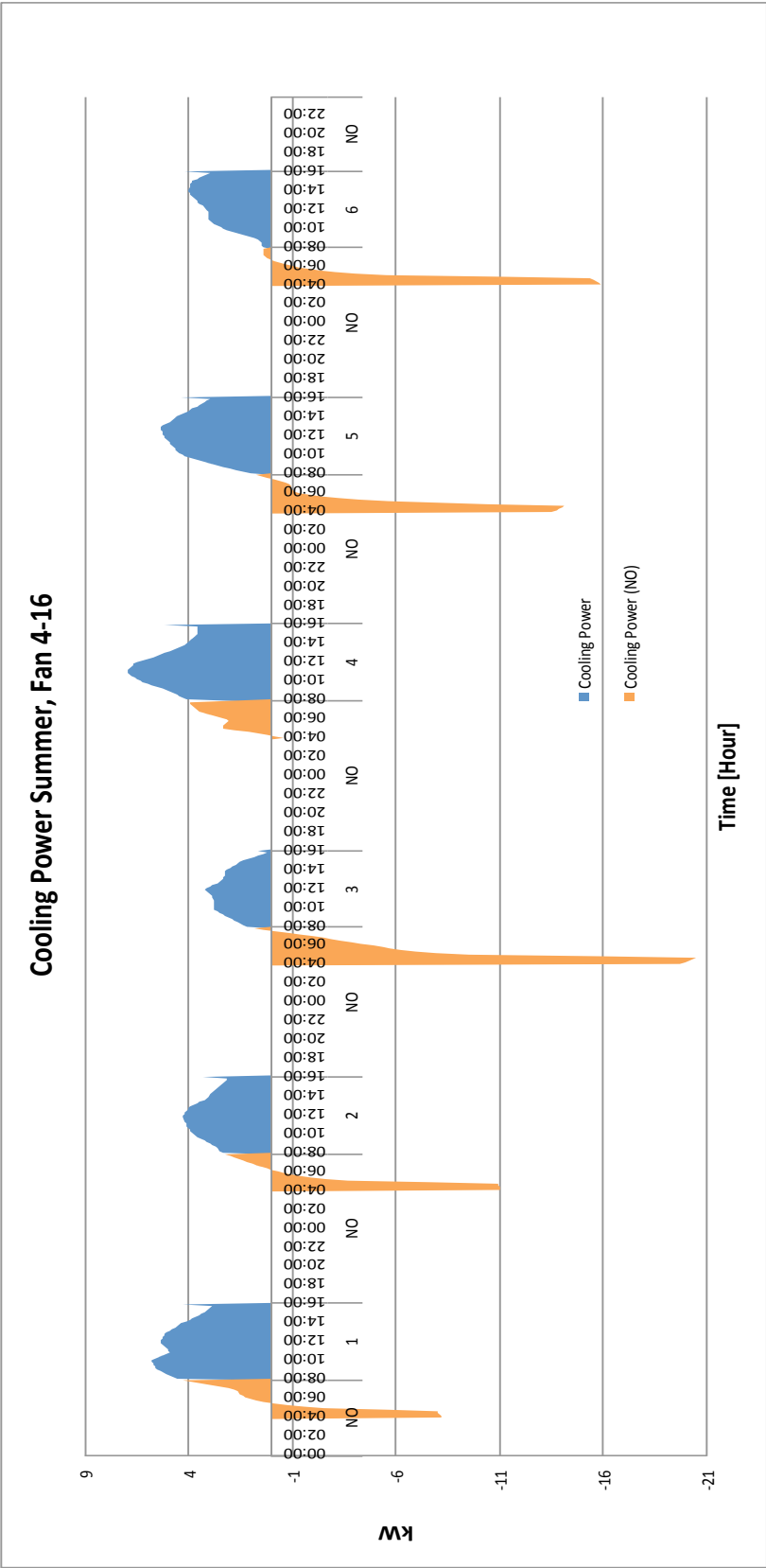
Figure 83: Cooling Power 18-23 July, Fan 4-16

95

For the constant fan mode, the highest amount of cooling is on day 1 and 4 where the intake air temperature is reduced by 2,5 K, which can be seen by observing Figure 79. Similar results are observed for the variable fan mode. This resulted in approximately 7 kW as the highest cooling power provided in both cases (Figure 80 and Figure 83). The average characteristics are summed up in the table below.

The highest cooling is achieved when the fan is running constantly. Day 3 is the day with the least amount of cooling. That day there was no cooling demand since the ambient temperature was below 18 °C the whole time.

Table 12: Average Cooling Power Summer

Summer	Constant Fan	Variable Fan
Day	Avg. Cooling Power (TOO)[kW]	Avg. Cooling Power (TOO)[kW]
1	5,05	4,75
2	3,71	3,35
3	2,79	2,14
4	5,34	5,18
5	4,49	4,11
6	3,28	2,81
Average period	4,11	3,72

8 Discussions

8.1 CFD: Uniform Flow

Both of the uniform cases had velocity profiles and temperature plots confirming that there was creation of boundary layers and that these were made bigger either in the ceiling or on the floor depending on the temperature differences between the surface and the air. The boundary layer decreased the local heat exchange on the surface it was closest to.

For uniform flow the heat exchange is approximately the same on the left and the right side. In a real case this will probably not be same, since the temperature is profile in the ground is bound to be non-uniform and vary in any given direction.

The mass flow rate affected the heat transfer coefficient. This was observed in the winter case when the model was tested with a higher mass flow rate. The reason is that the boundary layers will not develop as easily when the velocities are bigger, thus allowing a higher heat exchange between the walls and the air.

8.2 CDF: Rotational Flow

The rotation increased the heat transfer coefficient in both the winter and the summer case. The temperature plots showed that boundary layers were still developed toward the exit of the duct, but now they were pushed a bit away from the floor or the ceiling and on to one of the walls. The result was a skewness in the heat transfer with a higher heat transfer coefficient on either the left or the right wall.

However, there was an insecurity of how much the tangential component should set to compared to the axial component, in order to simulate a flow downstream of an axial fan most realistically. For the moderate rotation cases, a wave shaped profile was observed as seen in Figure 36 and Figure 40. When comparing these with the velocity profile belonging to the strong rotation case as seen in Figure 45, the strong rotation profile seems to have a greater similarity with the measured velocity profile measured at Grong in 2005 (Figure 13).

The development of the axial vorticity was greatly enhanced for the strong rotational case. When the normalized axial velocity development was plotted throughout the duct (Figure 48), it shared a great similarity with was measured by Chen et al. as seen in Figure 11.

All the predicted heat transfer coefficients were much lower than what had already been reported in the measurements in the literature search. A probable reason for the underestimation is that the CFD model only relied on the k-ε

turbulence model, when ideally it should have been constructed as a two turbulence model with k-ε on the main flow and k-ω in the near wall regions. According to the Ansys user–guide the k-ε is intended for fully developed turbulent flows. However due to the complexity of implementing the two turbulence model, it was omitted. However characteristics of the flow picture seem quite plausible.

An interesting result was the improvement in the average heat transfer coefficient between the uniform flow and strong rotational case for the summer case. It was augmented from 4,29 to 9,69 W/m^2K, i.e. an improvement of 125%. This result is very close to the same improvement reported by Chen et al. with and improvement of 117% between the uniform and the rotational case.

8.3   ESP-r Model

The ESP-r model was updated with a constant heat transfers coefficient on all the surfaces for all the different cases. The value of 30 W/m^2K seems justifiable when comparing with the experimental data of Wachenfeldt, Zhang and Chen et al. as discussed in chapter 3. In a real case the heat transfer coefficient is likely to change along the duct with the highest magnitude at the entrance and falling value until reaching fairly constant level after certain length as illustrated for the Nusselt number in Figure 6.

A one-dimensional heat conduction model with a monthly average undisturbed ground temperature is not the most accurate model, but it has obvious advantages of being easier to implement than the alternatives and requires less input data. For this case, it is important that the model captures the thermal storage effect of the ground and that the undisturbed ground temperatures should have the right impact on the culvert walls. Since the thermal properties of the ground have not been measured, the default values of heavy mix concrete, clay and ground were chosen from the ESP-r standard library.

8.4   Ground Temperature Plots

The ground temperature plots are an attempt to get a better understanding of how the temperature flux propagates through the earth layers, but also how the impact of an enhanced heat transfer coefficient will have on the model. It was seen to have huge effect in the layers closest to the concrete surface, because a bigger heat transfer coefficient allows a higher heat flux given a temperature difference between the culvert air and the surface temperature.

The spread was biggest for the scenarios done with constant fan running the whole time. This is because the culvert surface will be subject to high daytime temperatures and cold nocturnal temperatures. The old model had a spread from 0 to 6 °C in the floor layer with the constant fan. This range was augmented to -4 to 4 °C for the new model, i.e. an increase of 6K to 8K.

When the fan was shut off outside the time of occupancy when the ambient temperature was mostly low, the temperatures rose with a several degrees and the ranges decreased. Now the ranges were 4-7 and 0-6 °C for the old and the new model respectively i.e. also an increase from 3K to 6K. This indicates that shutting off the fan is beneficial in terms of charging the culvert walls when the outside ambient temperatures are low during a heating period.

8.5   Culvert Performance For Heating

Firstly a comparison of the old and the new model was done for the fall. In the case of constant fan the old model supply air is seen to follow the fluctuations of the ambient air more closely than the new model. This is a natural result since the new model allows the culvert surfaces to influence the temperature of the intake air more in terms of heat exchange, thus giving a bigger difference between the supply air and the ambient temperature.

In order to evaluate and quantify the heating outcome of using the culvert, two graphs showing the temperature difference between the supply air and the ambient temperature (heating/cooling potential) and the heating/cooling power were made.

For the heating seasons, keeping the fan closed outside the time of occupancy when ambient temperatures are low, is seen to be quite beneficial, if not crucial to avoid a negative impact of the culvert on certain days. The culvert performance at a given day is extremely connected the ambient temperature prior to that period. In Figure 60 for November one can see how the duct is mostly cooling down the intake air during the time of occupancy because the temperature was colder on the day before. The exception is day 1 in which the duct has positive contribution due to the relative high ambient temperature the day and night before. However, by shutting off the fan during time of no occupancy, the situation changes radically. From having a negative contribution on five out of six days, the duct will only have a minor negative effect on day 5. By looking at Figure 65 of the heating power supplied, one can see how the effect of the duct is most positive during the first few hours of the time of occupancy. This is because the surface layers are warmest right before the fan is turned on and then the heat is released as cold ambient air starts flowing through the duct.

The same observations are also done during the winter. The effect of the culvert depends on the ambient temperature prior to the day of assessment. Day 1, 3 and 6 are the three hottest days in this period and the culvert cools the air all of these days in the constant fan scenario. Changing to variable fan this negative trend changes, and the duct manages to provide heating on four out of six days. Day 1 had an almost neutral contribution and day 6 was negative.

For the spring the duct is not providing the intake air with much heating, quite on the contrary. For both modes the average contribution is negative, meaning that overall the duct was cooling the intake air instead of heating it. This is confirmed by Table 11 and by looking at the graphs of heating power for the

spring. The negative contribution during the spring and the positive contribution during the winter and fall can be explained by comparing the ground temperatures vs. the ambient temperature for each season. In the first two seasons, the ground temperatures are higher than the ambient temperature. But in the spring, the ground temperatures are at their lowest point while the ambient temperature is rising. This is confirmed by looking at Figure 63, Figure 69 and Figure 75 where the temperature in the duct rises when the fan is shut off for the first two periods and how it falls in the spring season.

8.6   Culvert Performance For Cooling

The cooling season was chosen to be for the week with the highest observed daytime temperatures. Unfortunately the available climate data doesn't contain days with hotter ambient temperature than just a few degrees above the level for which cooling is required. The ambient temperatures are mostly within the comfort zone, and therefore the requirement for cooling is diminished. However for the days when the temperature is above 22 °C the culvert offers cooling of 1-2K for the hottest days for both modes. The highest cooling effects were measured to be approximately 7kW for in both cases.

This is considerably lower than what was observed in 2002 as shown in Figure 14 when the ambient temperatures where much higher. There the culvert was seen to be able to cool the intake air from 30 °C to 23 °C on day 5, i.e. 7K cooling with the highest cooling power reported to be 17kW. It would have been interesting to see how the culvert model would have responded to ambient temperatures that high to have a direct comparison.

Un unwanted effect is when the duct cools the ambient air below 19 °C, which is seen for the first few hours on day 1, 2 and 4. For day 3 the ambient is too low to induce any need for cooling, hence the cooling provided that day should have been avoided.

9 Conclusion

A CFD-model was created in order to explore the effects different inlet flow conditions. The flow conditions and the heat transfer characteristics were seen to be strongly affected by varying the inlet flow from uniform to rotational. In the uniform and moderate rotational cases clear effects of buoyancy could be seen from the temperature plots and in the velocity and temperature profiles. When the axial-vorticity and the velocity profile were compared to the results from the literature research, it was decided to increase the tangential component even more in order to simulate these results better. The result was a flow with no sign of buoyancy effects shown in the temperature plots, and the velocity profile resembled the velocity profile shown in Figure 13. The velocity in the near wall regions had grown considerably and the overall heat transfer coefficient was augmented by 125%; a number close to was measured experimentally by Chen et al. The magnitude of the measured heat transfer coefficients was about 3 times lower than the numbers from the literature. The reason for this deviation might be a result of using k-ε for the whole flow domain instead of using the k-ε combined with k-ω for the near wall regions. If this accounts the whole deviation is unknown.

The previous ESP-r model that was made for the preparation thesis was updated with fixed heat transfer coefficients on the surfaces inside the culvert. This was seen to have a noticeable impact on the model when compared with each other for the November period. The result was a model with bigger sensitivity to the ambient temperature as the culvert performance for a particular day was seen to be very influenced by the ambient temperature prior that day. Other influencing parameters were the ground temperatures versus the ambient temperatures. If the ground temperatures were several degrees higher than the ambient temperatures, the culvert would have a good effect on the energy performance. However this effect could be made even bigger or even turn from negative to positive when the fan was shut down during the coldest parts of the day. For those reasons, a good heating effect was observed during the fall and the winter. However, for the spring an alternative preheating strategy should be found, or the culvert will cool the air most of the time.

In the case of cooling during a hot summer, the culvert is able to provide this the few days there was a need for cooling. For this particular season, the model could provide more cooling power when the fan was run the whole time. The reason for this was the summer nights had lower temperatures than the surface layers of the culvert.

The only comparable data from the site that is available was the data provided in Figure 14. However that summer the ambient temperature was particularly high, and the culvert provided a cooling of more degrees than observed for the summer case.

10 Further Studies

The CFD model should be further developed with a two-turbulence model as mentioned earlier. And further improvements of and possible refinements of the mesh should be tested out.

The ESP-r model could be updated with a three-dimensional representation of the ground heat conduction to see if that would make a significant impact on the model. In this case, more data on the ground should be collected experimentally.

More experimental data for different seasons and different mass flow rates would be desirable in order to compare with the results provided by the ESP-r model.

11 References

1. "http://www.esru.strath.ac.uk/Documents/ESP-r_cookbook_july_2011.pdf." 322.

2. Ansys (2011). "Ansys User Guide."

3. Bejan, A. K., J. (1982). Entropy Generation Through Heat and Fluid Flow, Journal of Applied Mechanics, vol. 50, issue 2, p. 475.

4. Darkwa, J., et al. (2011). "Theoretical and practical evaluation of an earth-tube (E-tube) ventilation system." Energy and Buildings **43**(2–3): 728-736.

5. Deisler, R. G. (1953). "Analysis of Turbulent Heat Transfer and Flow in the Entrance Regions of Smooth Passages." NACA TN 3016.

6. ESP-r. "http://www.esru.strath.ac.uk/Programs/ESP-r.htm."

7. F. Williams, J. W. (1970). "The development of rough surfaces with improved heat transfer performance and a study of mechanisms involved\ Proceedings of the 3th International Heat Transfer Conference\ Paris 2 ".

8. Incropera, F. P. and D. P. De Witt (1985). "Fundamentals of heat and mass transfer."

9. Labs, K. (1979). "Underground Building Climate. Solar Age, 4(10), 44-50."

10. Lienhard, J. I. L. J. V. (2005). "A Heat Transfer Textbook."

11. Per O. Tjelflaat, J. Z. a. F. H. (2011). "Measurements of Cooling Performance for an Earth-to-Air Heat Exchanger with an Axial Entrance Fan ".

12. R. Karwa, S. C. S. J. S. S. (1998). "Heat transfer coe.cient and friction factor correlations for the transitional ~ow regime in rib!roughened rectangular ducts." International Journal of Heat and Mass Transfer 42.

13. Roaf, S. (2005). Air-conditioning avoidance: lessons from the windcatchers of Iran. Passice and Low Energy Cooling for the Built Environment. Santorini, Greece.

14. S.M. Jafarian, P. H., M. Taheri (2009). "Performance analysis of a passive cooling system using underground channel (Naghb)."

15. T.Y. Chen , H. T. S. (2003). "Flow structures and heat transfer characteristics in fan flows with and without delta-wing vortex generators."

16. Wachenfeldt, B. J. (2003). <u>Natural ventilation in buildings : detailed prediction of energy performance</u>. Trondheim, Norges teknisk-naturvitenskapelige universitet, Institutt for energi- og prosessteknikk.

17. White, F. M. (2006). <u>Viscous fluid flow</u>, McGraw-Hill Professional Publishing.

18. Zhang, J. (2009). "Investigation of Airflow and Heat Transfer in Earth-to-Air Heat Exchangers."

Appendix

A: Risk Assessment

There was no need for any laboratory work or any possible harmful situations. For that reason, no risk assessment was done.

B: Additional Ansys Fluent Simulation Pictures

Summer Uniform Flow Density Plots
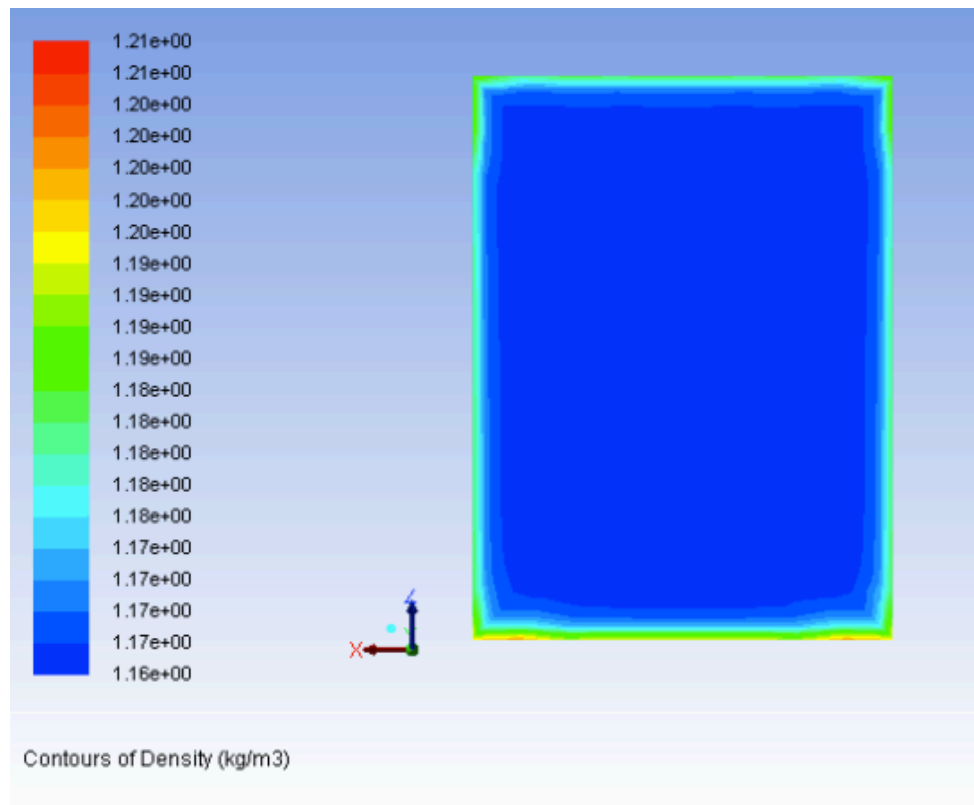
Figure 84: Density At Y= 3m
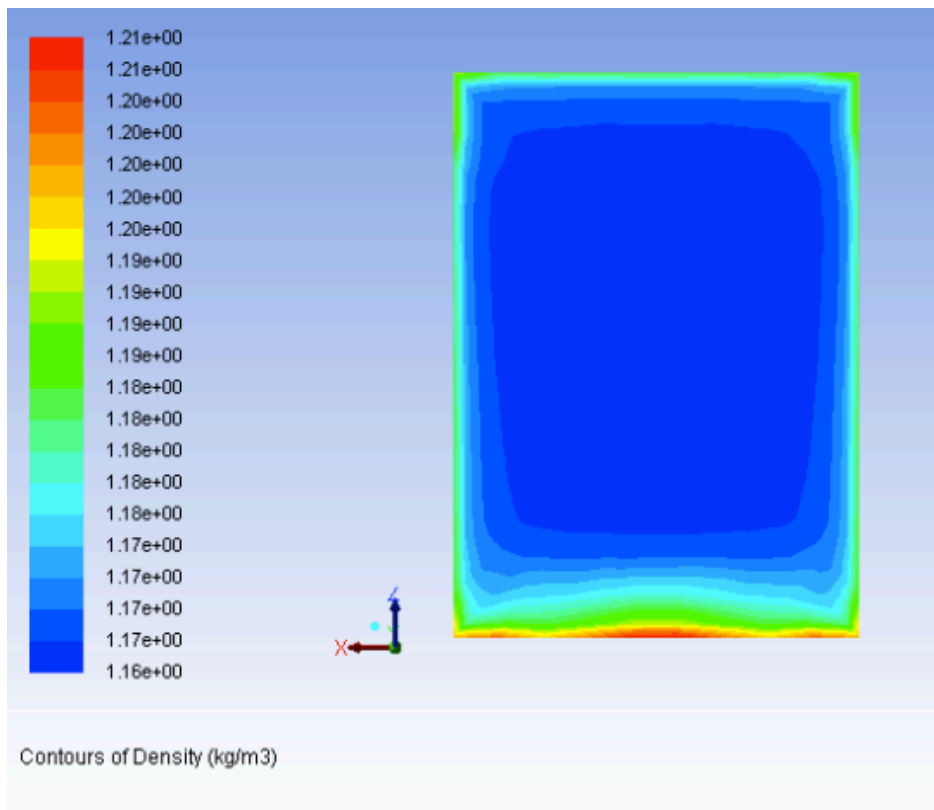
Figure 85: Density At Y= 6m
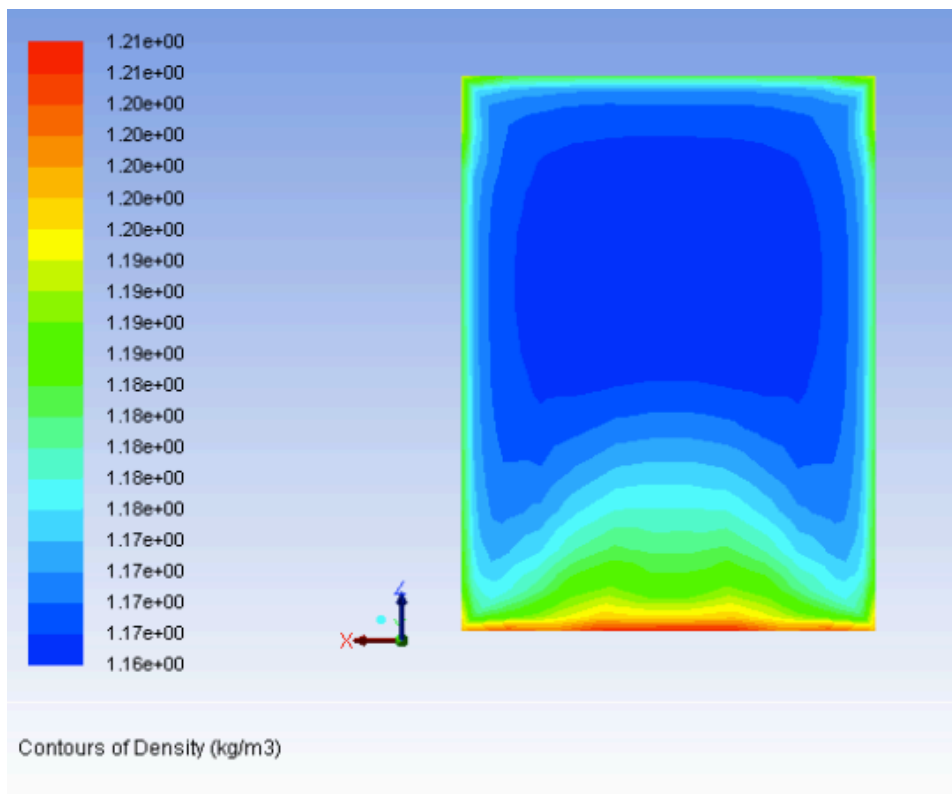
Figure 86: Density At Y= 11m

Winter Uniform Flow Density Plots
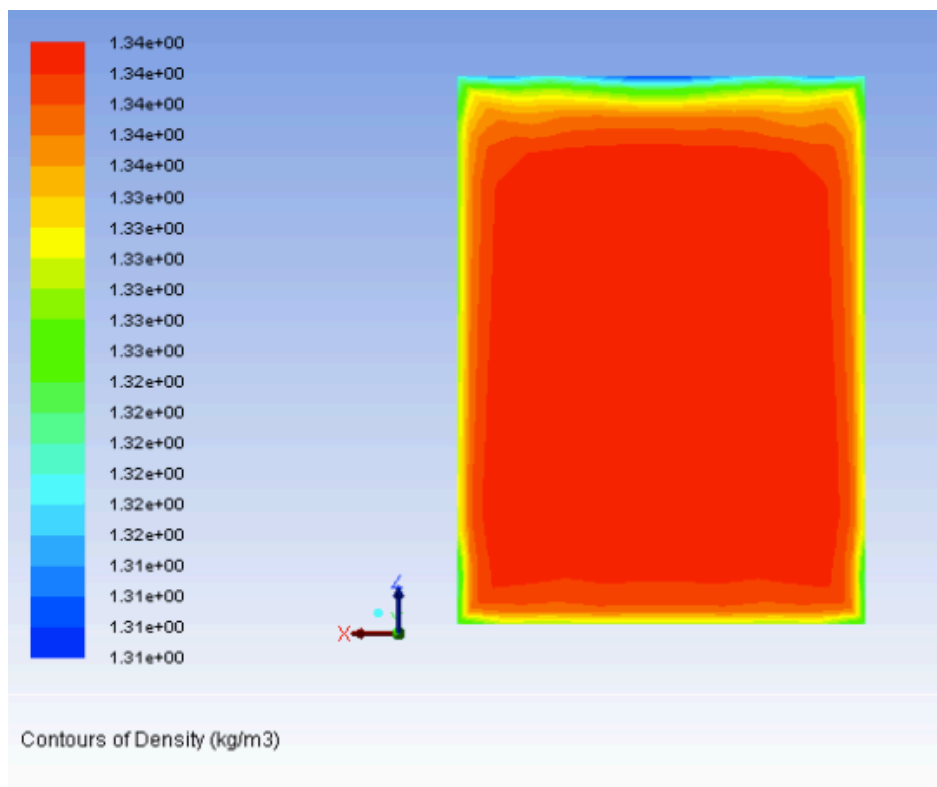
Figure 87: Density At Y= 3m

Figure 88: Density At Y= 6m
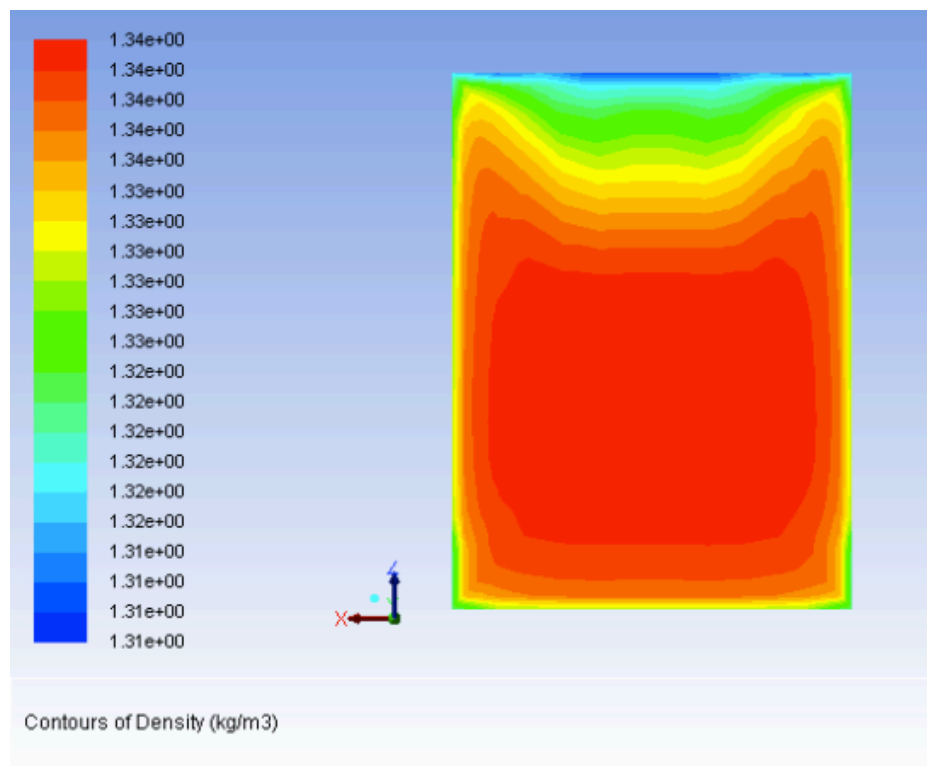
Figure 89: Density At Y= 11m

Calculation Tables

Table 13: Entire Table For Summer Uniform Flow

Summer, uniform		Luft 30 C , grav, ideal gas			
mass flow	2,68	kg/s			
Tin	303,1499	K	Q conv ceiling	1196,54	W
Tout	301,42651	K	Q conv ground	779,70673	W
			Q wall left	1333,322	W
Tair	302,288205	K	Q wall right	1333,1553	W
T surf ceiling	288,89819	K	Area		
T surf ground	287,24405	K	Ceiling	18	m^2
T surf wall left	290,10233	K	Ground	18	m^2
T surf wall right	290,10156	K	Wall left	24	m^2
			Wall right	24	
ΔT air/ceiling	-13,36321		h ceiling	4,974436864	W/m^2K
ΔT air/ground	-15,01735		h ground	2,884466338	W/m^2K
ΔT air/wall left	-12,15907		h wall left	4,569024056	W/m^2K
ΔT air/wall right	-12,15984		h wall right	4,56816352	W/m^2K
			h total	4,294675708	W/m^2K

Table 14: Entire Table For Winter Uniform Flow

Winter, rotational	Luft -10 C				
mass flow	1,5	kg/s			
Tin	263,1499	K	Q conv ceiling	309,8334	W
Tout	264,5296	K	Q conv ground	561,789	W
			Q wall left	604,27924	W
Tair	263,83975	K	Q wall right	604,3667	W
T surf ceiling	271,9205	K	Area		
T surf ground	270,92068	K	Ceiling	18	m^2
T surf wall left	270,45233	K	Ground	18	m^2
T surf wall right	270,45193	K	Wall left	24	m^2
			Wall right	24	
ΔT air/ceiling	8,04698		h ceiling	2,139059208	W/m^2K
ΔT air/ground	7,04716		h ground	4,428805363	W/m^2K
ΔT air/wall left	6,57881		h wall left	3,827181765	W/m^2K
ΔT air/wall right	6,57841		h wall right	3,827968435	W/m^2K
			h total	3,594585322	

Table 15: Entire Table For Winter Uniform Flow With Increased Mass Flow Rate

mass flow, uniform	2,68	kg/s			
Tin	263,1499	K	Q conv ceiling	402,96686	W
Tout	264,04004	K	Q conv ground	616,25818	W
			Q wall left	689,19733	W
Tair	263,59497	K	Q wall right	689,23596	W
T surf ceiling	271,5509	K	Area		
T surf ground	270,70453	K	Ceiling	18	m^2
T surf wall left	270,07321	K	Ground	18	m^2
T surf wall right	270,07306	K	Wall left	24	m^2
			Wall right	24	
ΔT air/ceiling	7,905515		h ceiling	2,831826614	W/m^2K
ΔT air/ground	7,059145		h ground	4,849959245	W/m^2K
ΔT air/wall left	6,427825		h wall left	4,467538462	W/m^2K
ΔT air/wall right	6,427675		h wall right	4,467893134	W/m^2K
			h total	4,199077426	

Table 16: Entire Table For Summer Rotational Flow, Tangential Component= 33%

Summer, rotatinal		Luft 30 C , grav, ideal gas		tan	0,4
				axial	0,8
mass flow	2,68	kg/s			
Tin	303,1499	K	Q conv ceiling	1319,491	W
Tout	301,2641	K	Q conv ground	930,6419	W
			Q wall left	1357,646	W
Tair	302,207	K	Q wall right	1472,86	W
T surf ceiling	289,3861	K	Area		
T surf ground	287,843	K	Ceiling	18	m^2
T surf wall left	290,2109	K	Ground	18	m^2
T surf wall right	290,7253	K	Wall left	24	m^2
			Wall right	24	
ΔT air/ceiling	-12,8753		h ceiling	5,693463885	W/m^2K
ΔT air/ground	-14,4184		h ground	3,5858575	W/m^2K
ΔT air/wall left	-12,0505		h wall left	4,694293459	W/m^2K
ΔT air/wall right	-11,5361		h wall right	5,319749887	W/m^2K
			h total	4,849581253	W/m^2K

Table 17: Entire Table For Winter Rotational Flow, Tangential Component= 33%

Winter, rotational	Luft -10 C			tan 0,4	
mass flow	1,5	kg/s			
Tin	263,1499	K	Q conv ceiling	327,11417	W
Tout	264,59714	K	Q conv ground	594,11279	W
			Q wall left	648,55341	W
Tair	263,87352	K	Q wall right	612,2584	W
T surf ceiling	271,85193	K	Area		
T surf ground	270,79239	K	Ceiling	18	m^2
T surf wall left	270,25467	K	Ground	18	m^2
T surf wall right	270,75845	K	Wall left	24	m^2
			Wall right	24	
ΔT air/ceiling	7,97841		h ceiling	2,277773321	W/m^2K
ΔT air/ground	6,91887		h ground	4,770470628	W/m^2K
ΔT air/wall left	6,38115		h wall left	4,234825815	W/m^2K
ΔT air/wall right	6,88493		h wall right	3,705305162	W/m^2K
			h total	3,77894684	

C: Temperature Plots For Wall Element WallA1 1-3 November
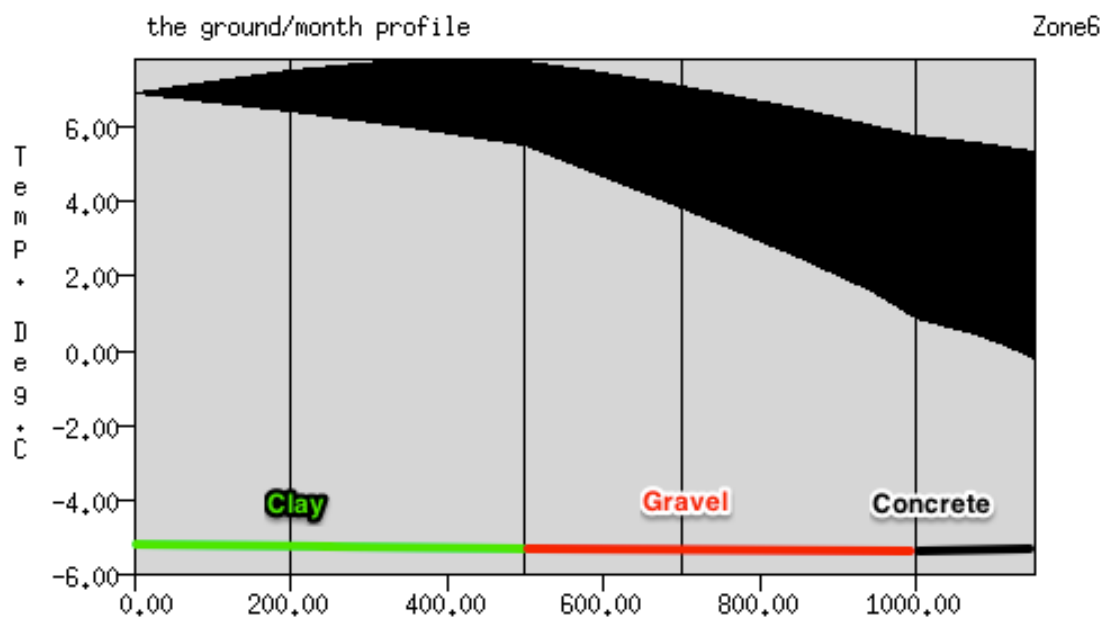
Figure 90: Accumulated Ground Temperature Plot For WallA1, Zone6, 1-3 November, Old Model, Constant Fan
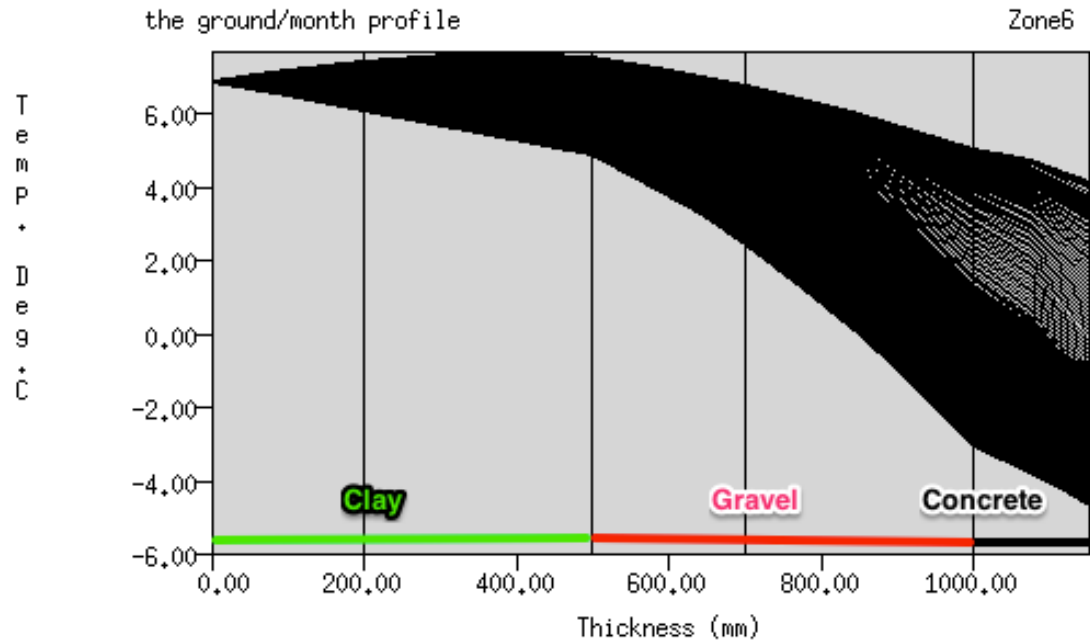
Figure 91: Accumulated Ground Temperature Plot For WallA1, Zone6, 1-3 November, New Model, Constant Fan
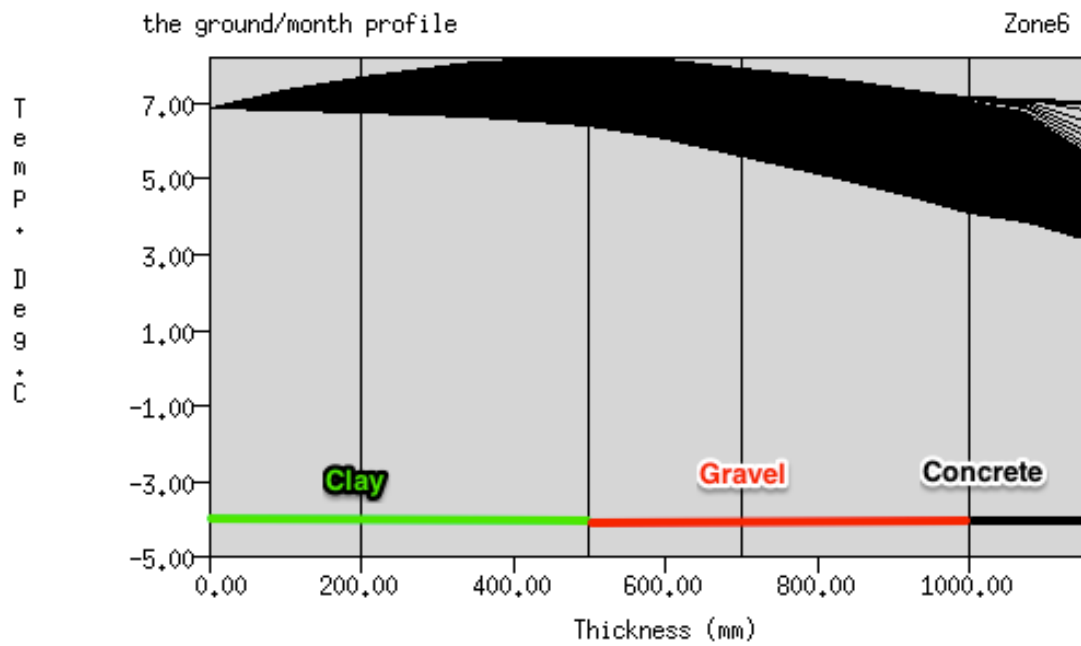
Figure 92: Accumulated Ground Temperature Plot For WallA1, Zone6, 1-3 November, Old Model, Fan 8-16
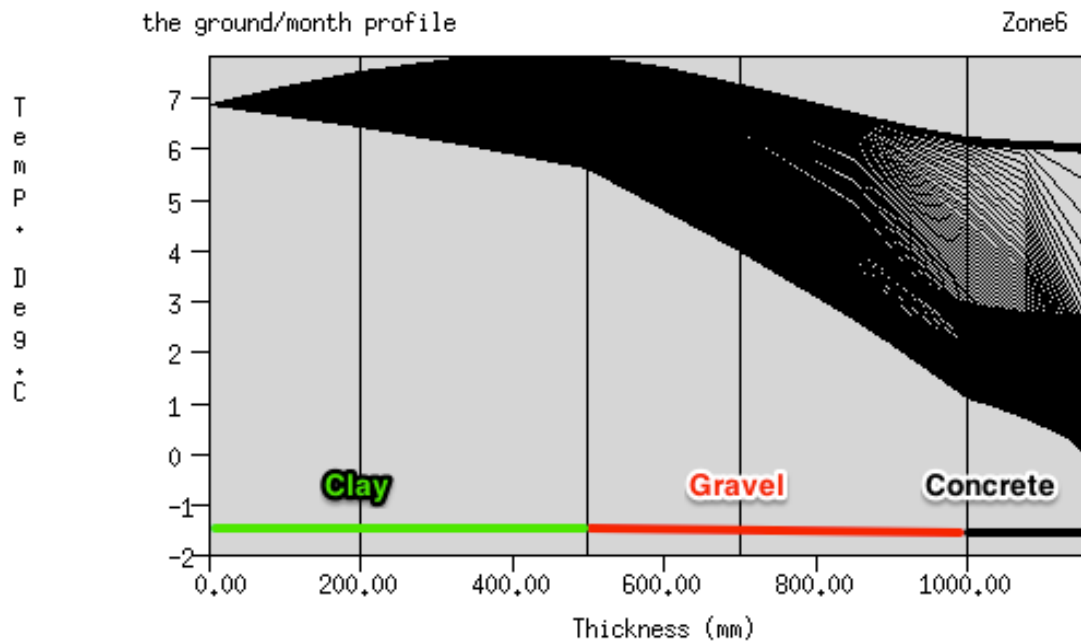
Figure 93: Accumulated Ground Temperature Plot For WallA1, Zone6, 1-3 November, New Model, Fan 8-16

D: ESP-r Fotran Code

Synopsis of the model Kulvert ved Grong Skole defined in Kulvert1.cfg generated on Sun Jun 16 12:36:12 2013. Notes associated with the model are in ../doc/Kulvert1.log

The model is located at latitude 63.42 with a longitude difference of -4.58 from the local time meridian. The year used in simulations is 2002 and weekends occur on Saturday and Sunday.
The site exposure is typical city centre and the ground reflectance is 0.20.

Simulationist name: not yet defined
Simulationist telephone: not yet defined
Simulationist address: not yet defined
Simulationist city: not yet defined
Simulationist postcode: not yet defined

The climate is: Grong, Norway and is held in:
/home/daniello/esp-r/Kulvert0/dbs/trondheim.clm with hour centred solar data.
 annual weather   : /home/daniello/esp-r/Kulvert0/dbs/trondheim.clm
Calculated ground temp at 0.5m depth
-2.8345 -3.6787 -2.1815 0.16138 6.2897 11.019 14.209 15.179 13.525 9.8538 4.9469 0.39406
Calculated ground temp at 1.0m depth
-1.6810 -2.8376 -1.8275 0.0900278 5.4787 9.8764 13.048 14.317 13.201 10.138 5.7801 1.5393
Calculated ground temp at 2.0m depth
0.27171 -1.2325 -0.92537 0.31914 4.4197 8.1267 11.092 12.683 12.344 10.262 6.8812 3.2965
Calculated ground temp at 4.0m depth
2.8429 1.3004 0.96312 1.4297 3.7507 6.2481 8.5376 10.131 10.504 9.6015 7.6161 5.1910

There are currently 2 user defined ground temperature profiles.
Ground temperatures Jan-Dec:
  0.3 -1.2 -0.9   0.3   4.4   8.1 11.1 12.7 12.3 10.3   6.9   3.3
Ground temperatures Jan-Dec:
  2.8   1.3   1.0   1.4   3.8   6.3   8.5 10.1 10.5   9.6   7.6   5.2

The model includes ground topology flat_booring which is defined in grnd.geo.

An Integrated Performance View is incomplete or missing.

Databases associated with the model:

standard pressure distr: pressc.db1
materials   : ../dbs/Kulvert1.materialdb
constructions   : ../dbs/Kulvert1.constrdb
standard plant comp   : plantc.db1
standard event profiles: profiles.db2.a
standard optical prop : optics.db2
standard UK NCM data   : SBEM.db1
standard mould isopleth: mould.db1

_____

The model includes ideal controls as follows:
Control description:
no overall control description supplied

Zones control includes 1 functions.
no zone control description supplied

 The sensor for function 1 senses the temperature of the current zone.
 The actuator for function 1 is the air point in Intake.
 There have been 1 day types defined.
 Day type 1 is valid Tue-01-Jan to Tue-31-Dec, 2002 with 1 periods.
 Per|Start|Sensing |Actuating | Control law | Data
   1 0.00 db temp > flux   basic control: max heating capacity 50000.0W min
heating capacity 0.0W max cooling capacity 0.0W min cooling capacity 0.0W.
Heating
setpoint 19.00C cooling setpoint 100.00C.

 Zone to contol loop linkages:
 zone (1) Entrance   << control 0
 zone (2) Zone2   << control 0
 zone (3) Zone3   << control 0
 zone (4) Zone4   << control 0
 zone (5) Zone5   << control 0
 zone (6) Zone6   << control 0
 zone (7) Intake   << control 1

 Flow control includes 1 loops.
no flow control description supplied

 The sensor for function 1 senses dry bulb temperature in Zone2.
 The actuator for function 1 is flow component: 1 fan
 There have been 1 day types defined.
 Day type 1 is valid Tue-01-Jan to Tue-31-Dec, 2002 with 3 periods.
 Per|Start|Sensing |Actuating | Control law | Data
  1 0.00 dry bulb > flow   on/off setpoint 50.00 direct action ON fraction 1.000.
  2 8.00 dry bulb > flow   on/off setpoint 50.00 inverse action ON fraction
1.000.

3 16.00 dry bulb > flow   on/off setpoint 50.00 direct action ON fraction 1.000.

_____

The model includes an air flow network.

 Flow network description.

  8 nodes, 4 components, 8 connections;   wind reduction = 1.000
  # Node   Fluid Node Type   Height Temperature Data_1   Data_2
  1 Entrance   air internal & unknown 1.0000 20.000   (-)   0.000 vol 6.000
  2 Zone2   air internal & unknown 1.0000 20.000   (-)   0.000 vol 6.000
  3 Zone3   air internal & unknown 1.0000 20.000   (-)   0.000 vol 6.000
  4 Zone4   air internal & unknown 1.0000 20.000   (-)   0.000 vol 6.000
  5 Zone5   air internal & unknown 1.0000 20.000   (-)   0.000 vol 6.000
  6 Zone6   air internal & unknown 1.0000 20.000   (-)   0.000 vol 6.000
  7 Intake   air internal & unknown 1.0000 20.000   (-)   0.000 vol 6.000
  8 ex   air boundary & known   1.0000 0.0000   (Pa) 0.000 (-) 1.000

 Component   Type C+ L+ Description

 fan   35 2 0 Constant mass flow rate component m = a
 Fluid 1.0 flow rate (kg/s)   1.3000

 Inlet   110 2 0 Specific air flow opening   m = rho.f(A,dP)
 Fluid 1.0 opening area (m) 3.000

 Opening   110 2 0 Specific air flow opening   m = rho.f(A,dP)
 Fluid 1.0 opening area (m) 3.000

 Outlet   110 2 0 Specific air flow opening   m = rho.f(A,dP)
 Fluid 1.0 opening area (m) 3.000

  # +Node   dHght -Node   dHght Component   Z @+   Z @-
  1 ex   0.000 Entrance   0.000 fan   1.000 1.000
  2 Entrance   0.000 Zone2   0.000 Opening   1.000 1.000
  3 Zone2   0.000 Zone3   0.000 Opening   1.000 1.000
  4 Zone3   0.000 Zone4   0.000 Opening   1.000 1.000
  5 Zone4   0.000 Zone5   0.000 Opening   1.000 1.000
  6 Zone5   0.000 Zone6   0.000 Opening   1.000 1.000
  7 Zone6   0.000 Intake   0.000 Opening   1.000 1.000
  8 Intake   0.000 ex   0.000 Opening   1.000 1.000
thermal zone to air flow node mapping:
thermal zone -> air flow node
Entrance   -> Entrance
Zone2   -> Zone2
Zone3   -> Zone3
Zone4   -> Zone4

```
Zone5      -> Zone5
Zone6      -> Zone6
Intake     -> Intake
```

_____

```
ID Zone       Volume|        Surface
   Name       m^3  | No. Opaque Transp ~Floor
1 Entrance     6.0  6   14.0   6.0    3.0  Entrance first part of culvert
2 Zone2        6.0  6   14.0   6.0    3.0  Zone2 describes a part 2 of model
3 Zone3        6.0  6   14.0   6.0    3.0  Zone3 describes a part 3 of model
4 Zone4        6.0  6   14.0   6.0    3.0  Zone4 describes a part 3 of model
5 Zone5        6.0  6   14.0   6.0    3.0  Zone5 describes last part of the model
6 Zone6        6.0  6   14.0   6.0    3.0  Zone6 describes part 6 of the model
7 Intake       6.0  6   14.0   6.0    3.0  Intake describes last part of model where
air gets heated
   all       42. 42   98.   42.   21.
```

Zone Entrance (1) is composed of 6 surfaces and 8 vertices.
It encloses a volume of 6.00m^3 of space, with a total surface
area of 20.0m^2 & approx floor area of 3.00m^2
Entrance first part of culvert
There is 3.0000m2 of exposed surface area.
Flat roof is 100.00 % of floor area & avg U of 0.533 & UA of 1.5991
Ground contact is 366.67 % of floor area & avg U of 0.614 & perimeter 0.00

A summary of the surfaces in Entrance(1) follows:

```
Sur| Area |Azim|Elev| surface   |  geometry    | construction |environment
   | m^2  |deg |deg | name      |optical|locat| use | name      |other side
1 3.00   180.  0. Inlet     SC_ficti VERT -   fictitious  ||< adiabatic
2 4.00    90.  0. Wall_A1    OPAQUE  VERT -   Wall_cu1    ||< user def grnd
profile 1
3 4.00   270.  0. Wall_B1    OPAQUE  VERT -   Wall_cu1    ||< user def grnd
profile 1
4 3.00     0. 90. Roof1      OPAQUE  CEIL -   Roof_cu1    ||< external
5 3.00     0. -90. Floor1     OPAQUE  FLOR -   Floor_cu1   ||< user def grnd
profile 2
6 3.00     0.  0. 0_out     SC_ficti VERT -   fictitious  ||< adiabatic
```

All surfaces will receive diffuse insolation (if shading not calculated).
No shading analysis requested.
No insolation analysis requested.

Opened existing hc control file.

Number of control periods: 1

Period 1 start   0.00 finish 24.00
User specified convection coefficients
User supplied hc values
  Surface orinetation Inside   Outside
1 Inlet   (VERT) default default
2 Wall_A1   (VERT) 30.000   default
3 Wall_B1   (VERT) 30.000   default
4 Roof1   (CEIL) 30.000   default
5 Floor1   (FLOR) 30.000   default
6 0_out   (VERT) default default

Ventilation & infiltration is assessed via network analysis
and the associated network node is: Entrance

Notes:
nothing happens in this zone in terms of occupants lights and small
power. There is not infiltration or ventilation.

Daytype	Gain Type No.	label	Period Hours	Sensible Magn.(W)	Latent Magn.(W)	Radiant Fraction	Convec Fraction
weekdays	1 OccuptW		0-24	0.0	0.0	0.50	0.50
weekdays	2 LightsW		0-24	0.0	0.0	0.50	0.50
weekdays	3 EquiptW		0-24	0.0	0.0	0.50	0.50
saturday	1 OccuptW		0-24	0.0	0.0	0.50	0.50
saturday	2 LightsW		0-24	0.0	0.0	0.50	0.50
saturday	3 EquiptW		0-24	0.0	0.0	0.50	0.50
sunday	1 OccuptW		0-24	0.0	0.0	0.50	0.50
sunday	2 LightsW		0-24	0.0	0.0	0.50	0.50
sunday	3 EquiptW		0-24	0.0	0.0	0.50	0.50

_____

Zone Zone2 (2) is composed of 6 surfaces and 8 vertices.
It encloses a volume of 6.00m^3 of space, with a total surface
area of 20.0m^2 & approx floor area of 3.00m^2
Zone2 describes a part 2 of model
There is 3.0000m2 of exposed surface area.
Flat roof is 100.00 % of floor area & avg U of 0.533 & UA of 1.5991
Ground contact is 366.67 % of floor area & avg U of 0.614 & perimeter 0.00

A summary of the surfaces in Zone2(2) follows:

Sur	Area m^2	Azim deg	Elev deg	surface name	geometry optical	locat	use	construction name	environment other side
1	3.00	180.	0.	0_in	SC_ficti	VERT	-	fictitious	||< adiabatic

```
 2 4.00   90.  0. Wall_A1    OPAQUE  VERT -    Wall_cu1    ||< user def grnd
profile  1
 3 4.00   270.  0. Wall_B1    OPAQUE  VERT -    Wall_cu1    ||< user def grnd
profile  1
 4 3.00    0.  90. Roof1     OPAQUE  CEIL -    Roof_cu1   ||< external
 5 3.00    0. -90. Floor1     OPAQUE  FLOR -    Floor_cu1  ||< user def grnd
profile  2
 6 3.00    0.  0. 0_out      SC_ficti VERT -    fictitious  ||< adiabatic
```

All surfaces will receive diffuse insolation (if shading not calculated).
No shading analysis requested.
No insolation analysis requested.

Opened existing hc control file.

Number of control periods: 1

Period 1 start 0.00 finish 24.00
User specified convection coefficients
User supplied hc values
  Surface orinetation Inside   Outside
1 0_in   (VERT) default default
2 Wall_A1   (VERT) 30.000 default
3 Wall_B1   (VERT) 30.000 default
4 Roof1   (CEIL) 30.000 default
5 Floor1   (FLOR) 30.000 default
6 0_out   (VERT) default default

Ventilation & infiltration is assessed via network analysis
and the associated network node is: Zone2

Notes:
nothing happens in this zone in terms of occupants lights and small
power. There is not infiltration or ventilation.

Daytype	Gain Type	Period	Sensible	Latent	Radiant	Convec
	No. label	Hours	Magn.(W)	Magn.(W)	Fraction	Fraction
weekdays	1 OccuptW	0-24	0.0	0.0	0.60	0.40
weekdays	2 LightsW	0-24	0.0	0.0	0.30	0.70
weekdays	3 EquiptW	0-24	0.0	0.0	0.40	0.60
saturday	1 OccuptW	0-24	0.0	0.0	0.60	0.40
saturday	2 LightsW	0-24	0.0	0.0	0.30	0.70
saturday	3 EquiptW	0-24	0.0	0.0	0.40	0.60
sunday	1 OccuptW	0-24	0.0	0.0	0.60	0.40
sunday	2 LightsW	0-24	0.0	0.0	0.30	0.70
sunday	3 EquiptW	0-24	0.0	0.0	0.40	0.60

_____

Zone Zone3 (3) is composed of 6 surfaces and 8 vertices.
It encloses a volume of 6.00m^3 of space, with a total surface
area of 20.0m^2 & approx floor area of 3.00m^2
Zone3 describes a part 3 of model
There is 3.0000m2 of exposed surface area.
Flat roof is 100.00 % of floor area & avg U of 0.533 & UA of 1.5991
Ground contact is 366.67 % of floor area & avg U of 0.614 & perimeter 0.00

A summary of the surfaces in Zone3(3) follows:

```
Sur| Area |Azim|Elev| surface   |  geometry    | construction |environment
  | m^2  |deg |deg | name     |optical|locat| use | name      |other side
 1 3.00   180. 0. 0_in      SC_ficti VERT -   fictitious  ||< adiabatic
 2 4.00    90. 0. Wall_A1    OPAQUE  VERT -   Wall_cu1   ||< user def grnd
profile  1
 3 4.00   270. 0. Wall_B1     OPAQUE  VERT -   Wall_cu1    ||< user def grnd
profile  1
 4 3.00    0. 90. Roof1      OPAQUE  CEIL -   Roof_cu1    ||< external
 5 3.00    0. -90. Floor1     OPAQUE  FLOR -   Floor_cu1   ||< user def grnd
profile  2
 6 3.00    0.  0. 0_out      SC_ficti VERT -   fictitious  ||< adiabatic
```

All surfaces will receive diffuse insolation (if shading not calculated).
No shading analysis requested.
No insolation analysis requested.

Opened existing hc control file.

Number of control periods: 1

Period 1 start 0.00 finish 24.00
User specified convection coefficients
User supplied hc values
  Surface orinetation Inside   Outside
1 0_in   (VERT) default default
2 Wall_A1   (VERT) 30.000 default
3 Wall_B1   (VERT) 30.000 default
4 Roof1   (CEIL) 30.000 default
5 Floor1   (FLOR) 30.000 default
6 0_out   (VERT) default default

Ventilation & infiltration is assessed via network analysis
and the associated network node is: Zone3

Notes:

nothing happens in this zone in terms of occupants lights and small power. There is not infiltration or ventilation.

Daytype	Gain	Type	Period	Sensible	Latent	Radiant	Convec
	No.	label	Hours	Magn.(W)	Magn.(W)	Fraction	Fraction
weekdays	1	OccuptW	0-24	0.0	0.0	0.60	0.40
weekdays	2	LightsW	0-24	0.0	0.0	0.30	0.70
weekdays	3	EquiptW	0-24	0.0	0.0	0.40	0.60
saturday	1	OccuptW	0-24	0.0	0.0	0.60	0.40
saturday	2	LightsW	0-24	0.0	0.0	0.30	0.70
saturday	3	EquiptW	0-24	0.0	0.0	0.40	0.60
sunday	1	OccuptW	0-24	0.0	0.0	0.60	0.40
sunday	2	LightsW	0-24	0.0	0.0	0.30	0.70
sunday	3	EquiptW	0-24	0.0	0.0	0.40	0.60

_____

Zone Zone4 (4) is composed of 6 surfaces and 8 vertices.
It encloses a volume of 6.00m^3 of space, with a total surface
area of 20.0m^2 & approx floor area of 3.00m^2
Zone4 describes a part 3 of model
There is 3.0000m2 of exposed surface area.
Flat roof is 100.00 % of floor area & avg U of 0.533 & UA of 1.5991
Ground contact is 366.67 % of floor area & avg U of 0.614 & perimeter 0.00

A summary of the surfaces in Zone4(4) follows:

Sur	Area	Azim	Elev	surface	geometry		construction	environment
	m^2	deg	deg	name	optical	locat	use	name	other side
1	3.00	180.	0.	0_in	SC_ficti	VERT -	fictitious	||< adiabatic
2	4.00	90.	0.	Wall_A1	OPAQUE	VERT -	Wall_cu1	||< user def grnd profile 1
3	4.00	270.	0.	Wall_B1	OPAQUE	VERT -	Wall_cu1	||< user def grnd profile 1
4	3.00	0.	90.	Roof1	OPAQUE	CEIL -	Roof_cu1	||< external
5	3.00	0.	-90.	Floor1	OPAQUE	FLOR -	Floor_cu1	||< user def grnd profile 2
6	3.00	0.	0.	0_out	SC_ficti	VERT -	fictitious	||< adiabatic

All surfaces will receive diffuse insolation (if shading not calculated).
No shading analysis requested.
No insolation analysis requested.

Opened existing hc control file.

Number of control periods: 1

Period 1 start 0.00 finish 24.00
User specified convection coefficients
User supplied hc values
  Surface orinetation Inside   Outside
1 0_in   (VERT) default default
2 Wall_A1   (VERT) 30.000 default
3 Wall_B1   (VERT) 30.000 default
4 Roof1   (CEIL) 30.000 default
5 Floor1   (FLOR) 30.000 default
6 0_out   (VERT) default default

Ventilation & infiltration is assessed via network analysis
and the associated network node is: Zone4

Notes:
nothing happens in this zone in terms of occupants lights and small
power. There is not infiltration or ventilation.

Daytype	Gain	Type No.	Period label	Sensible Hours	Latent Magn.(W)	Radiant Magn.(W)	Convec Fraction	Fraction
weekdays	1	OccuptW	0-24	0.0	0.0	0.60	0.40	
weekdays	2	LightsW	0-24	0.0	0.0	0.30	0.70	
weekdays	3	EquiptW	0-24	0.0	0.0	0.40	0.60	
saturday	1	OccuptW	0-24	0.0	0.0	0.60	0.40	
saturday	2	LightsW	0-24	0.0	0.0	0.30	0.70	
saturday	3	EquiptW	0-24	0.0	0.0	0.40	0.60	
sunday	1	OccuptW	0-24	0.0	0.0	0.60	0.40	
sunday	2	LightsW	0-24	0.0	0.0	0.30	0.70	
sunday	3	EquiptW	0-24	0.0	0.0	0.40	0.60	

_____

Zone Zone5 (5) is composed of 6 surfaces and 8 vertices.
It encloses a volume of 6.00m^3 of space, with a total surface
area of 20.0m^2 & approx floor area of 3.00m^2
Zone5 describes last part of the model
There is 3.0000m2 of exposed surface area.
Flat roof is 100.00 % of floor area & avg U of 0.533 & UA of 1.5991
Ground contact is 366.67 % of floor area & avg U of 0.614 & perimeter 0.00

A summary of the surfaces in Zone5(5) follows:

Sur	Area m^2	Azim deg	Elev deg	surface name	geometry optical	locat	use	construction name	environment other side
1	3.00	180.	0.	0_in	SC_ficti	VERT	-	fictitious	||< adiabatic
2	4.00	90.	0.	Wall_A1	OPAQUE	VERT	-	Wall_cu1	||< user def grnd profile 1
3	4.00	270.	0.	Wall_B1	OPAQUE	VERT	-	Wall_cu1	||< user def grnd profile 1

```
4 3.00    0. 90. Roof1      OPAQUE  CEIL -    Roof_cu1    ||< external
5 3.00    0. -90. Floor1     OPAQUE  FLOR -   Floor_cu1   ||< user def grnd
profile 2
6 3.00    0.  0. 0_out      SC_ficti VERT -    fictitious  ||< adiabatic
```

All surfaces will receive diffuse insolation (if shading not calculated).
No shading analysis requested.
No insolation analysis requested.

Opened existing hc control file.

Number of control periods: 1

Period 1 start 0.00 finish 24.00
User specified convection coefficients
User supplied hc values
  Surface orinetation Inside   Outside
1 0_in   (VERT) default default
2 Wall_A1   (VERT) 30.000 default
3 Wall_B1   (VERT) 30.000 default
4 Roof1   (CEIL) 30.000 default
5 Floor1   (FLOR) 30.000 default
6 0_out   (VERT) default default

Ventilation & infiltration is assessed via network analysis
and the associated network node is: Zone5

Notes:
nothing happens in this zone in terms of occupants lights and small
power. There is not infiltration or ventilation.

Daytype	Gain	Type	Period	Sensible	Latent	Radiant	Convec
	No.	label	Hours	Magn.(W)	Magn.(W)	Fraction	Fraction
weekdays	1	OccuptW	0-24	0.0	0.0	0.60	0.40
weekdays	2	LightsW	0-24	0.0	0.0	0.30	0.70
weekdays	3	EquiptW	0-24	0.0	0.0	0.40	0.60
saturday	1	OccuptW	0-24	0.0	0.0	0.60	0.40
saturday	2	LightsW	0-24	0.0	0.0	0.30	0.70
saturday	3	EquiptW	0-24	0.0	0.0	0.40	0.60
sunday	1	OccuptW	0-24	0.0	0.0	0.60	0.40
sunday	2	LightsW	0-24	0.0	0.0	0.30	0.70
sunday	3	EquiptW	0-24	0.0	0.0	0.40	0.60

_____

Zone Zone6 (6) is composed of 6 surfaces and 8 vertices.
It encloses a volume of 6.00m^3 of space, with a total surface

area of 20.0m^2 & approx floor area of 3.00m^2
Zone6 describes part 6 of the model
There is 3.0000m2 of exposed surface area.
Flat roof is 100.00 % of floor area & avg U of 0.533 & UA of 1.5991
Ground contact is 366.67 % of floor area & avg U of 0.614 & perimeter 0.00

A summary of the surfaces in Zone6(6) follows:

```
Sur| Area |Azim|Elev| surface   |  geometry    | construction |environment
  | m^2 |deg |deg | name     |optical|locat| use | name       |other side
 1 3.00  180. 0. 0_in     SC_ficti VERT -  fictitious  ||< adiabatic
 2 4.00   90. 0. Wall_A1   OPAQUE  VERT -   Wall_cu1   ||< user def grnd
profile 1
 3 4.00  270. 0. Wall_B1   OPAQUE  VERT -   Wall_cu1   ||< user def grnd
profile 1
 4 3.00    0. 90. Roof1     OPAQUE  CEIL -   Roof_cu1   ||< external
 5 3.00    0. -90. Floor1    OPAQUE  FLOR -   Floor_cu1  ||< user def grnd
profile 2
 6 3.00    0.  0. 0_out     SC_ficti VERT -   fictitious  ||< adiabatic
```


All surfaces will receive diffuse insolation (if shading not calculated).
No shading analysis requested.
No insolation analysis requested.

Opened existing hc control file.

Number of control periods: 1

Period 1 start 0.00 finish 24.00
User specified convection coefficients
User supplied hc values
  Surface orinetation Inside   Outside
1 0_in   (VERT) default default
2 Wall_A1   (VERT) 30.000 default
3 Wall_B1   (VERT) 30.000 default
4 Roof1   (CEIL) 30.000 default
5 Floor1   (FLOR) 30.000 default
6 0_out   (VERT) default default

Ventilation & infiltration is assessed via network analysis
and the associated network node is: Zone6

Notes:
nothing happens in this zone in terms of occupants lights and small
power. There is not infiltration or ventilation.

Daytype Gain Type Period Sensible Latent   Radiant Convec

```
         No. label  Hours Magn.(W) Magn.(W)  Fraction  Fraction
weekdays   1 OccuptW  0-24   0.0    0.0    0.60    0.40
weekdays   2 LightsW  0-24   0.0    0.0    0.30    0.70
weekdays   3 EquiptW  0-24   0.0    0.0    0.40    0.60
saturday   1 OccuptW  0-24   0.0    0.0    0.60    0.40
saturday   2 LightsW  0-24   0.0    0.0    0.30    0.70
saturday   3 EquiptW  0-24   0.0    0.0    0.40    0.60
sunday     1 OccuptW  0-24   0.0    0.0    0.60    0.40
sunday     2 LightsW  0-24   0.0    0.0    0.30    0.70
sunday     3 EquiptW  0-24   0.0    0.0    0.40    0.60
```

_____

Zone Intake (7) is composed of 6 surfaces and 8 vertices.
It encloses a volume of 6.00m^3 of space, with a total surface
area of 20.0m^2 & approx floor area of 3.00m^2
Intake describes last part of model where air gets heated

A summary of the surfaces in Intake(7) follows:

```
Sur| Area |Azim|Elev| surface  |  geometry    | construction |environment
  | m^2 |deg |deg | name     |optical|locat| use | name      |other side
 1 3.00   180.  0. 0_in      SC_ficti VERT -  fictitious   ||< adiabatic
 2 4.00    90.  0. Wall_A1    OPAQUE  VERT -   Wall_cu1    ||< adiabatic
 3 4.00   270.  0. Wall_B1    OPAQUE  VERT -   Wall_cu1    ||< adiabatic
 4 3.00    0. 90. Roof1      OPAQUE  CEIL -   Roof_cu1    ||< adiabatic
 5 3.00    0. -90. Floor1     OPAQUE  FLOR -   Floor_cu1   ||< adiabatic
 6 3.00    0.  0. 0_out      SC_ficti VERT -   fictitious   ||< adiabatic
```

All surfaces will receive diffuse insolation (if shading not calculated).
No shading analysis requested.
No insolation analysis requested.

Opened existing hc control file.

Number of control periods: 1

Period 1 start 0.00 finish 24.00
User specified convection coefficients
User supplied hc values
  Surface orinetation Inside   Outside
1 0_in   (VERT) default default
2 Wall_A1   (VERT) default default
3 Wall_B1   (VERT) default default
4 Roof1   (CEIL) default default
5 Floor1   (FLOR) default default
6 0_out   (VERT) default default

Ventilation & infiltration is assessed via network analysis
and the associated network node is: Intake

Notes:
nothing happens in this zone in terms of occupants lights and small
power. There is not infiltration or ventilation.

Daytype	Gain	Type	Period	Sensible	Latent	Radiant	Convec
	No.	label	Hours	Magn.(W)	Magn.(W)	Fraction	Fraction
weekdays	1	OccuptW	0-24	0.0	0.0	0.60	0.40
weekdays	2	LightsW	0-24	0.0	0.0	0.30	0.70
weekdays	3	EquiptW	0-24	0.0	0.0	0.40	0.60
saturday	1	OccuptW	0-24	0.0	0.0	0.60	0.40
saturday	2	LightsW	0-24	0.0	0.0	0.30	0.70
saturday	3	EquiptW	0-24	0.0	0.0	0.40	0.60
sunday	1	OccuptW	0-24	0.0	0.0	0.60	0.40
sunday	2	LightsW	0-24	0.0	0.0	0.30	0.70
sunday	3	EquiptW	0-24	0.0	0.0	0.40	0.60

_____

Project floor area is 21.000m2, wall area is 0.00m2, window area is 0.00m2.
Sloped roof area is 0.00m2, flat roof area is 18.000m2, skylight area is 0.00m2.
In contact with ground 66.000m2.
There is 18.000m2 of outside surface area.

Flat roof is 85.714 % of floor area & avg U of 0.533 & UA of 9.5944
Ground contact is 314.29 % of floor area & avg U of 0.614 & perimeter 0.00 &
max MLC thickness 1.150
CIBSE ground beta!66.000 dt 2.503 Ufleft 0.014 Ufright 4.429 Uf 0.063 R extra @
virtual layer14.165

_____

Multi-layer constructions used:

Details of transparent construction: fictitious with SC_fictit optics and overall
thickness 0.004

Layer	Matr	Thick	Conduc-	Density	Specif	IR	Solar	Diffu	R	Description
	db	(mm)	tivity		heat	emis	abs	resis	m^2K/W	
1	245	4.0	20.000	10.	10.	0.99	0.01	19200.	0.00	fict : fictitious material

(almost not there) with matching single layer optics
ISO 6946 U values (horiz/upward/downward heat flow)= 5.875 7.133 4.757
(partition) 3.843

: with id of: SC_fictit
with 3 layers [including air gaps] and visible trn: 0.76
Direct transmission @ 0, 40, 55, 70, 80 deg
 0.611 0.583 0.534 0.384 0.170

```
Layer| absorption @ 0, 40, 55, 70, 80 deg
   1  0.157 0.172 0.185 0.201 0.202
   2  0.001 0.002 0.003 0.004 0.005
   3  0.117 0.124 0.127 0.112 0.077
 Total area of fictitious is    42.00
```

Details of opaque construction: Wall_cu1 linked to Wall_culvert & with overall thickness 1.150

```
Layer|Matr|Thick |Conduc-|Density|Specif|IR |Solar|Diffu| R   |Description
     |db |(mm) |tivity |       |heat |emis|abs |resis|m^2K/W
 Ext  263 200.0    1.280 1460.  879. 0.90 0.85    5.  0.16 earth std : Clay_1
   2 263 300.0    1.280 1460.  879. 0.90 0.85    5.  0.23 earth std : Clay_1
   3 262 200.0    0.520 2050.  184. 0.90 0.85    2.  0.38 gravel based : Gravel_1
   4 262 300.0    0.520 2050.  184. 0.90 0.85    2.  0.58 gravel based : Gravel_1
 Int  50 150.0    1.400 2100.  653. 0.90 0.65   19.  0.11 mat_050 : Heavy mix
concrete_Grong1
 ISO 6946 U values (horiz/upward/downward heat flow)= 0.614  0.625  0.599
(partition) 0.582
 Total area of Wall_cu1 is    56.00
```

Details of opaque construction: Floor_cu1 and overall thickness 1.100

```
Layer|Matr|Thick |Conduc-|Density|Specif|IR |Solar|Diffu| R   |Description
     |db |(mm) |tivity |       |heat |emis|abs |resis|m^2K/W
 Ext  263 200.0    1.280 1460.  879. 0.90 0.85    5.  0.16 earth std : Clay_1
   2 263 300.0    1.280 1460.  879. 0.90 0.85    5.  0.23 earth std : Clay_1
   3 262 200.0    0.520 2050.  184. 0.90 0.85    2.  0.38 gravel based : Gravel_1
   4 262 300.0    0.520 2050.  184. 0.90 0.85    2.  0.58 gravel based : Gravel_1
 Int   1 100.0    0.960 2000.  840. 0.93 0.70   12.  0.10 Paviour brick : Paviour
brick
 ISO 6946 U values (horiz/upward/downward heat flow)= 0.615  0.626  0.600
(partition) 0.583
 Total area of Floor_cu1 is    21.00
```

Details of opaque construction: Roof_cu1 and overall thickness 1.150

```
Layer|Matr|Thick |Conduc-|Density|Specif|IR |Solar|Diffu| R   |Description
     |db |(mm) |tivity |       |heat |emis|abs |resis|m^2K/W
 Ext  263 200.0    1.280 1460.  879. 0.90 0.85    5.  0.16 earth std : Clay_1
   2 263 300.0    1.280 1460.  879. 0.90 0.85    5.  0.23 earth std : Clay_1
   3 262 200.0    0.520 2050.  184. 0.90 0.85    2.  0.38 gravel based : Gravel_1
   4 262 300.0    0.520 2050.  184. 0.90 0.85    2.  0.58 gravel based : Gravel_1
   5 207  50.0    0.160 1379. 1004. 0.90 0.60   70.  0.31 PVC : PVC
 Int  50 100.0    1.400 2100.  653. 0.90 0.65   19.  0.07 mat_050 : Heavy mix
concrete_Grong1
 ISO 6946 U values (horiz/upward/downward heat flow)= 0.525  0.533  0.514
(partition) 0.501
 Total area of Roof_cu1 is    21.
```